Addis Ababa University

Addis Ababa Institute of Technology

School of Graduate Studies

Energy Center

Simulation, Modeling and Control of Distributed Hybrid Generation System

Case Study: *Berehet Woreda*

A Thesis submitted to the School of Graduate Studies of Addis Ababa Institute of Technology in partial fulfillment of the Degree of Master of Science in Energy Technology

Mohammed Shikur

Advisor: Dr. Tesfaye Dama

June 2015

Addis Ababa University

Addis Ababa Institute of Technology

Energy Center

Simulation, Control and Modeling of Distributed Hybrid Generation System: A Case Study of Berehet Woreda

By: Mohammed Shikur Sherif

APPROVED BY BOARD OF EXAMINERS

Dr. Solomon Abebe	_____	_____
Head, Energy Center	Signature	Date
Dr. Tesfaye Dama	_____	_____
Advisor	Signature	Date
Dr. Solomon Abebe	_____	_____
Internal Examiner	Signature	Date
Dr.-Ing. Abebayehu Assefa	_____	_____
External Examiner	Signature	Date

Declaration

I hereby declare that this thesis is my own work and effort and that it has not been submitted anywhere for any award. Where other sources of information have been used, they have been acknowledged

Signature: …….

Date: …….

Acknowledgement

I would like to express my gratitude to all those who gave me the possibility to complete this thesis. I am deeply indebted to my supervisor Dr. Tesfaye Dama from the Addis Ababa University, Mechanical Engineering Department for stimulating suggestions and encouragement that helped me in all the time of research and writing of this thesis. My sincere appreciation also goes to Dr.-Ing Abebayehu Assefa for his devoted support during my graduate years .My family and friends supported me in my research work, I want to thank them for all their help, support, interest and valuable hints.

.

Abstract

An autonomous decentralized distributed generation hybrid system supplies electricity to the user load both in grid tied or standalone modes. This kind of decentralized system is frequently located in remote and inaccessible areas. It is essential for about one third of the world populations who are living in undeveloped or isolated regions and have no access to utility grid. Most people live in remote and rural areas, with low population density, lacking even the basic infrastructure. The grid extension to these locations might not be cost effective option and sometimes technically not feasible even. This decentralized energy generation system is essential for countries which has low installed capacity.

The purpose of this thesis is modeling, simulation and control of a grid ties hybrid power system. It couples wind turbines, photovoltaic generators (PV), alkaline water electrolyser, a storage gas tank, fuel cell (SOFC) to give different system topologies. The system is intended to be an environmentally friendly solution since it tries maximizing the use of a renewable energy source. Besides the grid, electricity is produced by a both wind turbines and PV generators to meet the requirements of user load. During periods of low solar radiation, wind speed and also when the grid system is disconnected because of some reason, the fuel cell stack serves as standby to supply the load required by users.

Different methodologies have been applied to address each objective of this study. Matlab Simulink software is used for the modeling and simulation of the hybrid system. Data were collected for the case study area in order to perform the optimization and financial analysis for the case study area using the Homer optimization software.

Based on the dynamic component models, a simulation model for the proposed hybrid wind/PV/FC energy system has been developed successfully using MATLAB/Simulink.

In the conclusion of this work the most optimum hybrid system is selected for the case study area from the output of Homer hybrid optimization software and comparison of the cost between the optimum homer output with that of the grid extension to the case study area is done.

Table of Content

List of Figures

List of Tables

CHAPTER 1

1.1 Introduction

Ethiopia is gifted with abundant renewable energy resources. Yet it is also a lowest energy consuming country in the world. Only 14 % of its people have a direct supply of electricity in their homes; among the 66 million who live in rural areas that figure is below one percent [1]. This is a major limitation on the country's growth and development.

Domestic energy requirements in rural and urban areas are mostly met from wood, animal dung and agricultural residues in Ethiopia. At the national level it is estimated that biomass fuels meet 88 % of total energy consumed in the country [3]. In urban areas access to petroleum fuels and electricity has enabled a significant proportion of the population there to employ these for cooking and other domestic energy requirements.

In the absence of other affordable power sources people still rely on traditional forms of energy, such as firewood. This is causing increased deforestation and soil erosion, and it also leads to health problems. To address the situation, Ethiopia needs to develop and use its renewable and environmentally sustainable energy resources.

Ethiopia's hydropower resources, which are distributed in nine major river basins and their innumerable tributaries, are estimated to generate 650 TWh per year. The technically feasible potential is estimated to be 40% of the theoretical potential i.e. 260 TWh per year (45 GW equivalent with 65% plant factor). This would constitute about 15% of the total technically feasible potential of Africa, which is 1750 TWh per year. In order to tap from these resources various studies are being undertaken both by Ministry of Water and Energy (MoWE) and the Ethiopian Electric Power Corporation (EEPCo) [34].

EEPCo is responsible for the generation, transmission, distribution and sales service of electric energy throughout Ethiopia. The corporation has two electric power supply systems: the Interconnected System (ICS) and the Self Contained System (SCS). The main energy source of ICS is hydropower plants, and for the SCS mini-hydro and diesel power generators allocated in various areas of the country.

The country's ICS consists of 12 hydro, one geothermal and 15 Diseal Power Plants and two wind farm with a total capacity of around 2000MW, of which 91% is generated from hydropower plants. The electric energy generated from the main hydropower plants is transported through high voltage transmission lines rated 45, 66, 132, 230 and 400 kV. The 400 kV transmission lines of 685.71 km were constructed and commissioned recently while 500kV and DC lines are going to be implemented in the near future. The total

length of the existing transmission lines is about 10,884.23 km. Regional interconnections with neighboring countries including Djibouti and Sudan are finished while that of to Kenya is under procurement phases [2].

The total energy sales of the Interconnected System (ICS), the main electricity grid and the Self-Contained System (SCS) separate mini grids, stand at 3844 GWh during the 2010/2011 fiscal year. Of this the sales in the ICS take about 98% of the total. Category-wise the domestic consumption takes the highest share at 38% seconded by the total industrial consumption (LV and HV) which is 37% [49]. Annual per capita consumption of electricity is 100 kWh per year. The same figure for the Sub-Saharan Africa is 510 kWh. This reveals that most of the energy usage is still from traditional energy sources such as wood and animal waste. Moreover it also informs the fact that with the country's economic development and improvement of the per-capita income, there will be huge potential for consumption of electricity within the country [3].

System losses as determined from the generation and sales figure stand at 23%. This figure represents both technical and non-technical losses and the major share is attributable to the distribution network poor design. Distribution system rehabilitation and power factor improvement projects are launched in major cities of the country in order to address this problem. In 2010/2011 fiscal year, the generated energy stood at 4980 GWh and the system peak was 913.93 MW [49]. The actual generation was constrained due to shortage of generation and transmission capacity. Implementation of distrusted generation systems would resolve such kind of problems.

The Adama I Wind Farm, with a capacity of generating 52 MW is the first ever renewable power generation project in the history of the country was officially inaugurated in December 2011. The 120 MW Ashegoda wind farm, 84-turbine farm 780 km north of Addis Ababa, is also inaugurated in 2013 as part of a plan to mitigate the impact of dry seasons on the country's dams.

1.2 Conventional Electric Power Generation

Lighting sources in Ethiopia can be divided between grid-connection, kerosene (and other traditional methods), modern off-grid technologies, and PV-battery based systems. Urban zones rely on an existing grid network, while in rural areas most lighting products are powered using kerosene fuel and conventional thermal generation. With 84 percent of Ethiopians living in rural areas, this represents more than 70 million people (15 million households) who do not have access to electricity. The UEAP is an umbrella program executed by EEPCo to provide grid-based electrification in rural towns and villages over a 10-year horizon. These rural towns and villages range in size from about 100 to 15,000 inhabitants.

The off-grid electrification program is progressing at a much slower pace than its grid-based counterpart. To date, there have been only a handful of decentralized projects serving to electrify a few thousand rural households. Presently, only 11,000 households are electrified with support from Rural Electrification Fund (REF), 10,000 of which are estimated to use Diesel generators, reflecting prior emphasis on thermal generation [11]. Currently, however, the emphasis is on renewable energy, particularly solar photovoltaic (PV) and micro hydropower. Yet it is been noted that the resources available for the off-grid rural electrification component are far less numerous than those available for the grid-based program. The study also estimated that even with tremendous investments to rapidly scale up grid connection in Ethiopia, more than 12 million families will still be living without electricity by 2025. For basic energy services like lighting, these families will continue to rely on carbon dioxide (CO_2) emitting, hazardous, and unhealthy traditional lighting sources such as kerosene, fuel wood, and candles. The latest census data (2004 E.C) indicated that about 80 percent of households in rural towns and villages rely on kerosene for lighting, compared to 23 percent of urban dwellers. Moreover, 18 percent of rural families use firewood as their primary source for lighting.

1.3 Recent Progress in Alternative/Renewable Energy Technologies in Ethiopia

Most traditional energy sources in Ethiopia are used for cooking and lighting, and thus energy consumption is dominated by the domestic sector, which represents 89 per cent of energy consumed, mostly rural homes.

Ethiopia has significant renewable energy resources. The vast majority of Ethiopia's existing capacity (85 per cent) is hydroelectric. Most of Ethiopia's electricity is generated from hydroelectric dams. To provide sufficient electricity to its people, the government of Ethiopia is currently constructing several hydropower plants, wind farms and also urban scaled solar powers. The government has also attached prime attention to the development of renewable energy sources in addition to the construction of hydroelectric power projects. It is developing water, geothermal, solar and wind renewable sources, which indeed are environmental friendly.

TABLE 1.1 The energy resource potential of Ethiopia

Resource	***Unit***	***Exploitable Reserve***	***Exploited***	
			Amount	***Percentag***
Hydropower	*MW*	*45,000*	*~2100*	*5%*
Solar/day	*kWh/m2*	*4 –6*	*<1%*	

Wind: Power Speed	*GW, m/s*	*1350, > 7*	*171MW Under construction*	*<1%*
Geothermal	*MW*	*7000*	*7.3 MW*	*<1%*
Wood	*Million tons*	*1120*	*560*	*50%*
Agricultural waste	*Million tons*	*15-20*	*~6*	*30%*
Natural gas	*Billion m3*	*113*	*-*	*0%*
Coal	*Million tons*	*>300*	*-*	*0%*
Oil Shale	*Million tons*	*253*	*-*	*0%*

Source: Ministry of Water and Energy June 22, 2013 Ethiopia's Renewable Energy Power Potential and Development Opportunities.

1.4 Objective of the Thesis

The objective of this work is to model, simulate and perform the optimization and economic evaluation of a hybrid system for the study area. The hybrid system comprises Wind/ Photovoltaic/ Fuel Cell Hybrid microgrid Distributed Generation system, which play a crucial role in building a scalable power grid that facilitates the use of renewable energy technologies. This effort may result in the distributed autonomous power grid that could integrate renewable energy technologies and minimize reliance on external energy resources.

Specific Objectives

- Development of Wind and Photovoltaic Hybrid Distributed Generation Systems device models;
- Formulating a mathematical model as well as a simulation for a typical connected to a distribution power network using MATLAB simulation tool;
- To propose a control design methodology for the Photovoltaic system.
- Select a photovoltaic module and wind turbine suitable to generate electricity.
- To perform optimization to determine the amount and type of PV modules, fuel cells and wind turbines needed to satisfy a predetermined demand at minimum cost using the wind and solar resource available for the selected study area.
- Perform an economic analysis to compute the Cost of Energy (COE) and net present value of the renewable energy systems proposed and compare different options.
- To create reliable power supply for “Berehet Woreda” and to get electricity access from potential renewable energy resource through their own alternative supply.

1.5 Problem Statement

At present, there is a need to design a distributed and autonomous subset of a larger grid or a microgrid to increase the security and reliability of electric power supply. The existing electricity network is facing frequent blackouts. Because of this there is a need by customers for better distribution reliability. Autonomous capability of distributed

energy generation systems enable better reliability by reducing effects of faults by isolating itself from the national grid and working independently. As part of the development of green world, distributed generation systems with renewable energy sources contribute to the future clean environment.

There are also a lot of rural areas in the country which are not electrified yet and need the electric supply in order to make their living simpler. Berehet, which is one of the Wordas not electrified yet, is selected as the case study area.

1.6 Scope

The main components of the distributed generation system consist of wind turbines, PV arrays, fuel cells and Electrolyzers. Dynamic models for the main system components, namely, wind energy conversion system and PV energy conversion system are developed. The optimization of the hybrid system and also the economic evaluation is done for the study area using HOMER simulation modeling tool software.

The pitch angle controls for wind energy conversion system, the maximum power point tracking (MPPT) control for PV energy conversion system are addressed in the thesis. Based on the dynamic component models, a simulation model for the proposed hybrid energy system is developed using MATLAB/Simulink.

1.7 Methodology

Different methodologies have been applied to address each objective of this study. Each methodology was selected to suit the different phases used to undertake this thesis.

The problem identification involved a literature survey in collecting general information about “Berehet Woreda” such as geography, climate, population, current electricity status of the Woreda

The potential solar resource, wind power resource for this Woreda were assessed. The wind speed, solar insolation and clearness index for a yearlong period were obtained from the NASA Surface Meteorology and Solar Energy database (SMSE). Wind and solar potential of the study area from NASA is compared with the solar radiation and wind data map of Ethiopia (SWERA).

For modeling and simulation of the hybrid system, MATLAB Simulink graphical block diagramming tool and a customizable set of block libraries is used. It offers tight integration with the rest of the MATLAB environment and can either drive MATLAB or be scripted from it. Simulink is widely used in control theory and digital signal processing for multidomain simulation and Model-Based Design.

For the optimization and economic analysis, the input data are wind speed, solar radiation, clearness index, wind turbines' cost, converter cost, PV panel cost, fuel cell cost, electrolyzer cost, hydrogen tank cost, wind power curve, efficiency of solar panel, nominal operating cell temperature, primary and deferrable load.

In order to simulate and sense the behavior of chosen power sources, all sources will be simulated in conjunction with each other. This will be done using the simulation tool HOMER, provided by NREL, National Renewable Energy Laboratory. A simulation tool can never reflect the true results of a project. It is, however, a useful tool when comparing different system arrangements in terms of economic and technical feasibility. A presentation of the HOMER simulation tool will be provided in connection to the simulation. The result of the simulations will then form a basis where conclusions and proposals can be drawn concerning system performance and reliability.

CHAPTER 2

Hybrid Energy Systems

Caisheng Wang (2006): In this paper the modeling and control of a hybrid wind/PV/FC DG system is discussed. Different small scale energy sources in the system are coupled to an AC bus. Dynamic models for the main system components, wind energy conversion system (WECS), PV energy conversion system (PVECS), fuel cell, electrolyzer, power electronic interfacing circuits, battery, hydrogen storage tank, gas compressor and gas pressure regulator, are developed. Based on the dynamic component models, a simulation model for the proposed hybrid energy system has been developed using MATLAB/Simulink. The overall power management strategy for coordinating the power flows among the different energy sources is presented in the dissertation. Simulation studies have been carried out to verify the system performance under different scenarios using a practical load profile and real weather data. The results show that the overall power management strategy is effective and the power flows among the different energy sources and the load demand is balanced successfully. The DG's impacts on the existing power system are also investigated in this dissertation. Analytical methods for finding optimal sites to deploy DG sources in power systems are presented and verified with simulation studies [5].

Mohamed A. H. El-Sayed et al. (2010): A hybrid wind/fuel cell renewable energy utilization scheme for electrical energy generation from renewable resources is digitally simulated and presented in this paper. The proposed hybrid renewable green energy scheme has four key subsystems or components to supply the required DC and AC electric loads. The first subsystem includes the renewable generation sources from wind turbine and fuel cell. The second is the interface converters used to connect the renewable energy generators to the common DC collection bus, where the generated energy is collected. The third device represents the added inverter between the common collection DC bus and the added AC bus interface to feed all AC loads before integration with the public grid. The fourth subsystem comprises all controllers including the modulated power filter. The controller main function is to ensure efficient energy utilization and dynamic matching between loads and green energy generation as well as voltage stabilization. The proposed controllers are coordinated dynamic error driven PI regulators to control the interfaced converters. The integrated hybrid green energy system with key subsystems are digitally simulated using the MATLAB/Simulink/Sim-Power software environment and fully validated for efficient energy utilizations and enhanced interface power quality under different operating conditions and load excursions [35].

Deepak Kumar Lal et al (2011): This paper proposed a hybrid power generation system suitable for remote area application. The concept of hybridizing renewable energy sources is that the base load is to be covered by largest and firmly available renewable source(s) and other intermittent source(s) should augment the base load to cover the peak load of an isolated mini electric grid system. The study is based on modeling, simulation and optimization of renewable energy system in rural area in Sundargarh district of Orissa state, India. The model has designed to provide an optimal system configuration based on hour-by-hour data for energy availability and demands. Various renewable/alternative energy sources, energy storage and their applicability in terms of cost and performance are discussed. The Homer software is used to study and design the proposed hybrid alternative energy power system model. The sensitivity analysis was carried out using Homer program. Based on simulation results, it has been found that renewable/alternative energy sources will replace the conventional energy sources and would be a feasible solution for distribution of electric power for standalone applications at remote and distant locations [36].

GM Shafiullah et al. (2010): Current power systems create environmental impacts due to utilization of fossil fuels, especially coal, as carbon dioxide is emitted into the atmosphere. In contrast to fossil fuels, renewable energy offers alternative sources of energy which are in general pollution free, technologically effective and environmentally sustainable. There is an increased interest in renewable energy, particularly solar and wind energy, which provides electricity without giving rise to carbon dioxide emissions. The paper presents economic analysis of a renewable hybrid system for a subtropical climate and also investigated the impact of renewable energy sources to the existing and future smart power system. Initially total net present cost (NPC), cost of energy (COE) and the renewable fraction (RF) have been measured as performances metrics to compare the performances of different systems. For better optimization, the model has been refined with sensitivity analysis which explores performance variations due to wind speed, solar irradiation and Diesel fuel prices [37].

PrabodhBajpai et al.(2010): In this paper decentralized distributed generation technologies based on renewable energy recourses such as Solar Photovoltaic (SPV)/ Wind Turbine Generators (WTG) address the major issues concerned with conventional Diesel generators to a large extent and are therefore considered as emerging alternate power solutions to stand alone applications. Three standalone WTG power systems using different energy storage technologies, i.e. WTG-Battery system, WTG-Fuel Cell (FC) system and WTG-FC-Battery system are optimized and compared in the paper. The analysis of such hybrid systems feeding a standalone load of 45.6 kWh/day energy consumption with a 2.3 kW peak power demand is carried out using Hybrid Optimization Model for Electrical Renewable (HOMER) software [38].

2.1 Working Principles of Photovoltaic, Wind Turbine and Fuel Cell

2.1.1 General working principles of Photovoltaic Cells

Solar energy is radiant energy from the sun. It is vital because it provides the world directly or indirectly with almost all of its energy. In addition to providing the energy that sustains the world, solar energy is stored in fossil fuels and biomass, and is responsible for powering the water cycle and producing wind.

Photovoltaic is the direct conversion of light into electricity at the atomic level. Some materials exhibit a property known as the photoelectric effect that causes them to absorb photons of light and release electrons.

Semiconductors can and cannot allow electric current to pass through them. These materials have a resistivity value that ranges between that of insulators and conductors. Silicon is the solar-industry's most common semiconductor material, however, in its pure crystalline form, silicon is a poor conductor. In order to make the silicon material usable for an electronic or solar application, the pure form must first be "doped" by having a small amount of boron or phosphorous added into the crystalline structure. By adding boron to the crystalline structure of silicon, an electron "hole" is left unfilled, as boron only has 3 valence electrons. This loss of an electron results in a slight positive charge to the material (p+ doped). Likewise, if phosphorous is added, (which has an extra valence electron), a slight negative charge is added to the material (n- doped).

A PV cell consists primarily of two layers of semi conductive material, which create something called a p-n junction. A p-n junction is just a fancy means of saying that one layer of negatively-doped material is connected physically to another layer of positively-doped material. The two layers are connected together by a flat surface, allowing as much surface area contact as possible to sunlight.

The photoelectric effect was first noted by a French physicist, Edmund Bequerel, in 1839, who found that semiconductors would produce small amounts of electric current when exposed to light. In 1905, Albert Einstein described the nature of light and the photoelectric effect on which photovoltaic technology is based, for which he later won a Nobel Prize in physics. The first photovoltaic module was built by Bell Laboratories in 1954. In the 1960s, the space industry began to make the first serious use of the technology to provide power aboard spacecraft. Through the space programs, the technology advanced, its reliability was established, and the cost began to decline. During the energy crisis in the 1970s, photovoltaic technology gained recognition as a source of power for non-space applications.

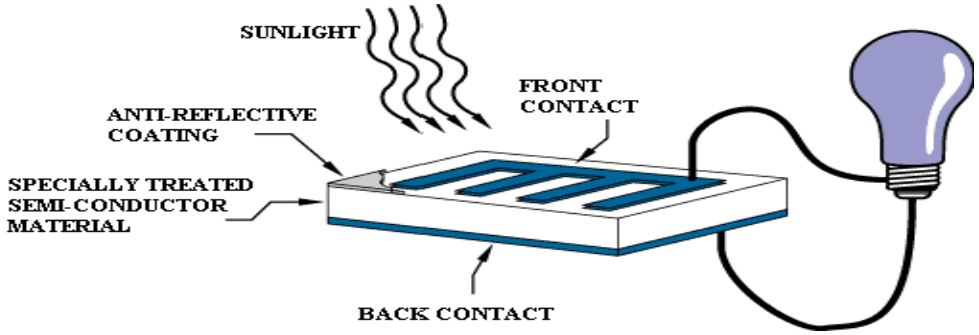

Figure 2.1 A photovoltaic cell changes light into electricity.

Figure 2.1 illustrates the operation of a basic photovoltaic cell, also called a solar cell. Solar cells are made of the same kinds of semiconductor materials, such as silicon, used in the microelectronics industry. For solar cells, a thin semiconductor wafer is specially treated to form an electric field, positive on one side and negative on the other. When light energy strikes the solar cell, electrons are knocked loose from the atoms in the semiconductor material. If electrical conductors are attached to the positive and negative sides, forming an electrical circuit, the electrons can be captured in the form of an electric current that is, electricity. This electricity can then be used to power a load, such as a light or a tool.

A number of solar cells electrically connected to each other and mounted in a support structure or frame is called a photovoltaic module. Modules are designed to supply electricity at a certain voltage, such as a common 12 volts system. The current produced is directly dependent on how much light strikes the module.

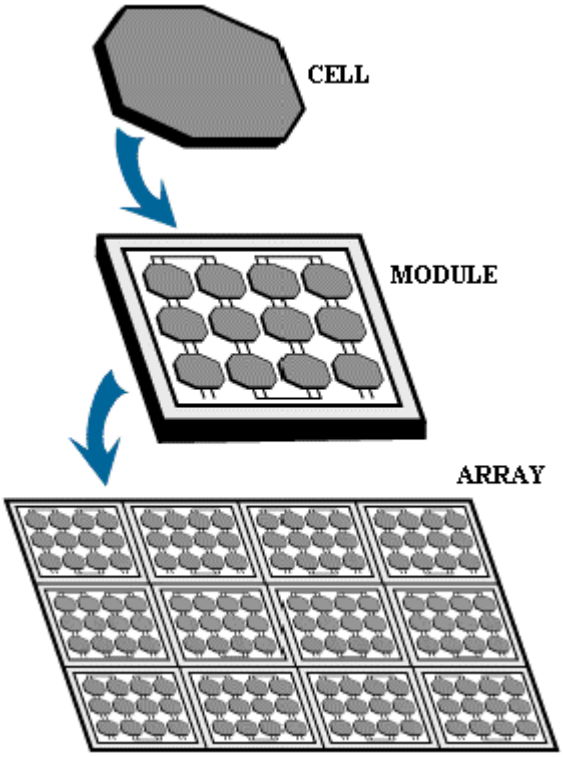

Figure 2.2 Photovoltaic cell, module and array

Multiple modules can be wired together to form an array. In general, the larger the area of a module or array, the more electricity that will be produced. Photovoltaic modules and arrays produce direct-current (DC) electricity. They can be connected in both series and parallel electrical arrangements to produce any required voltage and current combination.

A module is an assembly of individual cells, connected in series and parallel arrangements designed to yield optimum performance.

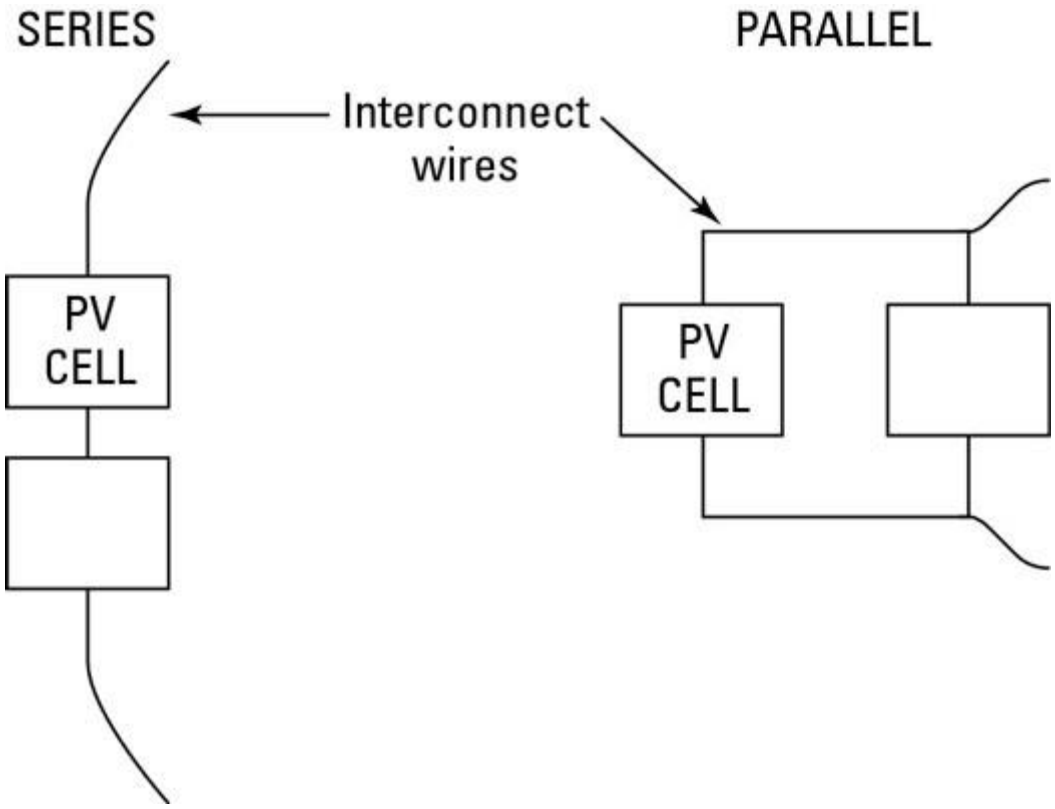

Figure 2.3 Interconnection of PV cells.

A typical PV cell produces around half a volt of electrical output. When 36 PV cells are connected in series, the result is an 18-volt module. A module or panel is a number of individual cells interconnected and housed into a finished product. A typical PV module in a residential application measures around 0.762m by 1.524m, in either bluish or black.

It is possible to achieve a wide range of voltage and current outputs, depending on how the individual cells are connected together. The amount of power a module can produce is a function of the total surface area, as well as the amount of sunlight that strikes the module.

Typical modules are available in a variety of sizes and configurations. Small modules (the kind used in hand-held calculators) output less than a single watt of power, while a typical residential module produces around 200W of power, more or less.

Modules are characterized by:

- Cell material, or the type of silicon process that is used
- Glazing material
- Frame and electrical connections

The short-circuit current and the open-circuit voltage are the maximum current and voltage respectively from a solar cell. However, at both of these operating points, the power from the solar cell is zero. The "fill factor", more commonly known by its abbreviation "FF", is a parameter which, in conjunction with V_{oc} and I_{sc}, determines the maximum power from a solar cell. The FF is defined as the ratio of the maximum power from the solar cell to the product of V_{oc} and I_{sc}. Graphically, the FF is a measure of the "Squareness" of the solar cell and is also the area of the largest rectangle which will fit in the IV curve. The FF is illustrated Figure 2.4.

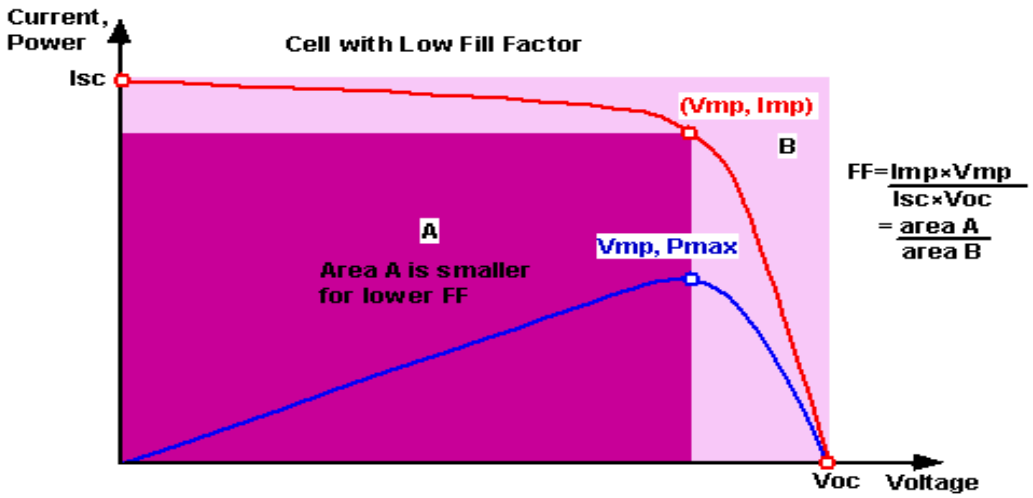

Figure 2.4 Solar cell fill factor

As FF is a measure of the "squareness" of the IV curve, a solar cell with a higher voltage has a larger possible FF since the "rounded" portion of the IV curve takes up less area. The maximum theoretical FF from a solar cell can be determined by differentiating the power from a solar cell with respect to voltage and finding where this is equal to zero.

2.1.2 Solar Module Power Characteristics and Operating Issue

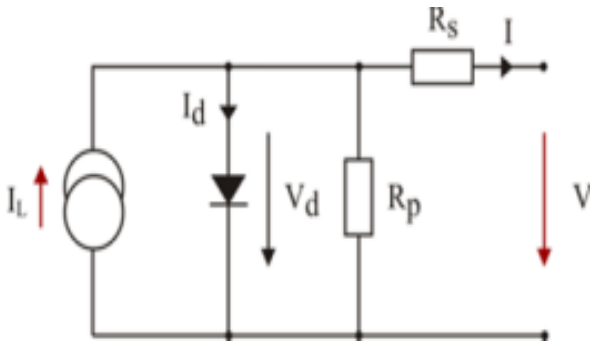

Figure 2.5 Real solar cell model

Some important factors responsible for the performance and efficiency of a solar cell are given below:

Characteristic resistance: The characteristic resistance of a solar cell is the output resistance of the solar cell at its maximum power point. If the resistance of the load is equal to the characteristic resistance of the solar cell, then the maximum power is transferred to the load and the solar cell operates at its maximum power point.

Parasitic Resistances: Resistive effects in solar cells reduce the efficiency of the solar cell by dissipating power in the resistances. The most common parasitic resistances are series resistance and shunt resistance. In most cases and for typical values of shunt and series resistance, the key impact of parasitic resistance is to reduce the fill factor. Both the magnitude and impact of series and shunt resistance depend on the geometry of the solar cell, at the operating point of the solar cell. Impact of both resistances on the solar cell could seriously reduce the fill factor. For an ideal solar cell, series resistance equals to 0 ohms while shunt resistances equals to infinity.

Temperature: Solar cells are sensitive to temperature. Increases in temperature reduce the band gap of a semiconductor, thereby effecting most of the semiconductor material parameters. In a solar cell, the parameter most affected by an increase in temperature is the open-circuit voltage. As the temperature increases, the open-circuit voltage decreases, thereby decreasing the fill factor and finally decreasing the efficiency of a solar cell. It is recommended to operate at 25 degree Celsius. The power output for different operating temperatures is shown in Figure 2.6 [43].

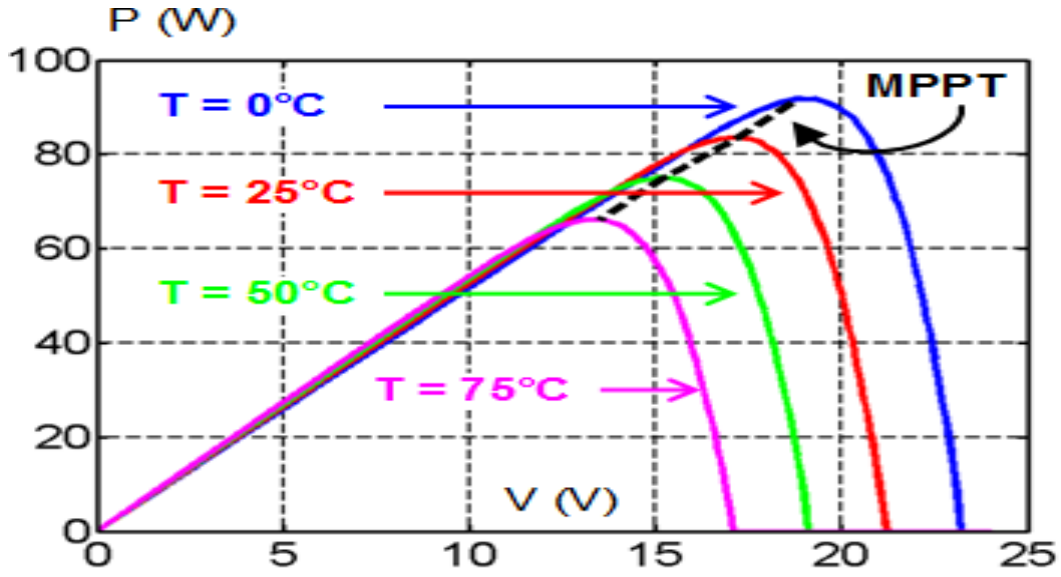

Figure 2.6 Solar cell power characteristics temperature dependency [48]

Light intensity: Changing the light intensity incident on a solar cell changes all solar cell parameters, including the short-circuit current, the open-circuit voltage, the fill factor, the efficiency and the impact of series and shunt resistances. The light intensity on a solar cell is called the number of suns, where 1 sun corresponds to standard illumination at AM1.5, or 1 kW/m2. Solar cells experience daily variations in light intensity, with the incident power from the sun varying between 0 and 1 kW/m^2. At low light levels, the effect of the shunt resistance becomes increasingly important. Consequently, under cloudy conditions, a solar cell with a high shunt resistance retains a greater fraction of its original power than a solar cell with a low shunt resistance.

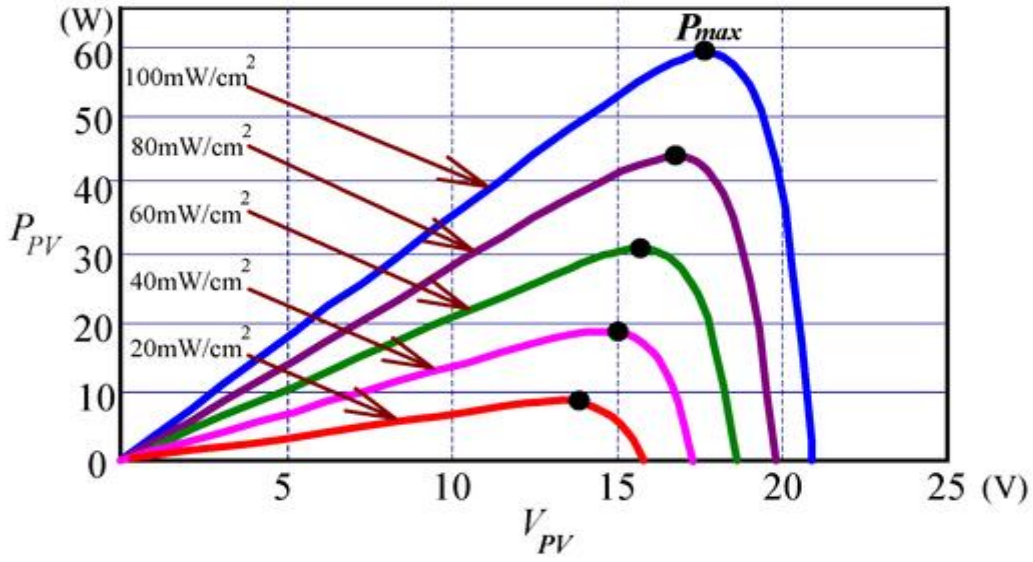

Figure 2.7 Solar cell power characteristics for different irradiation values [47]

Ideality factors: The ideality factor of a diode is a measure of how close the diode follows the ideal diode equation. The derivation of the simple diode equation uses certain assumptions about the cell. In practice, there are second-order effects so that the diode does not follow the simple diode equation and the ideality factor provides a way of describing them.

2.1.3 Wind Power System

Winds are produced by uneven solar heating of the earth's land and sea surfaces. Thus, they are a form of "solar" energy. On the average, the ratio of total wind power to incident solar power is on the order of two percent, reflecting a balance between input and dissipation by turbulence and drag on the surface.

Wind is the movement of air caused by the irregular heating of the Earth's surface. It happens at all scales, from local breezes created by heating of land surfaces that lasts some minutes, to global winds caused from solar heating of the Earth. Wind power is the transformation of wind energy into more utile forms, typically electricity using wind turbines.

Wind is a source of free energy which has been used since ancient times in windmills for pumping water or grinding flour. The technology of high power, geared transmissions was developed centuries ago by windmill designers and the fantail wheel for keeping the main sales pointing into the wind was one of the world's first examples of an automatic control system.

Though modern technology has made dramatic improvements to the efficiency of windmills, they are still dependent on the vagaries of the weather. Not just on the wind direction but on the intermittent and unpredictable force of the wind. Too little wind can't deliver sufficient sustained power to overcome frictional losses in the system. Too much and they are susceptible to damage. Between these extremes, cost efficient installations have been developed to extract energy from the wind.

Theoretical Power

The power **P** available in the wind impinging on a wind driven generator is given by:

$$\boldsymbol{P = \frac{CA\rho V^3}{2}} \qquad \textbf{(2.1)}$$

where $\boldsymbol{C}$ is an efficiency factor known as the Power Coefficient which depends on the machine design, **A** is the area of the wind front intercepted by the rotor blades (the swept

area), **ρ** is the density of the air (averaging 1.225 kg/m^3 at sea level) and **v** is the wind velocity.

Note that the power is proportional to area swept by the blades, the density of the air and to the cube of the wind speed. Thus doubling the blade length will produce four times the power and doubling the wind speed will produce eight times the power. Note also that the effective swept area of the blades is an annular ring, not a circle, because of the dead space around the hub of the blades.

2.1.4 Practical Power and Conversion Efficiency

German aerodynamicist Albert Betz showed that a maximum of only 59.3% of the theoretical power can be extracted from wind, no matter how good the wind turbine is, otherwise the wind would stop when it hits the blades. He demonstrated mathematically that the optimum occurs when the rotor reduces the wind speed by one third. After inefficiencies in the design and frictional losses are taken into account the practical power available from the wind will rarely exceed 40% of the theoretical power [41].

Note that the power output from commercially available wind turbines is usually specified at a steady, gust free, wind speed of 12.5 m/s. In the many locations, particularly urban installations, the prevailing wind will rarely reach this speed.

2.1.5 Yaw Control

Wind turbines can only extract the maximum power from the available wind when the plane of rotation of the blades is perpendicular to the direction of the wind. To ensure this the rotor mount must be free to rotate on its vertical axis and the installation must include some form of yaw control to turn the rotor into the wind.

For small, lightweight installations this is normally accomplished by adding a tail fin behind the rotor in line with its axis. Any lateral component of the wind will tend to push the side of the tail fin causing the rotor mount to turn until the fin is in line with the wind. When the rotor is facing into the wind there will be no lateral force on the fin and the rotor will remain in position. Friction and inertia will tend to hold it in position so that it does not follow small disturbances.

Large turbine installations have automatic control systems with wind sensors to monitor the direction of the wind and a powered mechanism to drive the rotor into its optimum position.

2.1.6 Pitch Angle Control

Pitch angle control is the most common means for adjusting the aerodynamic torque of the wind turbine when wind speed is above rated speed and various controlling variables may be chosen, such as wind speed, generator speed and generator power. Variable pitch control can be used to shed the aerodynamic power generated by the wind turbine. Thus, the aerodynamic power produced by the wind turbine can be controlled by adjusting the pitch angle of the wind turbine. Conventional pitch control usually use PI controller.

The acceleration and deceleration is the result of the difference between the input power to the generator and the aerodynamic power captured by the wind turbine. Theoretically, at constant electric load, the acceleration and deceleration can be made zero if the pitch can be controlled fast enough to react to the wind speed such that the power captured from the wind is equal to the electric power ($P_{captured} = P_{electric}$). In the high wind speed region when the rotor speed limit is reached, the pitch can be controlled to keep the rotor rpm from exceeding its limit.

2.1.7 Capacity Factor

Electrical generating equipment is usually specified at its rated capacity. This is normally the maximum power or energy output which can be generated in optimal conditions. Since a wind turbine rarely works at its optimal capacity the actual energy output over a year will be much less than its rated capacity. The capacity factor is simply the wind turbine generator actual energy output for a given period divided by the theoretical energy output if the machine had operated at its rated power output for the same period. Typical capacity factors for wind turbines range from 0.25 to 0.30, currently turbines with 0.37 capacity factor are observed. Thus a wind turbine rated at 1M will deliver on average only about 250kW of power.

2.1.8 Different Types of Turbines

A wind turbine is a machine that converts the kinetic energy from the wind into mechanical energy. If the mechanical energy is used directly by machinery, such as a pump or grinding stones, the machine is usually called a windmill. If the mechanical energy is then converted to electricity, the machine is called a wind generator.

There are a number of different wind turbine types available. The horizontal axis turbine, HAWT is by far the most common type of turbine. They come in two different types: the up wind, which faces the wind (tower behind rotor) and the downwind arrangement that works away from the wind (tower in front). Another kind of turbine is the vertical axis,

VAWT arrangement that uses drag and lift as the driving forces; the horizontal also uses drag and lift, but in other proportions.

The advantages with upwind turbines are that the tower does not act as an obstacle for the wind hitting the rotor. Despite this, the flow behind the passing blade is affected by the tower and causes a slight drop in power. When the blade passes the tower it also decreases the drag on the construction which can cause an on/off bending process causing fatigue stress. This has of course been taking into account when designing the turbine. The upwind design needs a control system that helps the nacelle turn straight to the wind. In downwind turbines, the tower shades a rotor blade each time it passes by and causes greater power losses compared to the upwind design. An advantage with downwind turbines is that the nacelle is self-adjusting and is not in need of a control system. One drawback with this is the problem with untwisting the cable inside when the nacelle has turned same direction repeatedly. The VAWT are not as commercial and economically competitive as the HAWT. Some of the VAWT types suffer from low efficiency due to design difficulties as well as the problem with operation close to the ground. Parts of the vertical turbines will therefore receive low quality winds causing power losses. To keep the construction upright it also needs to be supported with guy cables attached to the ground. The vertical turbine is not in need of yaw control, which of course is an advantage and the wind always hits the turbine tangentially.

The modern wind turbine is a sophisticated piece of machinery with aerodynamically designed rotor and efficient power generation, transmission and regulation components. The size of these turbines ranges from a few Watts (Small Wind Turbines) to several Million Watts (Large Wind Turbines). The modern trend in the wind industry is to go for bigger units of several MW capacities in places where the wind is favorable, as the system scaling up can reduce the unit cost of wind-generated electricity. Most of today's commercial machines are horizontal axis wind turbines (HAWT) with three bladed rotors.

A typical system employs a fixed speed rotor with three variable pitch blades which are controlled automatically to maintain a fixed rotation speed for any wind speed. The rotor drives a synchronous generator through a gear box and the whole assembly is housed in a nacelle on top of a substantial tower with massive foundations requiring hundreds of cubic meters of reinforced concrete.

Large rotor blades are necessary to intercept the maximum air stream but these give rise to very high tip speeds. The tip speeds however must be limited, mainly because of unacceptable noise levels, resulting in very low rotation speeds which may be as low as 10 to 20 rpm for large wind turbines. The operating speed of the generator is however is much higher, typically 1200 rpm, determined by the number of its magnetic pole pairs

and the frequency of the grid electrical supply. Consequently a gearbox must be used to increase the shaft speed to drive the generator at its synchronous speed.

2.1.9 Wind Farms

A wind farm or wind park is a group of wind turbines in the same location used to produce energy. A large wind farm may consist of several hundred individual wind turbines and cover an extended area of hundreds of square miles, but the land between the turbines may be used for agricultural or other purposes. A wind farm can also be located offshore.

Many of the largest operational onshore wind farms are located in the United States and China. For example, the Gansu Wind Farm in China has a capacity of over 5,000 MW of power with a goal of 20,000 MW by 2020. The Alta Wind Energy Center in California, United States is the largest onshore wind farm outside of China, with a capacity of 1,020 MW [14].

2.1.10 Hybrid PV-Wind Energy Systems

Renewable energy resources like solar and wind offer clean and economically competitive alternatives to conventional power generation where high wind speed and high solar radiation are available. For meeting the energy demand, PV-wind hybrid power generating systems can be beneficial in enhancing the economic and environmental sustainability of renewable energy systems.

Solar and wind energy which change randomly are individually less reliable. However, in many regions, when solar and wind resources are combined for power generation, they complement each other by means of daily and seasonal variations. Combining these two renewable energy sources could make the system more reliable, and the system costs might slightly decrease depending on the regional conditions.

Photovoltaic-wind hybrid power systems are complex in sizing and optimization process, where renewable energy resources and storage components must be sized to match the given load profile and the estimated ease of use of solar radiation and wind speed.

2012-01-17–China's first integrated wind-solar power demonstration project has been completed and put into operation on December 25 in Zhangbei of north China's Hebei province with installed capacity of 100 Megawatt (MW) wind power, 40-MW solar PV power and a storage capacity of 20 MW [31].

Several economic viability and technical availability studies are carried out to assess choice of PV-wind hybrid power systems configurations that serve power to the load with

the certain reliability criteria [19–20]. The number of PV panels, wind turbines, battery cells, load profiles and available renewable resources play significant role in sizing of PV-wind hybrid power system. Researchers and scientists mostly use deterministic and probabilistic methods to size and simulate the PV-wind hybrid power system. In deterministic method, time-series data such as wind speed, solar radiation, ambient temperature, load profile, and site geographic position like latitude, longitude, and altitude are assumed to be known. Resource data like wind speed, solar radiation, ambient temperature, and load profile are needed, at least hourly basis for whole year [21–23]. Also on the chronological order of the resource data is really important. Frequency of time-series resource data is defined according to the chosen simulation step time period. In probabilistic method, resource data and load profile are assumed as random variables, and these variables may not be in the chronological order. Probabilistic method tries to develop appropriate stochastic model for power generation and power consumption and then combines these two models to determine a hybrid system risk model. A group of researchers reported two sizing methods for autonomous PV-wind hybrid power systems. The first one assesses hybrid system performance using energy to load ratio which is based on the yearly average of monthly hybrid system energy outputs [24, 25]. The second one realizes battery to load ratio using the worst monthly scenario [25–27]. The other probabilistic method is proposed by Yang et al. [28]. The authors proposed to use a typical meteorological year (TMY) to find out a precise assessment of energy output of a PV-wind hybrid power system. Tina and Gagliano [29] sized a PV-wind hybrid power system with probabilistic method that is based on convolution technique by probability density function. Deterministic and probabilistic sizing and simulation methods have their own advantages and disadvantages. Sizing procedure utilizing deterministic approach has severe computational efforts and it gives suboptimum solutions depending on the type of the used resource data, whereas stochastic procedures are simple and also they may use daily or monthly average resource data instead of time-series resource data.

In this paper, the hybrid system model sizing is done using stochastic procedures since the resource data available are monthly resources.

2.1.11 Fuel Cells and Electrolyzes

The electrolysis of water is considered a well-known principle to produce oxygen and hydrogen gas. In figure 2.8 a schematic of an electrochemical cell is presented. The core of an electrolysis unit is an electrochemical cell, which is filled with pure water and has two electrodes connected with an external power supply. At a certain voltage, which is called critical voltage, between both electrodes, the electrodes start to produce hydrogen gas at the negatively biased electrode and oxygen gas at the positively biased electrode. The amount of gases produced per unit time is directly related to the current that passes

through the electrochemical cell. In water, there is always a certain percentage found as ionic species; H^+ and OH^- represented by the equilibrium equation:

$$H_2O \rightarrow H^+ + OH^-$$

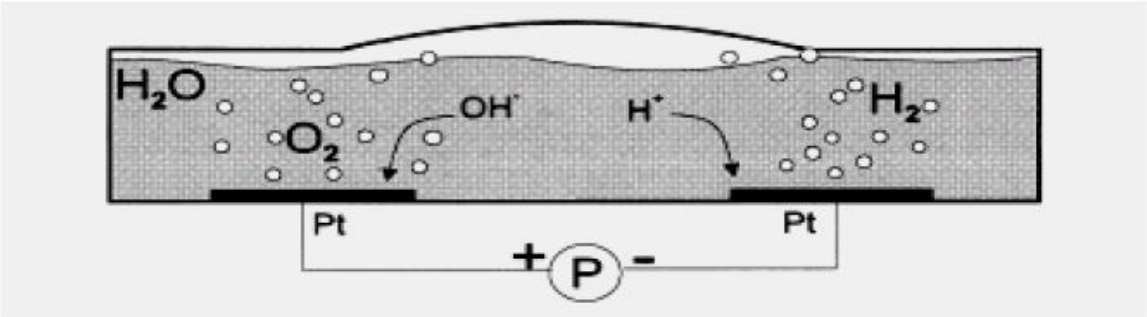

Figure 2.8 Sketch of an electrochemical cell

The electrolysis of one mole of water produces a mole of hydrogen gas and a half-mole of oxygen gas in their normal diatomic forms. A detailed analysis of the process makes use of the thermodynamic potentials and the first law of thermodynamics [30].

2.1.12 Fuel Cells

A fuel cell is a device that generates electricity by a chemical reaction. Every fuel cell has two electrodes, one positive and one negative, called, respectively, the anode and cathode. The reactions that produce electricity take place at the electrodes.

Every fuel cell also has an electrolyte, which carries electrically charged particles from one electrode to the other, and a catalyst, which speeds the reactions at the electrodes.

Hydrogen is the basic fuel, but fuel cells also require oxygen. One great appeal of fuel cells is that they generate electricity with very little pollution, much of the hydrogen and oxygen used in generating electricity ultimately combine to form a harmless byproduct, namely water.

There are several kinds of fuel cells and each operates a bit differently. But in general terms, hydrogen atoms enter a fuel cell at the anode where a chemical reaction strips them of their electrons. The hydrogen atoms are now "ionized," and carry a positive electrical charge. The negatively charged electrons provide the current through wires to do work. If alternating current (AC) is needed, the DC output of the fuel cell must be routed through a conversion device called an inverter.

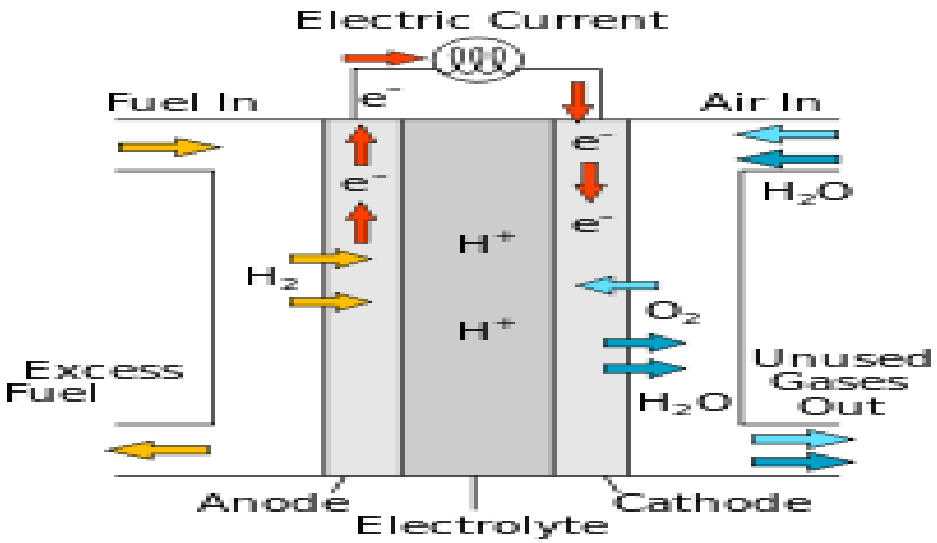

Figure 2.9 Fuel Cell [45]

There are many types of fuel cells, but they all consist of an anode, a cathode and an electrolyte that allows charges to move between the two sides of the fuel cell. As like illustrated in Figure 2.9, electrons are drawn from the anode to the cathode through an external circuit, producing direct current electricity. As the main difference among fuel cell types is the electrolyte, fuel cells are classified by the type of electrolyte they use followed by the difference in startup time ranging from 1 second for proton exchange membrane fuel cells (PEM fuel cells, or PEMFC) to 10 minutes for solid oxide fuel cells(SOFC)

The electrolyte plays a key role. It must permit only the appropriate ions to pass between the anode and cathode. If free electrons or other substances could travel through the electrolyte, they would disrupt the chemical reaction.

Whether they combine at anode or cathode, together hydrogen and oxygen form water, which drains from the cell. As long as a fuel cell is supplied with hydrogen and oxygen, it will generate electricity.

Even better, since fuel cells create electricity chemically, rather than by combustion, they are not subject to the thermodynamic laws that limit a conventional power plant. Therefore, fuel cells are more efficient in extracting energy from a fuel. Waste heat from some cells can also be harnessed, boosting system efficiency still further [39].

2.1.13 Energy and the EMF of the Hydrogen Fuel Cell

The change in energy is the reason for the production of electricity in fuel cells. In a fuel cell, it is the change in this Gibbs free energy of formation, ΔGf that gives the energy

released. This change is the difference between the Gibbs free energy of the products and the Gibbs free energy of the inputs or reactants.

$$\Delta G_f = \Delta G_f of\ Products - \Delta G_f of\ reacta \quad \textbf{(2.2)}$$

To make comparisons easier, it is nearly always most convenient to consider these quantities in their 'per mole' form. These are indicated by over the lower case letter, for example, (g_f) H_2O is the molar specific Gibbs free energy of formation for water

A mole of any substance always has the same number of entities (e.g. molecules) 6.022 $\times$ 10^{23} called Avogadro's number. This is represented by the letter N or Na. A 'mole of electrons' is 6.022 $\times$ 10^{23} electrons. The charge is N $\times$e, where e is 1.602 $\times$ 10^{-19} C (the charge on one electron). This quantity is called the Faraday's constant, and is designated by the letter F.

$$F = N \times e = 96{,}485C \quad \textbf{(2.3)}$$

Consider the basic reaction for the hydrogen/oxygen fuel cell:

$$2H_2 + O_2 \rightarrow 2H_2 \quad \textbf{(2.4)}$$

Which is equivalent to

$$H_2 + 1/2O_2 \rightarrow H_2 \quad \textbf{(2.5)}$$

The 'product' is one mole of H_2O and the 'reactants' are one mole of $H_2$and half a mole of O_2. Thus,

$$g_f = (g_f)_{\text{products}} - (g_f)_{\text{reactants}} \quad \textbf{(2.6)}$$

$$\Delta\overline{g_f} = (\bar{g}_f)_{H2O} - (\bar{g}_f)_{H2} - \frac{1}{2}(\bar{g}_f)_{O2} \quad \textbf{(2.7)}$$

This equation seems straightforward and simple enough. However, the Gibbs free energy of formation is not constant; it changes with temperature and state (liquid or gas).Table 2.1 shows $\Delta g_f$for the basic hydrogen fuel cell reaction [30].

Table 2.1 The Gibbs free energy of formation for the basic hydrogen fuel cell reaction

Form of Water Product	Temperatures[^{o}C]	Δg_f (kJ mol^{-1})
Liquid	25	-237.2
Liquid	80	-228.2

Gas	80	-226.1
Gas	100	-225.2
Gas	200	-220.4
Gas	400	-210.3
Gas	600	-199.6
Gas	800	-188.6
Gas	1000	-177.4

For the hydrogen fuel cell, two electrons pass round the external circuit for each water molecule produced and each molecule of hydrogen used. So, for one mole of hydrogen used, 2N electrons pass round the external circuit – where N is Avogadro's number. If −e is the charge on one electron, then the charge that flows is

$$-2\,Ne = -2F \text{ coulombs}$$

F being Faraday's constant or the charge on one mole of electrons. If E is the voltage of the fuel cell, then the electrical work done moving this charge round the circuit is

$$\text{Electrical work done} = \text{charge} \times \text{voltage} = -2FE \text{ joules}$$

If the system is reversible (or has no losses), then this electrical work done will be equal to the Gibbs free energy releasedΔg_f, so

$$\Delta g_f = (-2F \times E) \quad \textbf{(2.8)}$$

Thus

$$E = -\frac{\Delta g_f}{2F} \quad \textbf{(2.9)}$$

This fundamental equation gives the electromotive force (EMF) or reversible open circuit voltage of the hydrogen fuel cell.

For example, a hydrogen fuel cell operating at 200◦C has Δg_f= −225.2 kJ, then

$$E = -\frac{-(225{,}200)}{2(96485)} = 1.17V \quad \textbf{(2.10)}$$

2.1.14 Different types of fuel cells

Alkali fuel cells operate on compressed hydrogen and oxygen. They generally use a solution of potassium hydroxide (chemically, KOH) in water as their electrolyte. Efficiency is about 70 percent, and operating temperature is 150 to 200 ^{o}C, Cell output ranges from 300 W to 5 kW. Alkali cells were used in Apollo spacecraft to provide both electricity and drinking water. They require pure hydrogen fuel, however, and their platinum electrode catalysts are expensive. And like any container filled with liquid, they can leak.

Proton Exchange Membrane (PEM) fuel cells work with a polymer electrolyte in the form of a thin, permeable sheet. Efficiency is about 40 to 50 percent, and operating temperature is about 80 degrees C (about 175 degrees F). Cell outputs generally range from 50 to 250 kW. The solid, flexible electrolyte will not leak or crack, and these cells operate at a low enough temperature to make them suitable for homes and cars. But their fuels must be purified, and a platinum catalyst is used on both sides of the membrane, raising costs.

Solid Oxide fuel cells (SOFC) use a hard, ceramic compound of metal (like calcium or zirconium) oxides (chemically, O_2) as electrolyte. Efficiency is about 60 percent, and operating temperatures are about 1,000 ^{o}C. Cells output is up to 100 kW. At such high temperatures a reformer is not required to extract hydrogen from the fuel, and waste heat can be recycled to make additional electricity. However, the high temperature limits applications of SOFC units and they tend to be rather large. While solid electrolytes cannot leak, they can crack.

They differ in their operating characteristics, temperatures, power densities and therefore in their most suitable end uses. The table 2.2 summarizes some characteristics of these fuel cell types and their most suitable uses.

Table 2.2 Characteristics of these fuel cell types and their most suitable use

Fuel cell type	Operating temperature [°C]	Module size range [kW]	Suitable applications				
			Domestic Power	Small-scale power	Large-scale cogeneration	Transport	Battery replacement
AFC	60 – 90	<1 – 200	✓	✓	✗	✓	✗
PEMFC	80 – 100	<1 – 500	✓	✓	✗	✓	✓
PAFC	200	5 – 500	✗	✓	✗	NA	✗
MCFC	650	250 – 5000	✗	✓	✓	✗	✗
SOFC	800 – 1000	5 – 5000	✓	✓	✓	✗	NA

Present materials' science has made the fuel cells a reality in some specialized applications. By far the greatest research interest throughout the world has focused on Proton Exchange Membrane (PEM) and Solid Oxide (SO) cell stacks. PEMs are well advanced type of fuel cell that are suitable for cars and mass transportation. SOFC technology is the most demanding from a materials standpoint and is developed for its potential market competitiveness SOFCs are the most efficient (fuel input to electricity output) fuel cell electricity generators currently being developed world-wide [50].

SOFCs are becoming more familiar because:

- SOFC technology is most suited to applications in the distributed generation (i.e., stationary power) market because its high conversion efficiency provides the greatest benefit when fuel costs are higher, due to long fuel delivery systems to customer premises.
- SOFCs have a modular and solid state construction and do not present any moving parts, thereby are quiet enough to be installed indoors.
- The high operating temperature of SOFCs produces high quality heat byproduct which can be used for co-generation, or for use in combined cycle applications.
- SOFCs do not contain noble metals that could be problematic in resource availability and price issue in high volume manufacture.
- SOFCs do not have problems with electrolyte management (liquid electrolytes, for example, which are corrosive and difficult to handle).
- SOFCs have extremely low emissions by eliminating the danger of carbon monoxide in exhaust gases, as any CO produced is converted to CO_2 at the high operating temperature.
- SOFCs have a potential long life expectancy of more than 40000–80000 h.

CHAPTER 3

COMPONENT MODELING of the HYBRID SYSTEM

In this chapter, the models for the main components of the proposed hybrid alternative energy system are developed. They are wind energy conversion system and PV energy conversion system.

3.1 Modeling of the Solar Park

PV arrays are built up with combined series/parallel combinations of PV solar cells, which are usually represented by a simplified equivalent circuit model such as the one given in Figure 3.1 and/or by an equation as in (3.1).

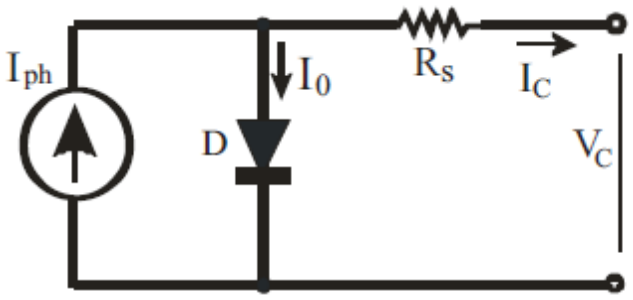

Figure 3.1 Simplified-equivalent circuit of photovoltaic cell.

The PV cell output voltage is a function of the photocurrent that mainly determined by load current depending on the solar irradiation level during the operation.

$$V_c = \frac{AKT_c}{e} \ln\left(\frac{I_{ph}+I_o-I_c}{I_o}\right) - R_s I_c \qquad \textbf{(3.1)}$$

The symbols are defined as follows:

The curve fitting factor A is used to adjust the I-V characteristics of the cell obtained from (3.1) to the actual characteristics obtained by testing.

K and T_c have the same temperature unit, either Kelvin or Celsius.

e: Eectron charge (1.602 × 10-19 C).

k: Boltzmann constant (1.38 × 10-23 J/K).

Ic: Cell output current, A.

I_{ph}: Photocurrent, function of irradiation level and junction temperature (5 A).

I_0: Reverse saturation current of diode (0.0002 A).

Rs: Series resistance of cell (0.001 Ω).

Tc: Reference cell operating temperature (20 °C).

Vc: Cell output voltage, V.

The shunt resistance is inversely related with shunt leakage current to the ground. In general the PV efficiency is insensitive to variation in shunt resistance if the PV is designed carefully making the shunt resistance infinity and the leakage current zero. Equation (3.1) gives the voltage of a single solar cell. Whereas, in order to calculate the whole array voltage it has to be multiplied by the number of solar cell connected in series. Since the array current is the sum of the currents flowing through the cells in parallel branches, the cell current I_C is obtained by dividing the array current by the number of the cells connected in parallel before being used in Equation (3.1), which is only valid for a certain cell operating temperature Tc with its corresponding solar irradiation level Sc. If the temperature and solar irradiation levels change, the voltage and current outputs of the PV array will follow this change. Hence, the effects of the changes in temperature and solar irradiation levels should also be included in the final PV array model. A method to include these effects in the PV array modeling is given by Buresch [40]. According to his method, for a known temperature and a known solar irradiation level, a model is obtained and then this model is modified to handle different cases of temperature and irradiation levels. Let Equation (3.1) be the benchmark model for the known operating temperature Tc and known solar irradiation level Sc as given in the specification. When the ambient temperature and irradiation levels change, the cell operating temperature also changes, resulting in a new output voltage and a new photocurrent value. The solar cell operating temperature varies as a function of solar irradiation level and ambient temperature. The variable ambient temperature Ta affects the cell output voltage and cell photocurrent. These effects are represented in the model by the temperature coefficients C_{TV} and C_{TI} for cell output voltage and cell photocurrent, respectively, as:

$$C_{TV} = 1 + \beta_T(T_a - T_X) \quad \textbf{(3.2)}$$

$$C_{TI} = 1 + \frac{\gamma_T}{S_C}(T_X - T_a) \quad \textbf{(3.3)}$$

where, β_T = 0.004 and γ_T = 0.06 for the cell used and Ta=20 ^oC is the ambient temperature during the cell testing. This is used to obtain the modified model of the cell

for another ambient temperature Tx. Even if the ambient temperature does not change significantly during the daytime, the solar irradiation level changes depending on the amount of sunlight and clouds. A change in solar irradiation level causes a change in the cell photocurrent and operating temperature, which in turn affects the cell output voltage. If the solar irradiation level increases from S_{x1} to S_{x2}, the cell operating temperature and the photocurrent will also increase from T_{x1} to T_{x2} and from I_{phl} to I_{ph2}, respectively. Thus the change in the operating temperature and in the photocurrent due to variation in the solar irradiation level can be expressed with two constants, C_{SV} and C_{SI}, which are the correction factors for changes in cell output voltage V_C and photocurrent Iph, respectively:

$$C_{SV} = 1 + \beta_T \alpha_S (S_X - S_C) \quad \textbf{(3.4)}$$

$$C_{SI} = 1 + \frac{1}{S_C}(S_X - S_C) \quad \textbf{(3.5)}$$

where S_C is the benchmark reference solar irradiation level during the cell testing to obtain the modified cell model. Sx is the new level of the solar irradiation. The temperature change, ΔTC, occurs due to the change in the solar irradiation level and is obtained using

$$\Delta T_C = \alpha_S (S_X - S_C) \quad \textbf{(3.6)}$$

The constant α_S represents the slope of the change in the cell operating temperature due to a change in the solar irradiation level and is equal to 0.2 for the solar cells used [40]. Using correction factors C_{TV}, C_{TI}, C_{SV} and C_{SI}, the new values of the cell output voltage V_{CX} and photocurrent I_{phx} are obtained for the new temperature T_x and solar irradiation S_x as follows:

$$V_{CX} = C_{TV} C_{SV} V_C \quad \textbf{(3.7)}$$

$$I_{phx} = C_{TI} C_{SI} I_{Ph} \quad \textbf{(3.8)}$$

V_C and I_{ph} are the benchmark reference cell output voltage and reference cell photocurrent, respectively.

3.2 Photovoltaic Array Modeling

A general block diagram of the photovoltaic array (PVA) model for GUI environment of Simulink is given in Figure 5.2. The block called PVA model for GUI is the last stage of the model. This block contains the sub models that are connected to build the final model, the sub models are shown in Appendix-4. The PVA can be configured to any number of cells all connected in series to have a desired voltage output. Depending on the load power required, the number of parallel branches can be increased to required level. The effects of the temperature and solar irradiation levels are represented by two variables gains. They can be changed by dragging the slider gain adjustments of these blocks named as variable temperature and variable solar irradiation.

The PVA functional model for the Simulink environment is shown in Figure 3.2. The developments of other parts of the operational block diagram are shown in the appendix part. However, just to describe the main diagram, as it can readily be seen, the system is modeled to supply power to ac loads.

The effects of the changing temperature and solar irradiation level are modeled inside the block called Effect of Temperature & Solar Irradiation (Appendix-3.2). This block represents the equations given from (3.2) to (3.8) with the modification of Equations (3.7) and (3.8) as follows

$$V_{CX} = C_V V_C \quad \textbf{(3.9)}$$

$$I_{CPhx} = C_I V_{ph} \quad \textbf{(3.10)}$$

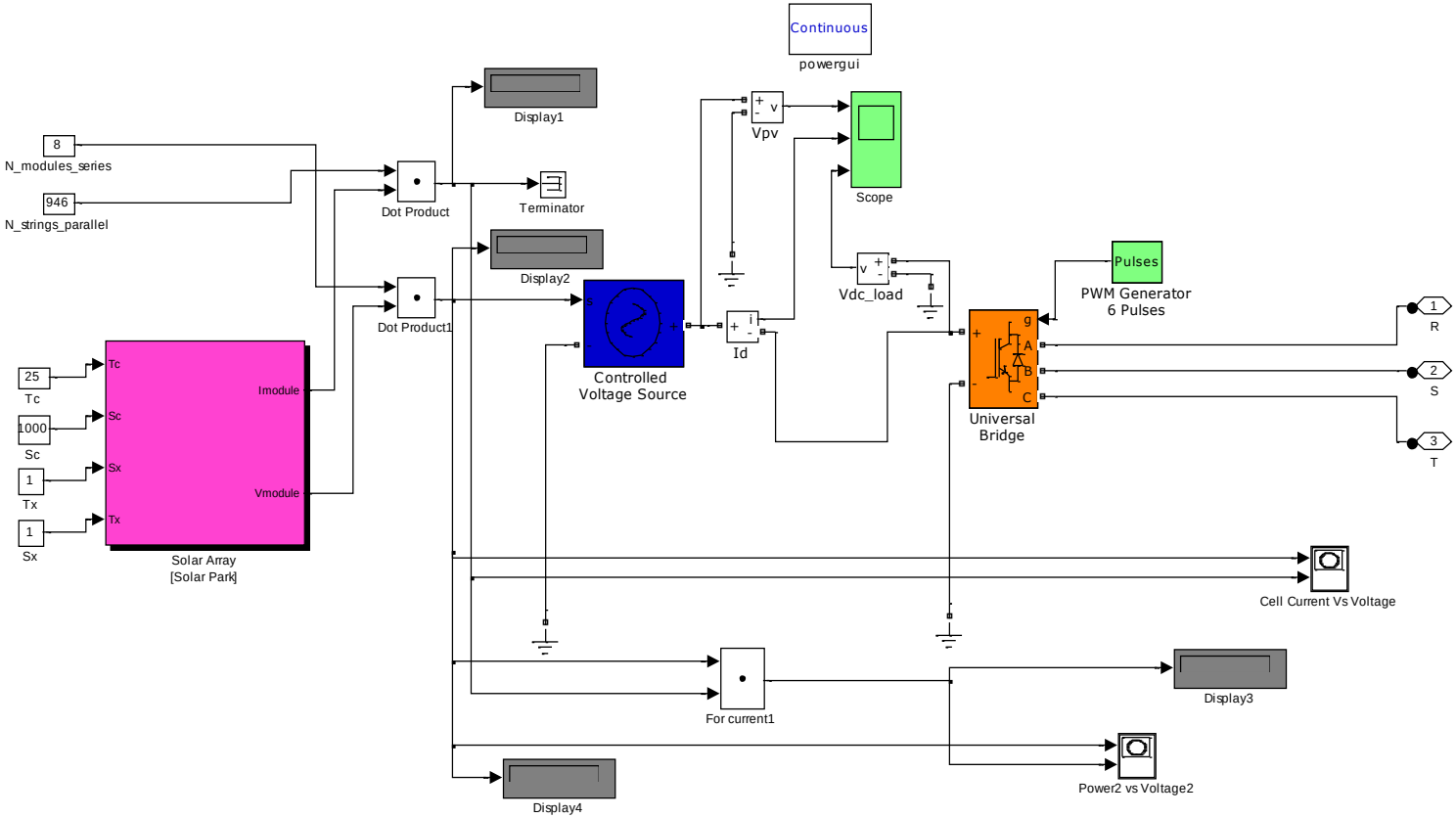

Figure 3.2 PVA Model

3.3 Modeling of the Wind Farm

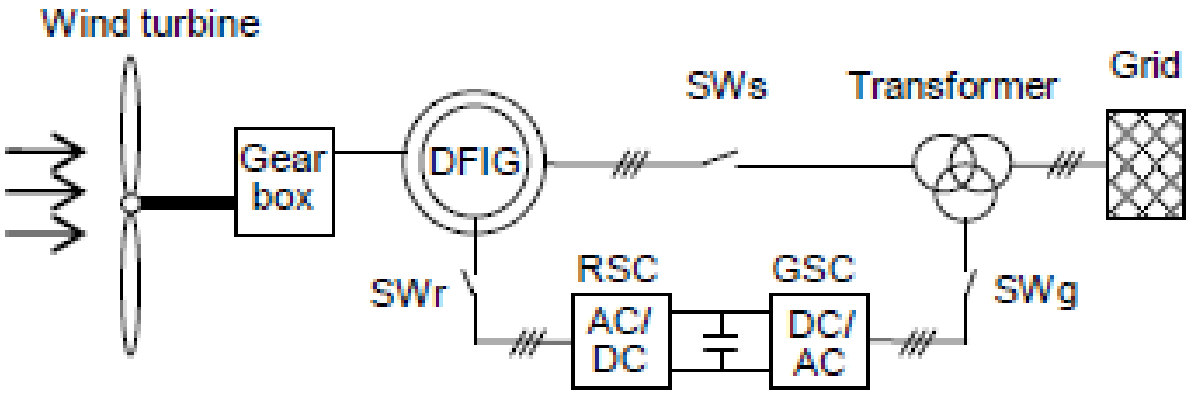

Figure 3.3 Doubly-fed induction generator (DFIG)

The Doubly-Fed Induction Generator (DFIG) technology allows extracting maximum energy from the wind for low wind speeds by optimizing the turbine speed, while minimizing mechanical stresses on the turbine during gusts of wind. Another advantage of the DFIG technology is the ability for power electronic converters to generate or absorb reactive power, thus eliminating the need for installing capacitor banks as in the case of squirrel-cage induction generator. Wind turbines using DFIG consist of a wound rotor induction generator and an AC/DC/AC IGBT-based PWM converter. The stator winding is connected directly to the 50 Hz grid while the rotor is fed at variable frequency through the AC/DC/AC converter.

A wound rotor induction machine, used as a DFIGwind turbines are nowadays becoming more widely used in wind power generation. The DFIG connected with back to back converter at the rotor terminals provide a very economical solution for variable speed application. Three-phase alternative supply is fed directly to the stator in order to reduce the cost instead of feeding through converter and inverter.

A schematic configuration of a DFIG wind turbine grid synchronization and power control are two control modes of a DFIG in a turbines system. For a better understanding of the control process, it is worth briefly stating the working process of the wind turbine systems. A schematic configuration of a DFIG wind turbine is shown in Figure 3.3. In the beginning from standstill, the DFIG is disconnected from the grid. Wind speed is measured by an anemometer. Once it reaches the cut-in value, the brake is released and the rotor blades are driven by the pitch regulation mechanism from the feathering position to a pre-optimized angle. The mechanical torque created by the aerodynamic lift from the

blades drives the shaft to rotate. At the same moment, the switch SWg is on, and the DC-link voltage in the bidirectional converter is soon charged. When the rotating speed of the wind turbine reaches a certain value (e.g. 70-80% of the rated speed), SWr is turned on and the soft grid synchronization process starts. For variable-speed wind turbines, grid synchronization is possible at any operational speed. Usually, grid synchronization process takes less than one second [16]. Once this process is accomplished, SWs is turned on and the stator of the DFIG is connected to the grid, and then the power control mode, which comprises active power optimization and reactive power control, starts.

Active power control is for tracking a predefined power-speed characteristics profile and reactive power control is to control the power factor at the grid terminals.

DFIG is controlled via the converters on the rotor. The grid side converter (GSC) is controlled to maintain a constant DC-link voltage and to guarantee the operation of the converter with unity power factor, i.e., zero reactive power [18]. The rotor side converter (RSC) is controlled for both grid synchronization and power optimization. To some degree, RSC can be considered as a current-controlled voltage source. Based on *d*,*q*-transformation with the stator-fluxoriented reference frame, control on the d,q-axis rotor current can be decoupled for active and reactive power. Considering that the stator resistance is comparatively very small, the grid flux orientation aligns with the stator flux orientation without any significant errors [17]. On this account, both the stator-flux-oriented reference and the grid-voltage-oriented reference can be used for vector control.

3.4 Simulation Methods of the DFIG

In the last years, MATLAB-Simulink has become the most used software for modeling and simulation of dynamic systems. It provides a powerful graphical interface for building and verifying new mathematical models as well as new control strategies particularly for non-linear systems. Then, using a dSPACE prototype, these new control strategies can be easily implemented and tested. The study of wind turbine systems generators are an example of such dynamic systems, containing subsystems with different ranges of the time constants: wind, turbine, generator, power electronics, transformer and grid.

This model is well suited for observing harmonics and control system dynamic performance over relatively short periods of times.

The Simulink diagram for a DFIG connected to grid side with wind turbine schemes is shown in figure 3.4.The system is connected to a 15 KV national grid system with the total capacity of 9MW wind farm (6 of 1.5 MW each) via. Step up transformers, fault

protection and pi- transmission line. The wind-turbine model is average model that allows transient stability type studies with long simulation times.

The model includes representation of power electronic IGBT converters. In order to achieve an acceptable accuracy with the 1620 Hz and 2700 Hz switching frequencies used in this model of the wind farm, the model is discretized at a relatively small time step (50 microseconds).

The DFIG wind turbine farm is simulated in MATLAB and the results are shown in the last section, Appendices, of this paper.

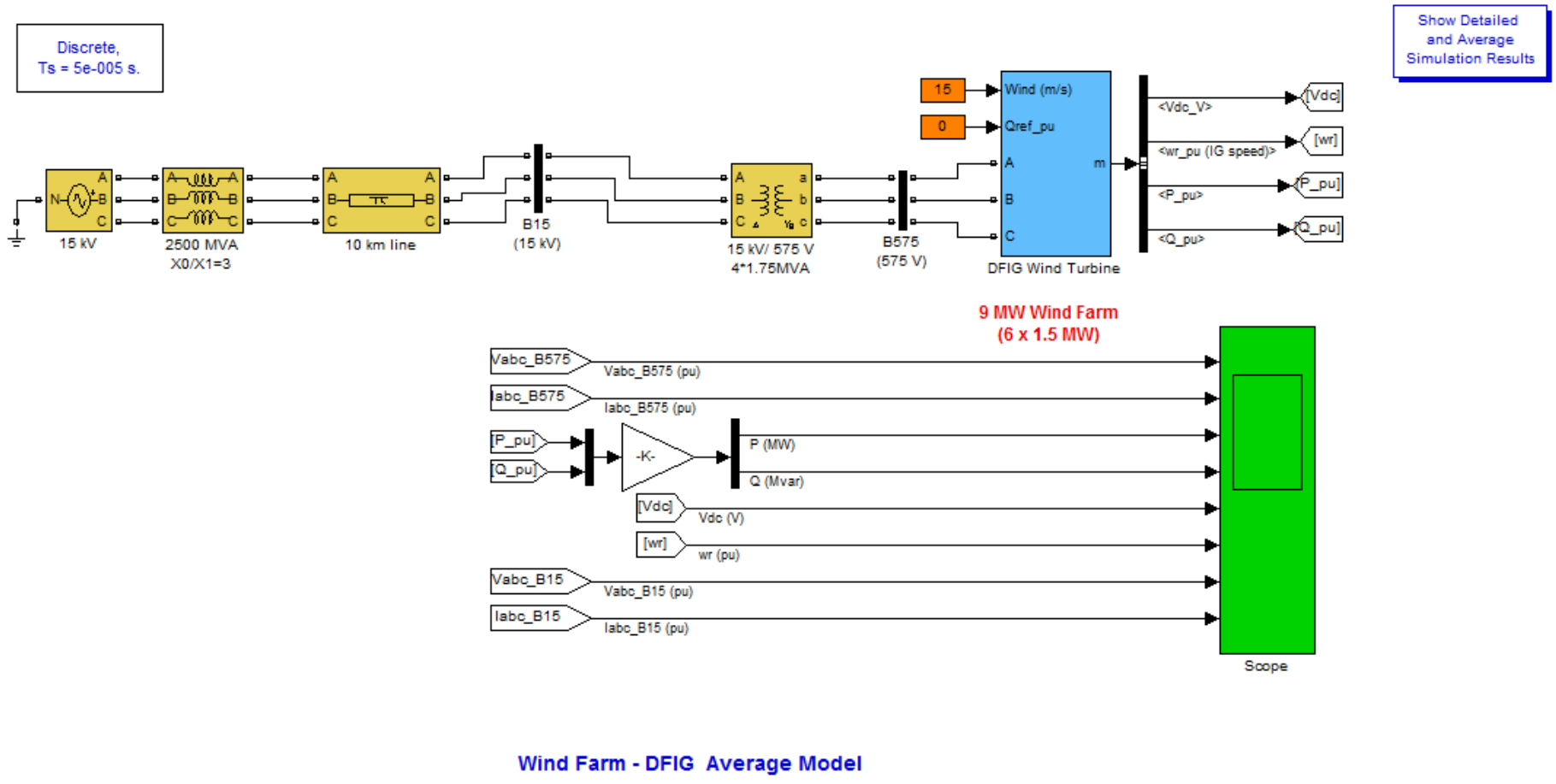

Figure 3.4 Wind farm model

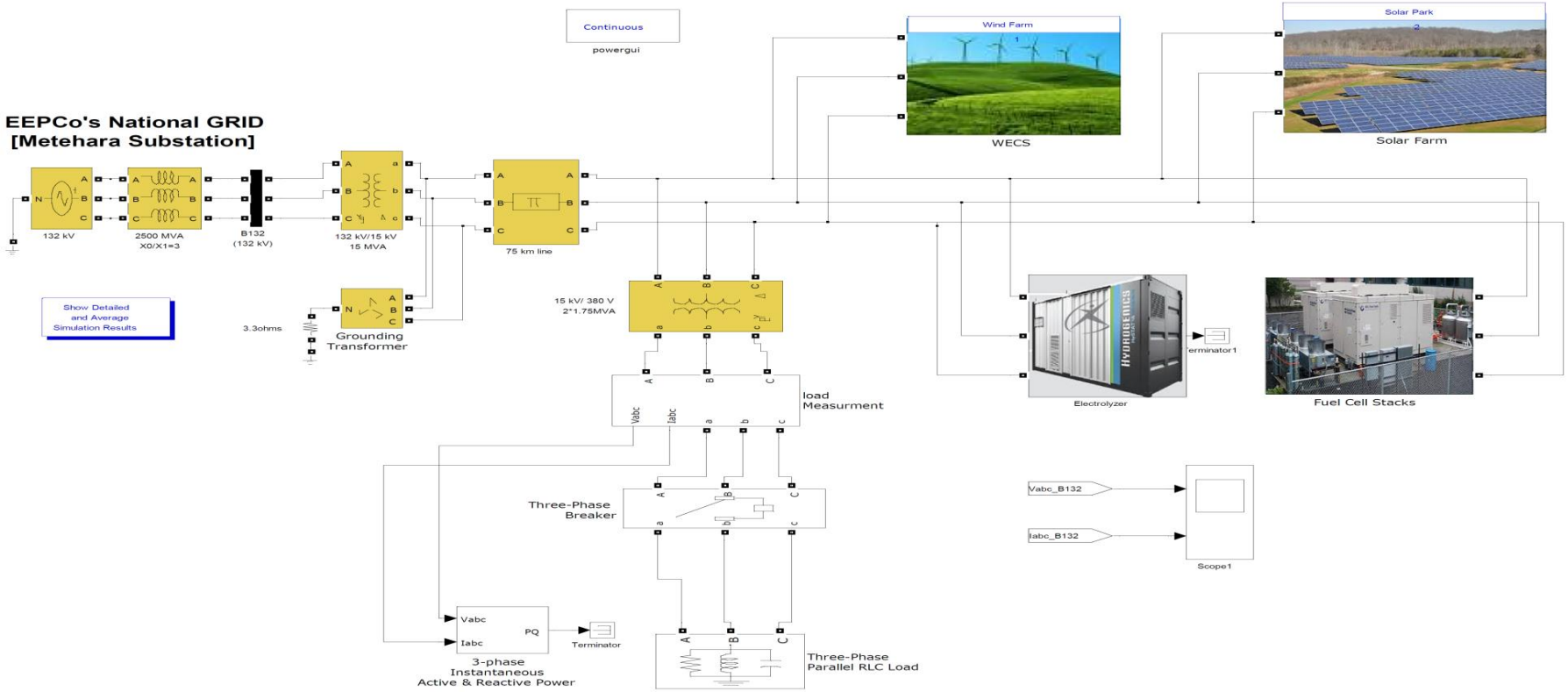

Figure 3.5 The Proposed Hybrid Model

3.5 Control Schemes

Even though the capital cost for installing a PV array is decreasing due to recent technology development, the initial investment on a PV system is still very high compared to conventional electricity generation techniques. Therefore, it is very natural to desire to draw as much power as possible from a PV array which has already been installed so that higher economic benefit gained. Maximum power point tracking (MPPT) is one of the techniques to obtain maximum power from a PV system. There are two kinds of Maximum Power Point Tracking systems.

3.5.1 Current-Based Maximum Power Point Tracking Control Scheme

The main idea behind the current-based MPPT is that the current at the maximum power point I_{mp} has a strong linear relationship with the short circuit current I_{sc}.I_{mp} has a very good linear dependence on I_{sc} which can be expressed as:

$$I_{mp} = K_{cmppt} \times I_{sc} \quad \textbf{(3.11)}$$

where K_{cmppt} is the current factor CMPPT control and is approximately equal to 0.86 for the silicon panel and has different values for different solar panels [5].

3.5.2 Voltage-Based Maximum Power Point Tracking Control Scheme

The VMPPT control is based on the observation from I–V curves that the ratio of the array's maximum power voltage, Vmp, to its open-circuit voltage, V_{oc}, is approximately constant, 0.72 [5]:

$$V_{mp} = V_{ompPt} \times V_{OC} \quad \textbf{(3.12)}$$

The voltage has a small variation in VMPPT; therefore, the controller is not always needed to control MPP. However, VMPPT cannot reach an accurate MPP at any irradiation and might encounter MPP confusion at low irradiation because of the PV array characteristics, On the other hand, CMPPT can always control the current; it can reach MPP easily and accurately because of the short circuit current characteristics in the PV array. Therefore, CMPPT is desired if the aim is to increase system efficiency.

In this thesis, the proposed maximum power tracking method used is current based maximum power point tracking.

The control scheme of the CMPPT for the PV system in the proposed hybrid system is shown in Figure 3.7. The value of Imp calculated form (3.11) is used as the reference signal to control the buck DC/DC converter so that the output current of the PV system matches Imp. This reference value is also used to control the inverter so that the maximum available of power is delivered to the AC bus, shown in Figure 3.7.

There are different maximum tracking algorithms for maximum power trucking. Implementing the perturbation and observation method is simple because it only increases or decreases reference voltage. However, this method cannot readily track any immediate and rapid change in the environment. One alternative is the incremental conductance method; it can track MPP accurately by comparing the incremental conductance and instantaneous conductance of a PV array [32], [43]. In this paper, the proposed CMPPT is selected from the perspective of the incremental conductance method.

The flowchart shown in Figure 3.6 presents the systematic progress of CMPPT, where $V_{pv(n)}$ and $I_{pv(n)}$ are the present voltage and current of the PV array, and $V_{pv(n-1)}$ and $I_{pv(n-1)}$ are their previous values, respectively. When $V_{pv(n)}/I_{pv(n)} + dV_{pv} / dI_{pv} < 0$ or $dI_{pv} = 0$ and $dV_{pv} < 0$, decreasing reference current Ipv^* forces $V_{pv(n)}/I_{pv(n)} + dV_{pv} / dI_{pv}$ to approach zero. When $V_{pv(n)}/I_{pv(n)} + dV_{pv} / dI_{pv} > 0$ or $dI_{pv} = 0$ and $dV_{pv} > 0$, increasing reference current I_{pv}^* forces $V_{pv(n)}/I_{pv(n)} + dV_{pv} /dI_{pv}$ to *approach zero. When* $V_{pv(n)}/I_{pv(n)} + dV_{pv} / dI_{pv} = 0$ *or* $dI_{pv} = 0$ *and* $dV_{pv} = 0$*, as the PV array is at the MPP, reference current* I_{pv}^* *is kept at a constant value, and thus, oscillation is reduced.*

The flow chart of Current Maximum Power Point Control is shown below

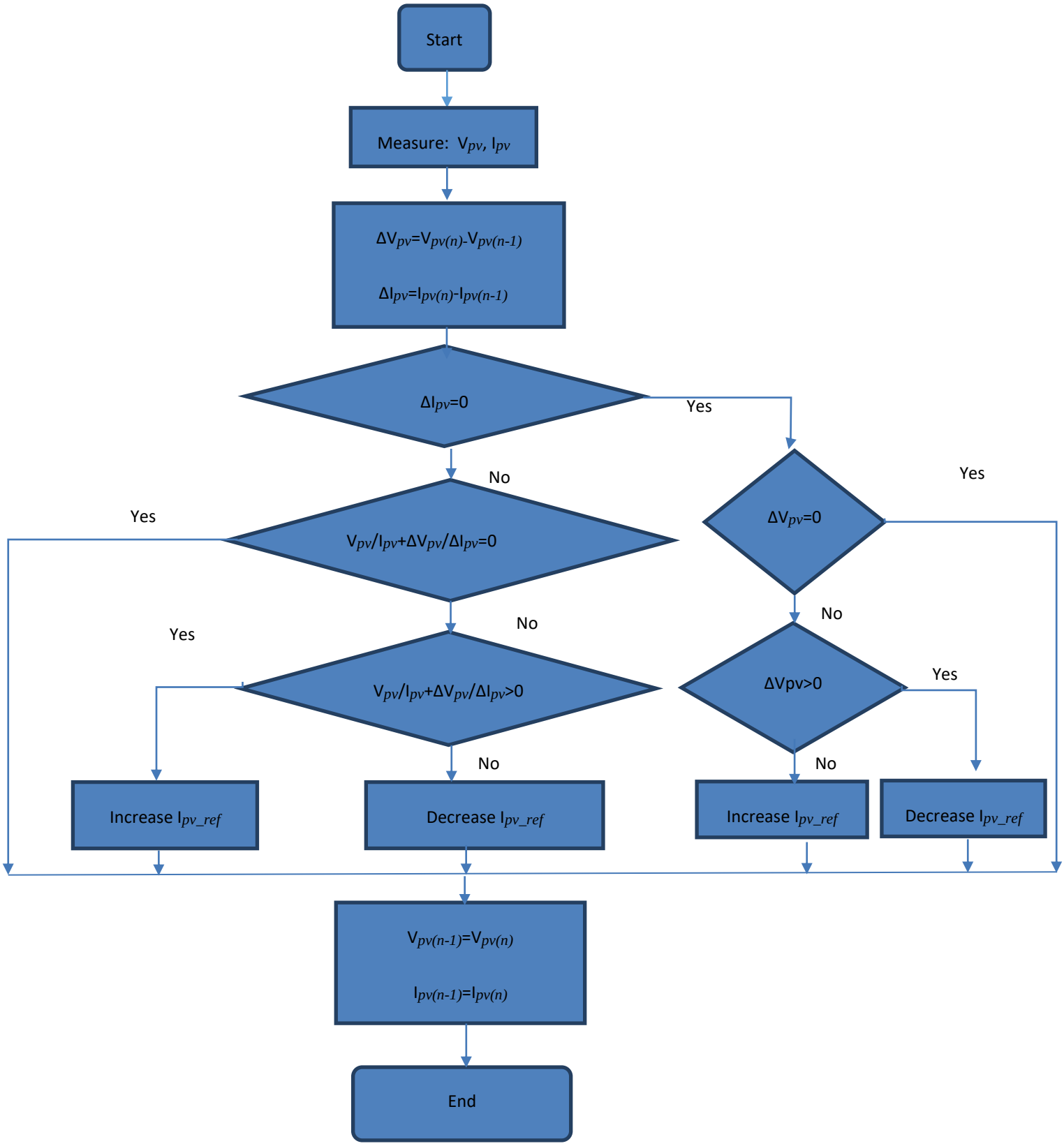

Figure 3.6 Flow chart for CMPPT

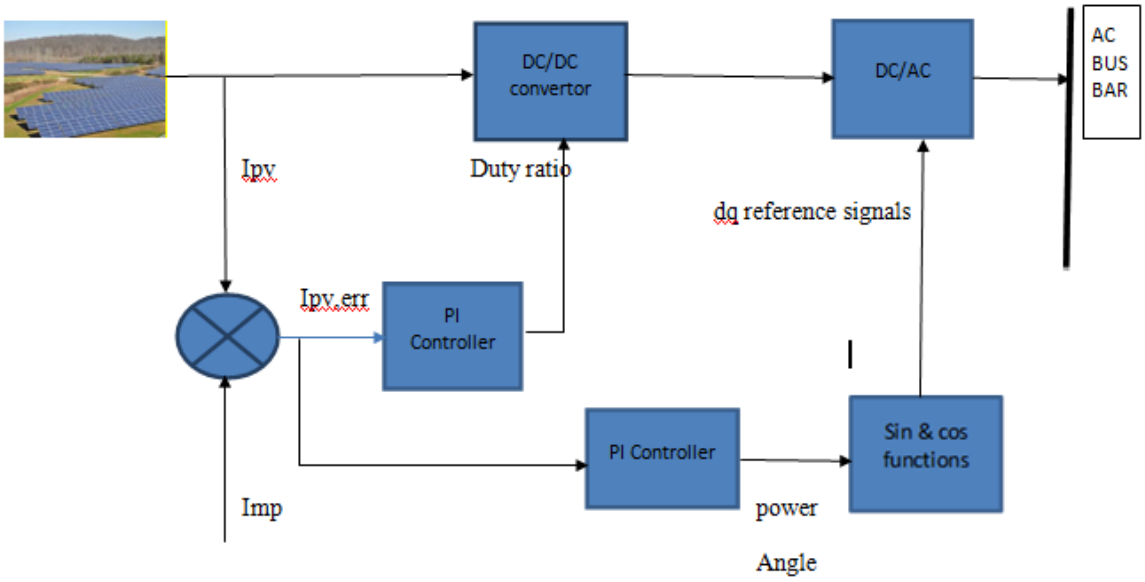

Figure 3.7 CMPPT Control Scheme

The average output voltage of buck DC/DC converter at steady-state is given as:

$$V_{dd\_out} = dV_{dd\_in}$$

Where d is the duty ratio of the switching pulse.

Since $0 \leq d < 1$, the output voltage of a buck converter is always lower than its input voltage. In contrast to a boost converter, a buck converter is a step-down DC/DC converter. Its output voltage can also be regulated by controlling the duty ratio (d) of the switching signals. The controller for the converter is to regulate the DC bus voltage within a desirable range. The output voltage is measured and compared with the reference value. The error signal is processed through the PWM controller, which can be a simple PI controller. The output of the controller is used to generate a PWM pulse with the right duty ratio so that the output voltage follows the reference value.

CHAPTER 4

CASE STUDY

4.1 Introduction

Berehet is one of the woredas in the Amhara Region of Ethiopia, part of the Semien Shewa Zone, Berehet is bordered on the south by the Germama River which separates it from Menjarna Shenkora, on the west by Hagere Mariamna Kesem, on the north by Asagirt, and on the east by the Afar Region. The main town in Berehet is Metiteh Bila.

Based on the data collected from Financial and Economic Development Office of Berehet Woreda, this woreda has a total population of 39,168 of whom 19,870 are men and 19297 are women. With an area of 791.44 square kilometers, Berehet has a population density of 43.98, which is less than the Zone average of 115.3 persons per square kilometer. A total of 6,976 households were counted in this woreda, resulting in an average of 5.61 persons to a household. The majority of the inhabitants practiced Ethiopian Orthodox Christianity, with 79.62% reporting that as their religion, while 20.19% of the population said they are Muslim.[2]

- In this woreda, there are 10 Kebeles, from which only one Kebele (Metiteh Bila) is electrified from Metehara substation with 15kV distribution line.
- The capacity of the existing Metahara substation is way out of fulfilling the demand load of the other 9 kebeles with the population of around 39,000.

The nearby substation to the study area is Metehara substations which is around 75km from the Woreda. The transformer capacity, the monthly and yearly load data from year 2003 to 2005 E.C from this substation is shown in Appendix 6. The capacity of the transformer is 15MVA. There are five 15kV feeders to Abomsa, Metehara Sugar Factory, Metehara line and Industry line. The line 5 is the one which feeds Metiteh Bila Kebele of the case study area. On average 200kW is delivered to this Metiteh Bila kebel from the national grid, which is by far less than the needed load demand of all the Kebeles. So it is a must to have energy source to satisfy all the demanded load of the woreda through other means. This is the reason why the hybrid system of “Wind/PV/Fuel Cell” for this case study area is needed. The fuel cell would supply the load demand for the Woreda in case there is no energy production from the solar and wind farms and it is used as standby power plant. The result of the optimum feasible hybrid system will be compared to that of

extension of the national grid form Metehara substation to the case study area in terms of finance.

4.2 System Unit Sizing

The load profile study and determination are the first steps for the design of any electric power system. Nature of operation of loads and behavior of consumers are the parameters that determine the load profile. In case of Berehet, most of the loads are lighting, Radio/TV, flour mills and work appliances. Nature of operation of these loads is shown in the Table 4.1.

4.3 Load Estimation

One of the basic inputs to HOMER is the load profile of the system. Electric load in the rural villages of Ethiopia can be assumed to be composed of lighting, radio and television, water pumps, health post and primary schools. As indicated previously, there are about 6,976. It is assumed that there will be four 18W fluorescent lamps and one elementary school and one health center per Kebele, a total of 10 schools and 10 health centers are required for the community. Each school consists of 8 classrooms and in each classroom will be installed with four 18W fluorescent lamps. Similarly for the 10 health centers, having 5 rooms each, one 18W fluorescent lamp per. A vaccine refrigerator of 120W working for 12 hours; a 60W capacity microscope; and a 2 kW water heater operational for 8 hours per day are also suggested for each health centers. For the community a total of 20 flour mills of 3kW working from 9:00 to 19:00 are assumed. Each family is assumed to use electric stove of 3kW rating for Injera baking oven for 1 hour twice a week which works for 3:00-16:00 daily.

Table 4.1 Load forecasting of the case study area

Service Type	Load Type	Rated Power [W]	Qty	Duration [hr]	Energy [kWh/day]
House	Lighting	18	20,928	8	3,013.63
	TV	80	3,488	11	3,069.44
	Radio	40	4,651	16	2,976.43
	Enjera Oven	3000	2,325	8	1,992.86

Agricultural	Pump	2500	20	10	500.00
Flour Mill	Mill	3000	20	12	720.00
School	Lighting	18	320	10	57.60
	Office Load	40	8	10	3.20
Churches & Mosques	Lighting	36	120	6	25.92
	Megaphone	80	40	4	12.80
Health Center	Lighting	18	50	24	21.60
	Microscope	60	10	10	6.00
	Refrigerator	120	10	24	28.80
	Water Heater	2000	10	8	160.00
11,010.00					
Total Energy of the town					**12,588.28**

The energy demand of the Woreda is forecasted to be 12,588.28 kWh/day. The demand of the Woreda is shown in Figure 4.1. The forecasting covers the daily peak load, total daily energy, and daily load curve as a series of 24 hourly forecasted hourly loads. The peak load hours are estimated to be from 5:00 PM to 10:00 PM.

Table 4.2 Load forecasting on hourly load demand basis [kW]

No	Service Type	Load Type	Energy (KWh/day)	Hour 1	Hour 2	Hour 3	Hour 4	Hour 5	Hour 6	Hour 7	Hour 8	Hour 9	Hour 10	Hour 11	Hour 12	Hour 13	Hour 14	Hour 15	Hour 16	Hour 17	Hour 18	Hour 19	Hour 20	Hour 21	Hour 22	Hour 23	Hour 24
1	House	Lighting	3,013.63																	376.70	376.70	376.70	376.70	376.70	376.70	376.70	376.70
2		TV	3,069.44														279.04	279.04	279.04	279.04	279.04	279.04	279.04	279.04	279.04	279.04	279.04
3		Radio	2,976.43							186.03	186.03	186.03	186.03	186.03	186.03	186.03	186.03	186.03	186.03	186.03	186.03	186.03	186.03	186.03	186.03		
4		Enjera Oven	1,992.86									249.11	249.11	249.11	249.11	249.11	249.11	249.11	249.11								
5	Agricultural	Pump	500.00						50	50	50	50	50	50	50	50	50	50									
6	Flour Mill	Mill	720.00								60.00	60	60	60	60	60	60	60	60	60	60	60					
7	School	Lighting	57.60								5.76	5.76	5.76	5.76	5.76	5.76	5.76	5.76	5.76	5.76							
8		Office Load	3.20								0.32	0.32	0.32	0.32	0.32	0.32	0.32	0.32	0.32	0.32							
9	Churches & Mosques	Lighting	25.92					4.32	4.32	4.32											4.32	4.32	4.32				
10		Megaphone	12.80					2.13	2.13	2.13										2.13	2.13	2.13					
11	Health Center	Lighting	21.60	0.90	0.9	0.9	0.9	0.9	0.9	0.9	0.9	0.9	0.9	0.9	0.9	0.9	0.9	0.9	0.9	0.9	0.9	0.9	0.9	0.9	0.9	0.9	0.9
12		Microscope	6.00							0.60	0.6	0.6	0.6	0.6			0.60	0.60	0.60	0.60	0.60						
13		Refrigerator	28.80	2.40		2.4		2.4		2.4		2.4		2.4		2.4		2.4		2.4		2.4		2.4		2.4	
14		Water Heater	160.00							20.00	20	20	20	20	20	20	20										
Total			12,588.28	3.30	0.90	3.30	0.90	9.75	57.35	266.38	323.61	575.11	572.71	575.11	572.11	574.51	851.75	834.15	781.75	913.88	909.72	911.52	846.99	845.07	842.67	659.04	656.64
				1	2	3	4	5	6	7	8	9	10	11	12	13	14	15	16	17	18	19	20	21	22	23	24

A graphical plot showing the variation in demand for energy of the consumers on a source of supply with respect to time is known as the load curve.

If this curve is plotted over a time period of 24 hours, it is known as daily load curve. If it is plotted for a week, month, or a year, then it is named as the weekly, monthly or yearly load curve respectively

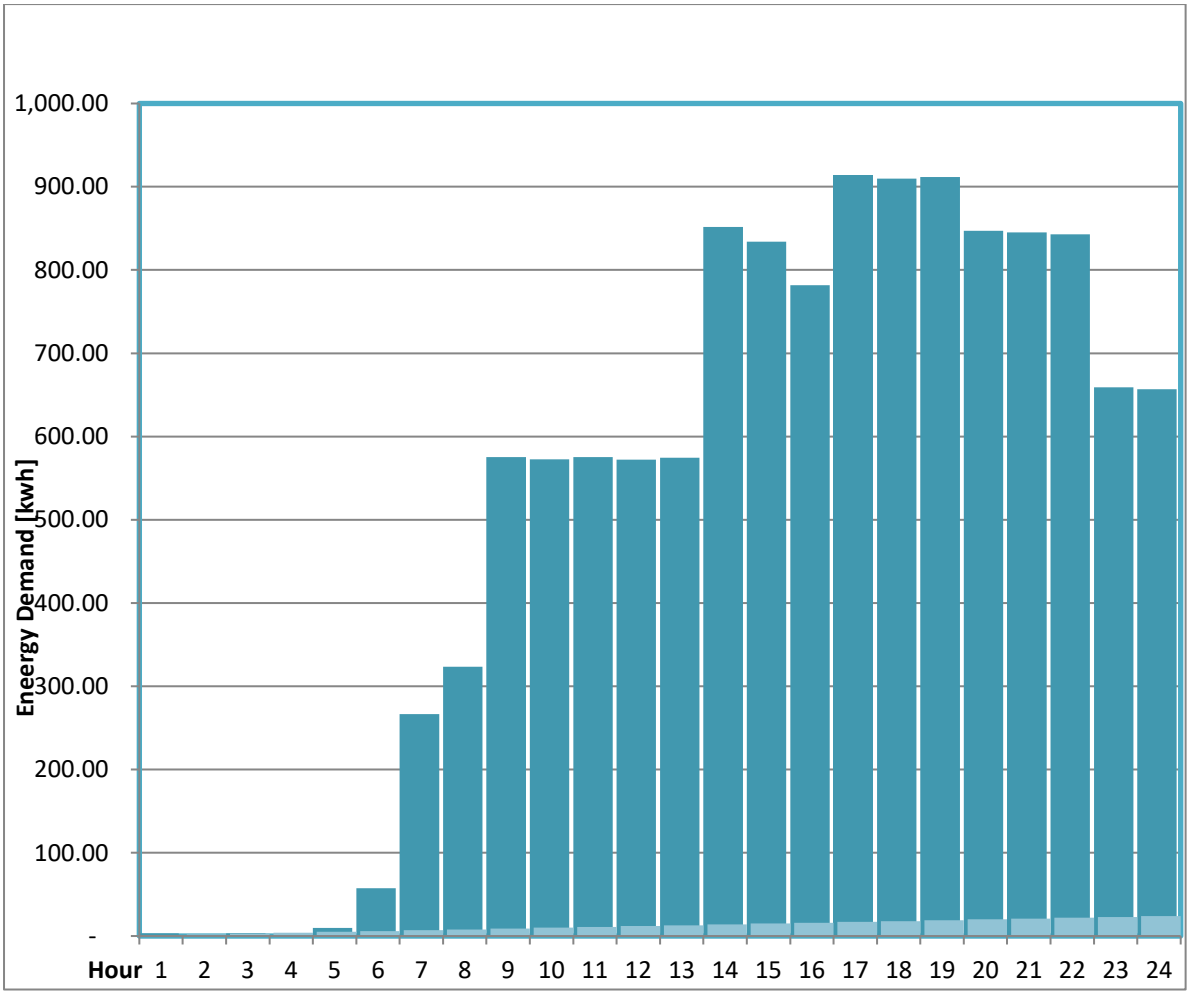

Figure 4.1 Daily Load Curve

The load duration curve reflects the activity of population quite accurately with respect to electrical power consumption over a given period of time. As we can see from the daily load curve, the minimum load is reached at about 1 to 6 hours in the evening, when most people are asleep. Whereas, the peak of the residential load demand starts at around 14 hrs and lasts up to 22 hrs at night, after which again the load drops, as most people retire to bed.

The load duration curve gives a graphical representation of the demand that the supply stations are required to meet throughout the day. And hence they are helpful in deciding

the total installed capacity of the DG system required, which should be capable of meeting the peak load demand, and the most economical size of various generating units.

4.4 Wind turbine sizing

The following are the major wind turbine selection criteria:

- Reasonable hub height
- Cut-in wind speed
- Rated capacity
- Rated wind speed

The most important criteria for choosing the wind turbine is to be able to work most of the time at its rated power which means that we need to consider a turbine with power curve that respond to the prevailing wind speed in the site of interest. For this case, we have considered the cut in speed as wind turbine selection criteria. A wind turbine with cut-in speed of 2m/s is selected for case study. This wind turbine works in the range of wind speeds from 2-25m/s.

There are still other important criteria affecting the selection of the wind turbine like:

1. The capacity of the transportation roads to come to the area of interest
2. The capacity of the connection point to the national grid
3. Turbulence intensity
4. The goals of the project
5. Price & availability of the turbines (many turbines have long waiting lists)

The production of wind energy from wind turbines is a function of wind speed. The relationship between wind speed and power is defined by a power curve, which is unique to each turbine model and, in some cases unique to site specific settings. In general, most wind turbines begin to produce power at wind speed of about 2-3m/s, achieve rated power at approximately 11-12m/s and stops power production at 25m/s [42].Variability in the wind resource results in the turbine operating at continually changing power levels. At good wind energy sites, this ability results in the turbine operating at approximately 35% of its total possible capacity when averaged over a year.

For this case study, 50kW Wind Turbine (ASWT-50kW) has been selected.The technical specifications and power curve data of the selected wind turbine are shown in Table 4.3 and Figure 4.2 respectively.

Table 4.3 The technical specifications of ASWT-50kW wind turbine

Model	ASWT.12.0-50KW
Rated Power	50KW
Maximum Output Power (W)	75000
Battery Bank Voltage (Vdc)	400
System output voltage (Vdc)	380
Start-up wind speed (m/s)	2
Rated wind speed (m/s)	11
Working wind speed (m/s)	2.5-25
Survival wind speed (m/s)	50
Generator efficiency	>.92
Wind energy utilizing ratio (cp)	0.42
Generator type	Permanent Magnet Alternator
Generator weight (kg)	1200
Blade material / quality	GRP/3
Blade diameter (m)	12.0
Speed regulation method	Yawning + Electromagnetism braking (Optional hydraulic braking)
Shutting down method	Manual + Automatic

Source : http://www.atlantissolar.com/turbine_50kw.html

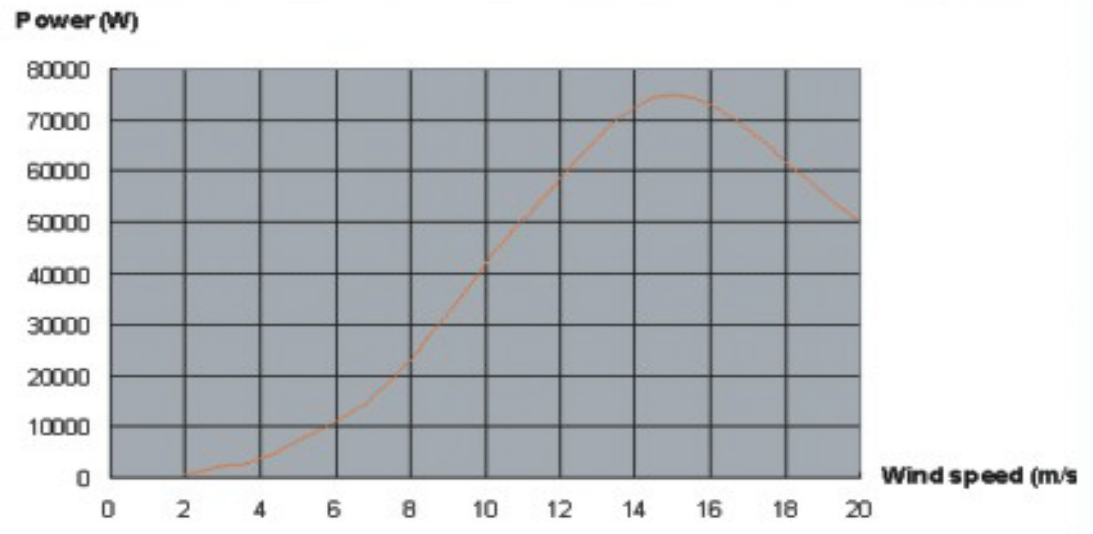

Figure 4.2 ASWT-50kW Power curve

Table 4.4 Power output of the selected wind turbine

No.	Wind speed [m/s]	Power [kW]
1	0.00	0.000
2	0.50	0.000
3	1.00	0.000
4	1.50	0.000
5	2.00	3.000
6	2.50	4.500
7	3.00	7.500
8	3.50	8.500
9	4.00	10.000
10	4.50	11.000
11	5.00	12.500
12	5.50	13.000
13	6.00	15.000
14	6.50	18.500
15	7.00	25.000
16	7.50	28.000
17	8.00	30.000
18	8.50	32.500
19	9.00	35.000
20	9.50	38.500
21	10.00	42.500
22	10.50	46.000
23	11.00	50.000

24	11.50	53.500
25	12.00	57.500
26	12.50	60.000
27	13.00	62.500
28	9.50	38.500
29	10.00	42.500
30	10.50	46.000
31	11.00	50.000
32	11.50	53.500
33	12.00	57.500
34	9.50	38.500
35	10.00	42.500
36	12.50	60.000
37	13.00	62.500
38	13.50	63.200
39	14.00	65.000
40	14.50	66.500
41	15.00	67.500
42	15.50	68.500
43	16.00	70.000
44	16.50	72.500
45	17.00	75.000
46	17.50	69.000
47	18.00	62.000

4.5 Optimization of the Hybrid System

HOMER, the micro-power optimization model, simplifies the task of evaluating designs of both off-grid and grid-connected power systems for a variety of applications. When designing a power system, one must make many decisions about the configuration of the system. What components does it make sense to include in the system design? How many and what size of each component should be used? The large number of technology options and the variation in technology costs and availability of energy resources make these decisions difficult. HOMER's optimization and sensitivity analysis algorithms make it easier to evaluate the many possible system configurations.

HOMER simulates the operation of a system by making energy balance calculations for each of the 8,760 hours in a year. For each hour, HOMER compares the electric and thermal demand in the hour to the energy that the system can supply in that hour, and calculates the flows of energy to and from each component of the system. For systems that include batteries or fuel-powered generators, HOMER also decides for each hour how to operate the generators and whether to charge or discharge the batteries.

HOMER performs these energy balance calculations for each system configuration that is considered. It then determines whether a configuration is feasible, i.e., whether it can meet the electric demand under the specified conditions, and estimates the cost of installing and operating the system over the lifetime of the project. The system cost calculations account for costs such as capital, replacement, operation and maintenance, fuel, and interest.

After simulating all of the possible system configurations, HOMER displays a list of configurations, sorted by net present cost (sometimes called lifecycle cost), that can be used to compare system design options.

When defining sensitivity variables as inputs, HOMER repeats the optimization process for each sensitivity variable that is specified. For example, if the wind speed is defined as a sensitivity variable, HOMER will simulate system configurations for the range of wind speeds that is specified.

HOMER helps determine how different conventional, renewable, and hybrid systems interact with end-use demand. Based on the availability and potential of renewable energies in the study area a hybrid energy system is modeled consisting of wind turbines and solar PV system along with DGs back-up. The details of various parameters such as solar and wind resource potential of the area, load profile and description of various components, i.e. size, number and cost of wind turbine, PV array, DG, converter, etc. in the proposed hybrid scheme have been collected from different resources.

The potential solar resource and wind power resource for Berehet Woreda were assessed. The wind speed, solar insolation and clearness index for a yearlong period were obtained from the NASA Surface Meteorology and Solar Energy database (SMSE) and it is compared with the wind and solar map of Ethiopian (SWERA).

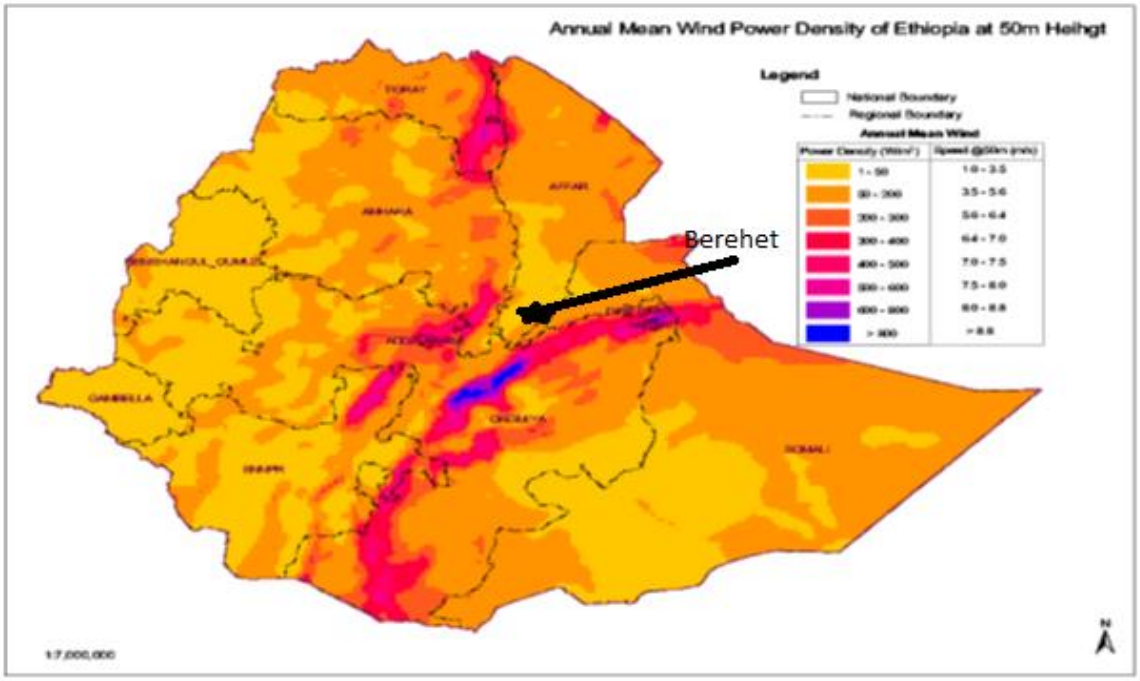

Figure 4.3 A GIS map showing wind resources of Ethiopia

The wind resource classifications, Class 1 to Class 7, are indicated by color-codes as indicated in the GIS map above, Class 7 indicating the strongest wind regions. Each color code has an assigned range of values to represent annual wind power density in W/m^2.

Table 4.5 Wind potential classification

Wind resource category	Wind class	Wind power density [W/m^2]	Wind speed @50m [m/s]	Total Area [km^2]
Poor	1	50-200	3.5-5.6	564,606
Marginal	2	200-300	5.6-6.4	96,801
Moderate	3	300-400	6.4-7.0	42,935
Good	4	400-500	7.0-7.5	23,975
Excellent	5	500-600	7.5-8.0	6,529
Excellent	6	600-800	8.0-8.8	3,814

Excellent	7	Above 800	Above 8.8	1,715
Total area covered by Marginal-to-Excellent wind regions				**740,376.00**

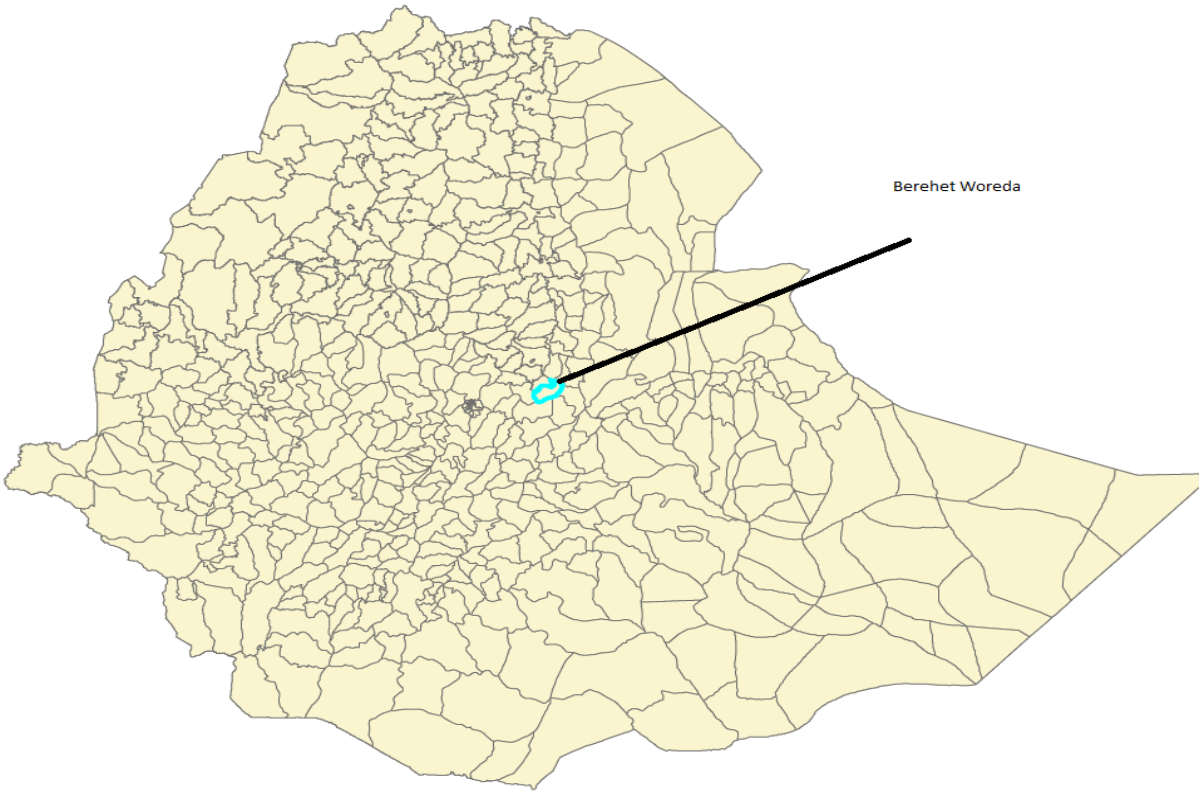

Figure 4.4 GIS Map, location of the case study area

As it can be seen from the SWERA map, it is estimated the class for Berehet Woreda fall in category 1. In addition to wind map from SWERA, there is another wind speed data obtained from NASA is presented in the table below.

TABLE 4.6 Monthly averaged Wind Speed at 50 m above the surface of the earth (m/s) for Berehet (Source: NASA)

Lat 9.20 ***Lon 39.3***	Jan	Feb	Mar	Apr	May	Jun	Jul	Aug	Sep	Oct	Nov	Dec	Annual Average
10-years Average	4.32	4.21	3.94	3.64	3.60	3.93	3.76	3.41	3.10	3.39	3.74	3.98	3.74

4.6 HOMER Simulation

4.5.1 Wind Turbine Model

The monthly wind speed data measured at 50m height is given in Table 4.5. The capital, replacement and O&M costs of the turbine are given in Table 4.6. The project lifetime of the wind turbine is 25 years i.e. end of the project.

Table 4.7 Costs of the components of the proposed hybrid

Component Detail	*Capital Cost [$]*	*Replacement Cost [$]*	*O & M Cost ($/yr)*
Solar PV System	1,960,000.00	523,833.00	1,789,671.00
Wind Turbine	5,180,000	-	61,360
Fuel Cell	1,600,000	-	
Hydrogen Tank	150,000	-	127,834
Electrolyzer	1,600,000	-	511,335
Converter	600,000	-	958,752.00

Details of the capital, replacement and O&M costs of various equipment employed in the proposed scheme.

4.5.2 PV array model

The latitude of the case study site is 9º20’ 0” North and the longitude is 39º 30’ 0”East. The daily radiation horizontal data are taken from NASA Surface Meteorology and Solar Energy database (SMSE) for simulation.

A PV module with a capacity of 230W is selected of this study and the technical specifications of the selected PV module are listed shown in Table 4.7.

The capital replacement and O&M costs of the PV farm is shown in table 4.6. The projected lifetime of the PV array is 25 years.

Table 4.8 Technical specifications of ATI-2000(230) solar module

Maximum power (Pmax)	*230W*
Maximum power voltage (Vpm)	*29.49V*
Maximum power current (Ipm)	*7.80A*
Open circuit voltage (Voc)	*37.20V*
Short circuit current (Isc)	*8.39A*
Module efficiency (η_m)	*14.3%*
No. & type solar cells	*60 in series/60"(156 ×156mm) multicry*

4.5.3 Fuel Cells

During any shortage or fault of the grid and also insufficient solar and wind energy generation fuel cell is used as standby power generation plant. The fuel cell system makes the distributed generation system to work autonomously. The fuel cell stacks may contain a number of fuel cells. The cost of a fuel cell, its replacement and O&M costs as used for simulation are shown in table 4.6.

The fuel cell energy generation system is for the times when there is insufficient solar radiation and wind resource or when there is no grid supply or when the grid is not sufficient to supply the load demand of the Woreda. The maximum load demand (peak load) of the Woreda is around 1MW. So it is safe to put fuel cell which has a capacity of 2MW fuel cell stack.

A fuel cell stack SR-12 is selected for this case study with power output of 500w. The voltage output of the stack is 58.9V

Table 4.9 Technical specifications for the SR-12 stack fuel

Specifications of SR-12	
Description	Value
Capacity	500W
Number of Cells	48
Operating Temperature	5^{o}C to 35^{o}C
Operating Pressure	P_{H2}=1.5atm

	P_{cathod}=1.0atm
Unit dimensions (WxDxH)	56.1x61.5x34.5cm
Weight	44Kg

Table 4.10 Electrical model parameter values for SR-12 stack

E0(V)	58.9	$C_h(F)$	22000
KE (V/K)	0.00085	$R_\tau(u)$	0.0347
$\tau_S(s)$	80.0	C(F)	0.1F(4.8F for each cell)
λ_e(u)	0.00333	$R_{ohm0}(\Omega)$	0.2793
A(v/K)	20.145	$R_{ohm1}(\Omega)$	0.001872xI
$\eta_o(V)$	-0.1373	$R_{ohm2}(\Omega)$	-0.0027312x(T-298)
$R_{act0}(u)$	1.2581	$R_{com0}(\Omega)$	0.080312
$R_{act2}(u)$	0.00112x(T-298)	$R_{com2}(\Omega)$	0.0002747x(T-298)
$R_{act1}(u)$	$-1.6777\times10^{-6}I^5+1.2232\times10^{-5}I^4$		
$R_{one1}(u)$	$-0.010089I^3+0.005554I^2-0.010542I$		

The number of fuel cell stacks per string is

$$= \frac{15000}{58.9} \cong 255$$

The number of strings is $= \frac{255}{16} \cong 16$

4.5.4 Electrolyzer

The Electrolyzer produces hydrogen from hydrolysis of water that will be fed to the fuel cell which is operated at times when the output from wind and solar systems fails to satisfy the load. The fuel cell stacks contain a number of fuel cells. The cost of

Electrolyzer, its replacement and O&M costs as used for simulation are shown in Table 4.6.

4.5.5 Converter

Here converter is used which can work both as an inverter and rectifier depending on the direction of flow of power. The inverter was rated based on the maximum output of the PV farm. It is assumed that the inverter has an efficiency of 90%. The initial cost of the inverter is 300$/kW, while the replacement cost is 200$/kW. The operating and maintenance cost estimated as 50 $/kw/yr.

4.5.6 Hydrogen Tank

The calorific energy content of Hydrogen is about 39kWh/kg [44], taking into account the process inefficiencies, it takes over 50 kWh of electricity to generate 1kg of Hydrogen. Assuming that the efficiency of the fuel cell is 60% and it supplies power for the Woreda at least for 10 hours, the storage capacity of the Hydrogen tank is 300kg.The initial cost of the tank is 150$/kg, while the replacement cost is 100$/kg [46]. The operating and maintenance cost estimated as 10 $/kw/yr.

4.5.7 Connected electric load

Electrical load is one or more devices that consume electric energy. The data were assumed for the total hourly basis daily electrical load requirement of a residential and public of Berehet Woreda. The expected load consumption profile of the area is shown in Figure below. The daily load requirement of the intended village cluster is found to be 12,588 kWh per day.

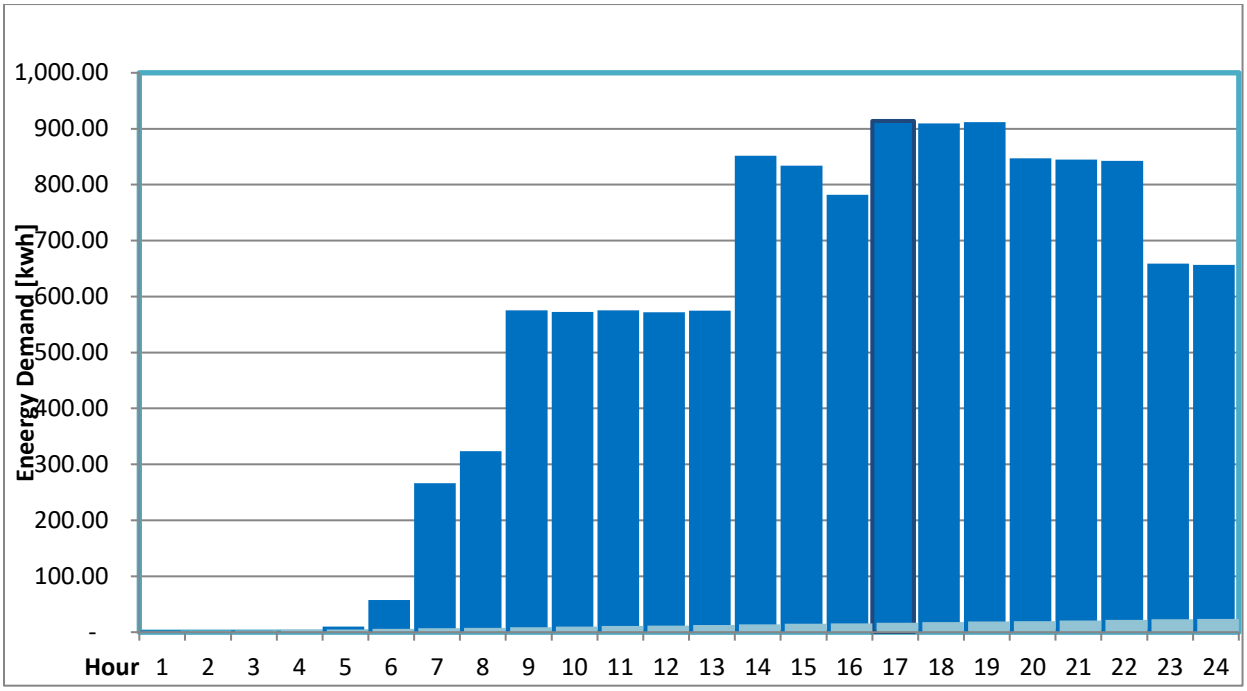

Figure 4.5 Hourly load consumption

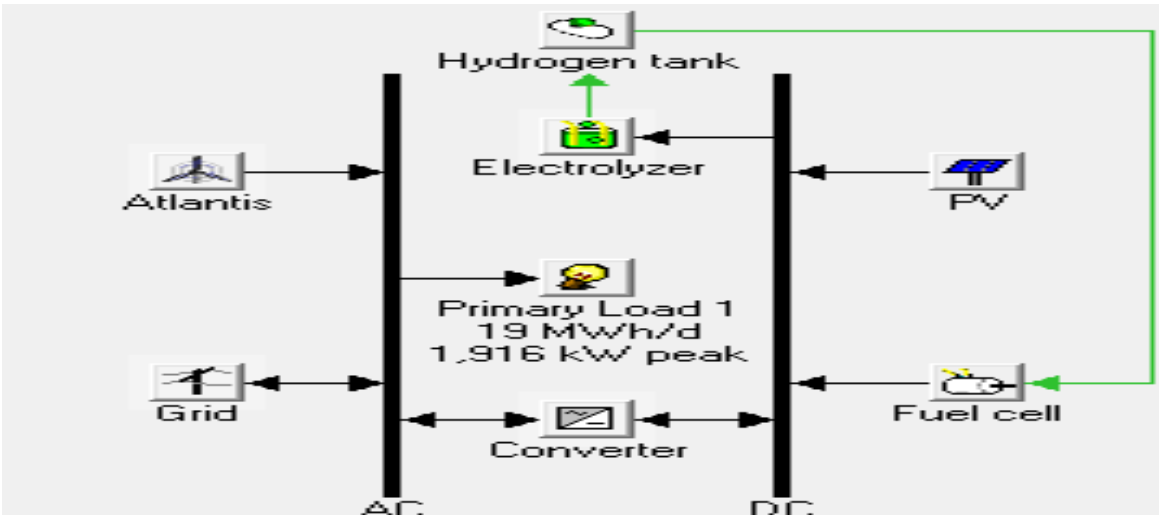

Figure 4.6 Proposed scheme of hybrid energy generation for the study area in Homer software model

CHAPTER 5

Results, Conclusion and Recommendations

5.1 Results and Discussions

The main part of the thesis focuses on the modeling, control, optimization and financial analysis of the hybrid system. The outputs of the simulation are shown in the appendix part of this paper.

HOMER simulates system configurations with all of the combinations of components that are specified in the component input. HOMER performs hundreds or thousands of hourly simulations (to ensure best possible matching of demand and supply) and offers a list of feasible schemes ranked on the basis of the NPC (net present cost). The strategy taken in this simulation is to ensure the power generator provide enough power to meet the demand. The renewable energy sources in collaboration with the utility grid were evaluated to determine the feasibility of the system. The system is also simulated in order to evaluate its operational characteristics, namely annual electrical energy production, annual electrical load served, excess electricity, renewable energy fraction, capacity shortage and unmet load as shown in Appendix-3.

HOMER presents a list of feasible systems classified by lifecycle cost as summarized in Figure 5.1; the three options are analyzed

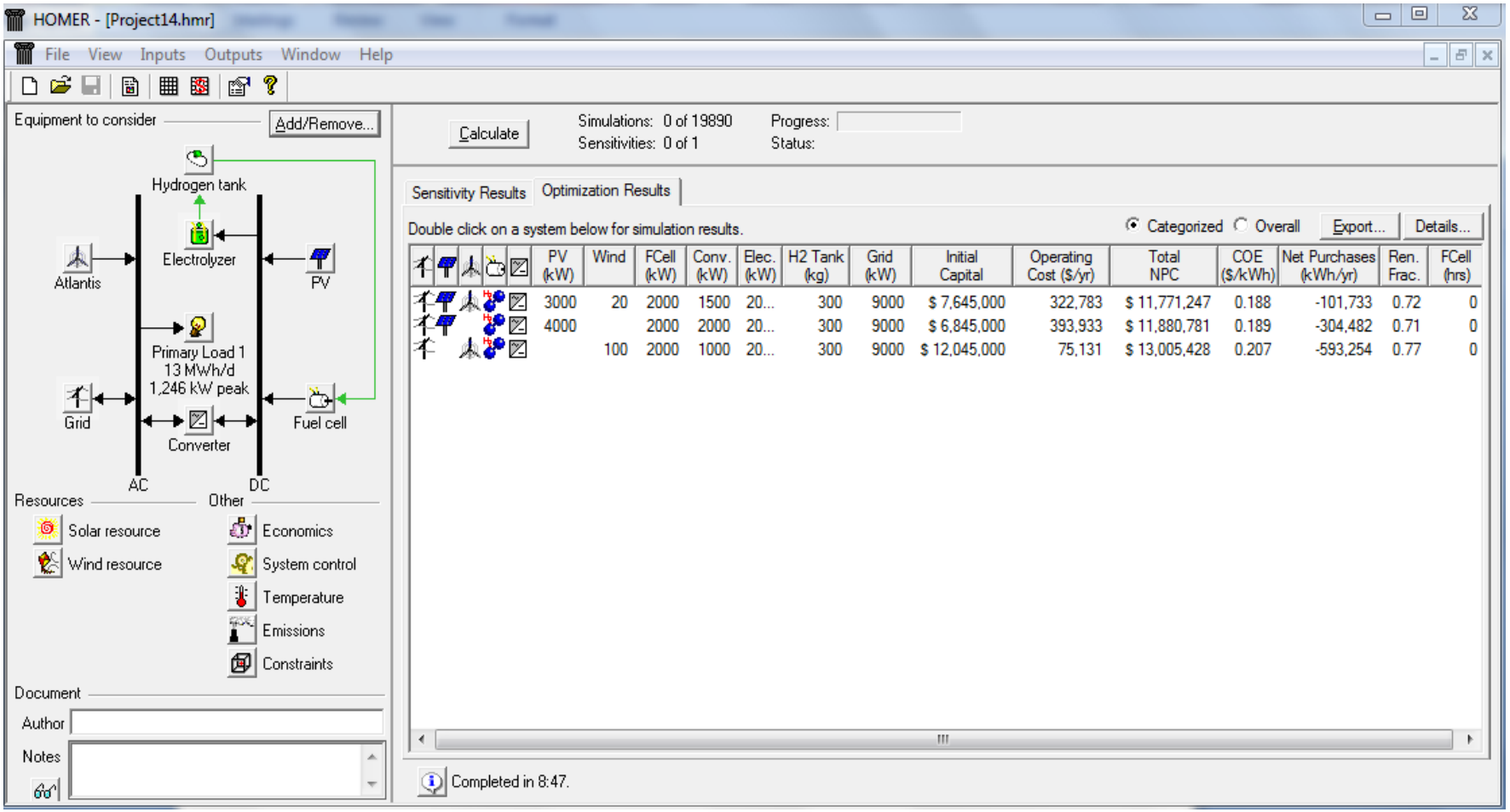

Figure 5.1 List of feasible solutions

From Figure 5.1, it can be observed that the first and the cheapest scenario is when electricity supplied to the Woreda and grid comes from the combinations of 300kW solar park and 20 wind turbines with 50kW rated capacity which sells 1kWh of electricity at 0.188$. The initial capital is USD 7,645,000.00. The replacement and O&M costs are 561,249.00$ and 4,152,157.00$ respectively. The second most cost-effective scenario is when the solar energy supports the grid by supplying 71% of the load. The wind energy has no place. With 29% from the grid and 71% from PVs, 1 kWh costs 0.189$. In the third scenario the wind turbine delivers yearly 77% of electricity to the house, the rest is supplied by the grid, without the participation of solar energy. The wind/grid connected loads buys electricity at 0.207$/kWh.

Based on the result of optimization from Homer, the total capacity of the solar farm is 3MW

The Current that is produced from the solar park is

$$\frac{3MW}{15kV} = 200A$$

ATI-2000(230) solar module is selected for this case study which has maximum power point current and voltages are 7.8 Ampere and 29.49V respectively. The number of strings in the solar park is

$$= \frac{188.667}{7.8} \cong 26$$

The number of modules per string is calculated to be

$$= \frac{15000}{29.49} \cong 510$$

There will be 13,260 PV modules each having a capacity of 230W to have total output of 3MW.

The fuel cell energy generation system is for the times when there is no enough grid supply, no solar and wind power. The maximum load demand (peak load) of the Woreda is around 1MW. So, it is safe to put fuel cell which has a capacity of 2MW.

5.2 Comparison of the Hybrid Distributed Generation System with the Extension of the Utility grid to the Woreda

The case study area is around 75km from the utility grid which is the nearby Metehara substation. The detail of cost analysis for the extension of the utility grid to this woreda is show in the Appendix 7.

The total summarized cost for distribution line and substation extension are as shown in Table 5.1 and 5.2. Single circuit 33kV distribution line is to be constructed to the case study area. Concrete pole with span length of 70m is considered. One new transformer bay and two 33kV feeders at Metehara substation are to be constructed. Four 400kVA distribution transformers will be installed in Berehet Woreda which will be interconnected. The total cost for the grid extension is around Birr 49,141,574.32 which is equivalent to USD 2,457,078.72. The grid sales energy at cost of 0.06/kWh.

Table 5.1 Summary of price for 33 kV distribution line

No	Description of Materials	Unit	Qty.	Unit PRICE	Total Price
1	CONCRETE POLE 12D 20 12MT LENGTH	ea	1072	10,494.10	11,249,675.20
2	Heavy angle Cross arm 2 mts	ea	1072	869.41	932,007.52
3	Dead end cross arm 2 mts	ea	5	872.88	4,364.40
4	Big collar	ea	1072	58.71	62,937.12
5	Bolt and Nut M10	ea	540	40.06	21,632.40
6	Insulator Pin, 15 kv	ea	3216	128.98	414,799.68
7	HT Insulator 15 kv 18/5mm^2	ea	3216	434.14	1,396,194.24
8	Gal steel wire 7x2.65	kg	410	36.23	14,854.30
9	AAC 95mm^2	mt	232500	27.5	6,393,750.00
10	AL-Al Clamp	ea	125	6.54	817.50
11	15 kV stay insulator	ea	270	34.71	9,371.70
12	Wire round aluminum for tie	kg	128	48.4	6,195.20

13	Long bolt 16 mm 40cm	ea	270	36.35	9,814.50
14	Chain insulator 16mm^2	ea	6800	121.63	827,084.00
15	Ball eye	ea	3233	21.22	68,604.26
16	socket eye	ea	3233	20.73	67,020.09
17	Small collar with nut	ea	3233	45	145,485.00
18	Strain clamp	ea	3233	81	261,873.00
19	CEMENT	KG	75051	20.95	1,572,318.45
20	SAND MOJO	MT^3	2250	550	1,237,500.00
21	GRAVEL	MT^3	2250	575	1,293,750.00
22	Washer 3/4" 5/8	kg	270	20	5,400.00
		Material Cost			25,995,448.56
		Transport Cost			1,300,000.00
		G. T O T A L			**27,295,448.56**

Source: - The Ethiopian Electric Power

Table 5.2 Summary of price for substation extension

Item	Description		SUPPLY (FOB)	Sea transport	Inland transport	Erection, test and commissioning (Birr)	
			Amount USD	USD	Amount Birr	Amount	AMOUNT
1	**132 kV SIDE, of 132/33 TRANSFORMER BAY**		64,837.50	9,262.50	18,525.00	15,641.30	**94,061.32**
2	**OUTDOOR TERMINAL CABINETS**		4,375.00	625.00	1,250.00	966.89	**6,335.40**
3	**CONTROL & PROTECTION PANELS**		82,250.00	11,750.00	23,500.00	12,942.45	**118,804.42**
4	**33 KV METAL CLAD SWITCHGEAR (INDOOR)**		28,000.00	4,000.00	8,000.00	3,500.00	**40,350.75**
5	**33 KV OUTDOOR SWITCHGEAR**		171,048.73	24,435.53	48,871.06	3,882.46	**244,755.27**
6	**STEEL STRUCTURES**		70,000.00	10,000.00	20,000.00	24,000.00	**101,427.73**
7	**AUTO TRANSFORMERS**		284,731.80	3,604.20	72,084.00	8,205.24	**361,979.61**
8	**CIVIL WORKS**		0.00	0.00	0.00	354,988.48	**20,411.84**
TOTAL CARRIED OUT TO FINAL SUMMARY OF PRICES		**USD**					**988,126.33**

Source: - The Ethiopian Electric Power

Exchange rage USD 1= Birr 20

Table 5.3 Cost of Installing Distribution Transformer

S.N	Description	Unit	Qty.	Unit price Birr	Total price Birr
09-02-120	Imp. Wooden pole 10mt.	ea	2	920.00	1,840.00
09-03-100	Cross arm for transformer	set	3	4825.28	14,475.84
03-02-450	Drop out fuse 33kv	ea	3	5723.39	17,170.17
03-05-160	Lightening arrester 33kv	ea	3	2833.08	8,499.24
03-02-400	Fuse mount 33KV	ea	3	411.98	1,235.94
03-01-010	33kv insulator	ea	6	434.14	2,604.84
03-01-010	33kv pin	ea	6	128.98	773.88
02-06-110	Hook n-95	ea	4	85.73	342.92
12-04-860	Long bolt5/8"	kg	6	66.13	396.78
04-05-040	Cu wire stranded 35mm	kg	35	198.91	6,961.85
04-05-580	Earthing rode	Mt.	2	235.85	471.70
12-02-310	Washer 5/8"	kg	5	25.30	126.50
02-07-190	Pole mount fuse 3*400A	ea	1	3714.44	3,714.44
05-02-262	Transformer 400 kva	ea	1	459,629.43	459,629.43

Material Cost	**518,243.53**
Transport Cost	**2,656.26**
GRAND TOTAL	**520,899.79**

Source:- The Ethiopian Electric Power

Since the load demand of the case study area is around 1MW, four 400kVA distribution transformers are required. The installation cost of the five transforms is Birr 2,083,599.16. Therefore, the total cost of extension work to connect the case study area to the utility grid is

$$Total\ cost = 988{,}126.33 * 20 + 27{,}295{,}448.56 + 2{,}083{,}599.16$$

$$Total\ cost = 49{,}141{,}574.32$$

5.3 Conclusion

The conclusions of the research work reported in this thesis are summarized below.

1. Environmentally friendly and sustainable alternative energy systems is developed which will play more important roles in the future electricity supply.
2. Dynamic models have been developed for the solar array and wind farm systems.
3. A hybrid wind/PV/FC DG system is proposed in this thesis. Wind and PV are the primary power sources of the system, and the combination of FC and electrolyzer is used as a backup and long term storage unit. The different energy sources in the system are integrated through an AC link bus. The system can be used as test-bed system for other related studies on hybrid alternative energy systems.
4. Based on the dynamic component models, a simulation model for the proposed hybrid wind/PV/FC energy system has been developed successfully using MATLAB/Simulink.

The PV/wind/grid hybrid system for the case study area, from the optimum result of HOMER, contains 3000 kW PV array, Twenty Atlantics wind turbines and 2000kW Fuel cell stack, with a total NPC of 7,645,000.00$ and a COE of 0.188$/kWh. The monthly energy yield of each component of the system is shown in Figure 5.2. As can be noticed, the share of PV in supplying the electricity is more than that of wind turbine in the whole year.

Even if the optimum result of the homer output for the hybrid system sales energy at cost of 0.188/kWh, when it is compared to the grid extension it is comparatively more expensive. The initial cost of the hybrid system is USD 7,645,000.00 while connecting the case study area to the utility grid costs USD 2,457,078.72. Based on the result of comparison, it is recommended to connect the Berehet Woreda to the existing national grid as the current market of renewable energy resources is more expensive. But the trend which is currently observed on price decrease of the solar, wind, fuel cell, electrolyzer…etc, clearly indicate in the near future the installation of Distributed Generation System's cost will be competitive to that of the Hydropower generation system.

Figure 5.2 Share of energy sources

5.4 Recommendation for Further Work

1. The study recommends collecting wind speed data at the actual site at three different heights for at least one complete year. This data then must be used for final feasibility of the hybrid system.
2. This study focus on only one Woreda/Village in Ethiopia. So, the future researchers should expand this research work in other sites and make the rural people beneficial with renewable energy resource.
3. In spite of the huge hydroelectric potential of Ethiopia, severe power cuts in recent years have a heavy impact on the country's economy. So in order to make the supply of power uninterrupted it is recommended to have a backup system. Replacing the fuel cell system with diesel generators is another recommendation so as to evaluate the hybrid system according to cost point of view.
4. The Software MATLAB and HOMER used for optimization in this study are not officially licensed and do not have capacity to solve different types of sensitivity analysis and other advanced features, and the licensed one is commercially available for the future use of similar assignments.

References

1. *http://www.giz.de/themen/en/30559.htm*
2. *www.eepco.gov.et*
3. *Federal Democratic Republic of Ethiopia Ministry of Water and Energy, " Scaling--Up Renewable Energy Program, Ethiopia Investment Plan".2012*
4. *http://en.wikipedia.org/wiki/Energy_in_Ethiopia*
5. *Modeling and Control of Hybrid Wind/Photovoltaic/Fuel Cell Distributed Generation Systems, by Caisheng Wang.2006*
6. *‹Optimization of PV/Wind/Micro-Hydro/Diesel Hybrid Power System in HOMER for the Study Area, International Journal on Electrical Engineering and Informatics - Volume 3, Number 3, 2011 Deepak Kumar Lal1, Bibhuti Bhusan Dash2, and A. K. Akella3›*
7. *Economic Analysis of Hybrid Renewable Model for Subtropical Climate Int. J. of Thermal & Environmental Engineering2010, GM Shafiullah*, a, Amanullah M.T. Ooa, ABM Shawkat Ali b, Dennis Jarvis b, Peter Wolfs c*
8. *]. Sizing Optimization and Analysis of a Stand-alone WTG System Using Hybrid Energy Storage Technologies, AIP Journal 2011,PrabodhBajpai, Sowjan Kumar, and N. K. Kishore**
9. *Jose´ L. Bernal-Agustı´n Rodolfo Dufo-Lo´ pez "Simulation and optimization of stand-alone hybrid renewable energy systems", 2009.*
10. *http://www.mpoweruk.com/wind_power.htm*
11. *Africa Renewable energy access program, Lighting Africa 2012.*

12. *J. Gow and C. Manning, "Controller arrangement for boost converter systems sourced from solar photovoltaic arrays or other maximum power sources," Proc.Inst. Electr. Eng. Electr. Power Appl., Jan. 2000.*
13. *J. Enslin, M.Wolf, D. Snyman, and W. Sweigers, "Integrated photovoltaic maximum power point tracking converter," IEEE Trans. Ind. Electron., Dec. 1997.*
14. *http://en.wikipedia.org/wiki/Wind_farm*
15. *http://www.hindawi.com/journals/ijp/2013/217526/*
16. *Gomez, S. A. and Amenedo, J. L. R., "Grid synchronisation of doubly fed induction generators using direct torque control", Proceedings of IEEE 28th Annual conference ofthe Industrial Electronics Society, Sevilla, Spain, Nov. 5-8, 2002.*
17. *Petersson, A., Analysis, modeling and control of Doubly-Fed Induction Generators for wind turbines, PhD thesis, Chalmers University of Technology, Göteborg, Sweden, 2005.*
18. *Hansen, A. D., Sørensen, P., Iov, F. and Blaabjerg, F., "Centralised power control of wind farm with doubly fed induction generators", Renewable Energy, 2006.*
19. *G. Bekele and B. Palm, "Feasibility study for a standalone solar-wind-based hybrid energy system for application in Ethiopia," Applied Energy, vol. 87, no. 2, pp. 487–495, 2010.*
20. *M. Lalwani, D. P. Kothari, and M. Singh, "Viability analysis by techno-economic aspects of grid interactive solar photovoltaic project in indiaon," in Proceedings of the International Conference on Advances in Engineering, Science and Management (ICAESM '12), 2012.*

21. *J. L. Bernal-Agustín and R. Dufo-López, "Simulation and optimization of stand-alone hybrid renewable energy systems," Renewable and Sustainable Energy Reviews, 2009.*
22. *A. N. Celik, "Optimisation and techno-economic analysis of autonomous photovoltaic-wind hybrid energy systems in comparison to single photovoltaic and wind systems," Energy Conversion and Management, 2002.*
23. *M. K. Deshmukh and S. S. Deshmukh, "Modeling of hybrid renewable energy systems, "Renewable and Sustainable Energy Reviews, 2008.*
24. *E. Koutroulis, D. Kolokotsa, A. Potirakis, and K. Kalaitzakis, "Methodology for optimal sizing of stand-alone photovoltaic/wind-generator systems using genetic algorithms," Solar Energy, 2006.*
25. *A. Gupta, R. P. Saini, and M. P. Sharma, "Steady-state modeling of hybrid energy system for off grid electrification of cluster of villages," Renewable Energy, 2010.*
26. *F. Giraud and Z. M. Salameh, "Steady-state performance of a grid-connected rooftop hybrid wind—photovoltaic power system with battery storage," IEEE Transactions on Energy Conversion, 2001.*
27. *M. P. McHenry, "Are small-scale grid-connected photovoltaic systems a cost-effective policy for lowering electricity bills and reducing carbon emissions A technical, economic, and carbon emission analysis," Energy Policy, 2012.*
28. *H. Yang, Z. Wei, and L. Chengzhi, "Optimal design and techno-economic analysis of a hybrid solar-wind power generation system," Applied Energy, 2009.*
29. *G. M. Tina and S. Gagliano, "Probabilistic modeling of hybrid solar/wind power system with solar tracking system," Renewable Energy, 2011.*
30. *James Larminie, Andrew Dicks, "Fuel Cell Systems Explained", 2003*

31. *http://www.chinatechgadget.com/china-to-complete-worlds-first-4in1-hybrid-green-power-station.html*
32. *O. Wasynzczuk, "Dynamic behavior of a class of photovoltaic power systems," IEEE Trans. Power App. Syst., Sep. 1983.*
33. *K. Hussein, I. Muta, T. Hoshino, and M. Osakada, "Maximum photovoltaic power tracking: An algorithm for rapidly changing atmosphere conditions," Proc. Inst. Electr. Eng., Jan. 1995.*
34. *http://aigaforum.com/articles/eth-energy-sector-bright2.php*
35. *Mohamed A. H. El-Sayed and Adel M. Sharaf "Hybrid Wind-Fuel Cell Renewable Energy Utilization Scheme for Village Electricity", 2010.*
36. *Deepak Kumar Lal1, Bibhuti Bhusan Dash2, and A. K. Akella3, "Optimization of PV/Wind/Micro-Hydro/Diesel Hybrid Power System in HOMER for the Study Area" International Journal on Electrical Engineering and Informatics - Volume 3, Number 3, 2011.*
37. *GM Shafiullah , Amanullah M.T. Oo, ABM Shawkat Ali , Dennis Jarvis , Peter Wolfs. "Economic Analysis of Hybrid Renewable Model for Subtropical Climate" Int. J. of Thermal & Environmental Engineering 2010.*
38. *Prabodh Bajpai, Sowjan Kumar, and N. K. Kishore, "Sizing Optimization and Analysis of a Stand-alone WTG System Using Hybrid Energy Storage Technologies", AIP Journal 2011.*
39. *http://americanhistory.si.edu/fuelcells/basics.htm*
40. *M. Buresch: Photovoltaic Energy Systems Design and Installation, McGraw-Hill, New York, 1983.*
41. *http://www.mpoweruk.com/wind_power.htm*

42. *http://setis.ec.europa.eu/setis-deliverables/technology-mapping/technology-map-chapters-2011/wind-power-generation*
43. *http://solarlove.org/solar-cell-model-and-its-characteristics*
44. *http://www.mpoweruk.com/hydrogen_fuel.htm*
45. *http://en.wikipedia.org/wiki/Fuel_cell*
46. *http://www.alibaba.com/product-detail/High-quality-hydrogen-storage-tank-vessel_1045723525.html*
47. *http://www.mdpi.com/energies/energies-0801373/article_deploy/html/*images */energies-08-01373-g008-1024.png*
48. *http://www.emrwebsite.org/uploads/images/EMR11/walter_pv_4.png*
49. *Ethiopian Electric Power Corporation, Facts in brief 2010/2011*

Appendixes

1. ATI-2000(230) Photovoltaic modules technical specification

PHOTOVOLTAIC ONGRID OPTIMIZED MODULE

36 Modules / Pallet
1,922 LBS / Pallet
130"H x 75"W x 55"L

Tel:(909)468-1800

ATI high efficiency module size is easy to handle and specifically designed for large and small scale grid interactive applications.

ATI 's module uses state of the art multicrystalline technology with a Silicon Nitride (SiN) coating that enhances cell efficiency. Encapsulation beneath high transmission tempered glass is accomplished using an advanced, UV resistant thermal setting plastic. The encapsulant, ethylene vinyl acetate, cushions the solar cells within the laminate and protect the cells from etching. The rear surface of the module is completely sealed from moisture and mechanical damage by a continuous high strength polymer sheet.

ATI 's module incorporates a reinforced anodised aluminium frame, designed to meet ATI's High Quality Standards for corrosion resistance.

ABSOLUTE MAXIMUM RATINGS		
Parameters	Rating	Unit
Operating temperature	-40 to +90	℃
Storage temperature	-40 to +90	℃
Dielectric voltage withstood	2200 max	V-DC

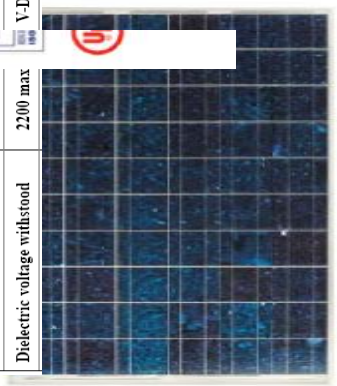

Weight: 45.34 LBS

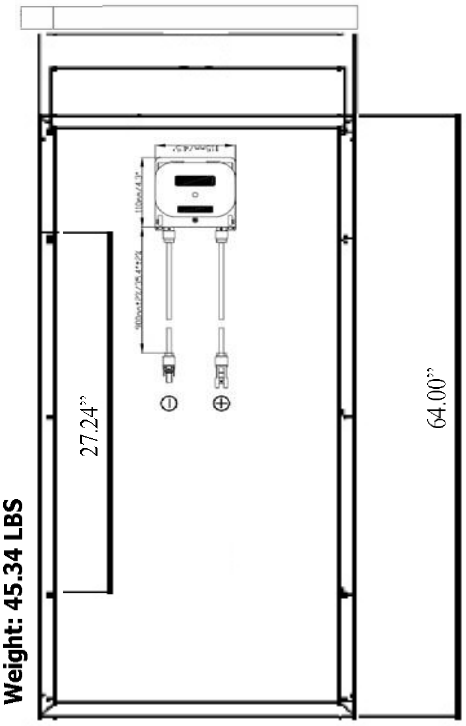

STC Power Rating	230.0W @ STC
CSI- PTC Power Rating	197.9W @ PTC
Maximum Power Voltage (Vpm)	29.4V
Maximum Power Current (Ipm)	7.80A
Open Circuit Voltage (Voc)	37.20V
Short Circuit Current (Isc)	8.39 A
Cell Type / # Cells	Poly / 60 Series
Nominal Voltage	20Vdc
Maximum System Voltage	DC 600V
Series Fuse Rating	15A
Performance Tolerance	+- 3%

Limited warranty : 25 years

Fax:(909)468-9880

Tel:(909)468-1800
Fax:(909)468-9880

3930-B Valley Blvd.
Walnut, CA 91789

Rev 11/16/08

Rev 11/16/08

MODEL: ATI-2000(230W)

PHOTOVOLTAIC ONGRID OPTIMIZED MODULE

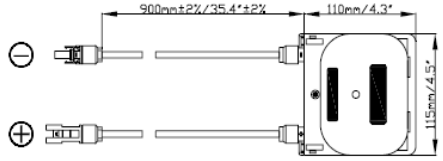

ELECTRICAL CHARACTERISTICS

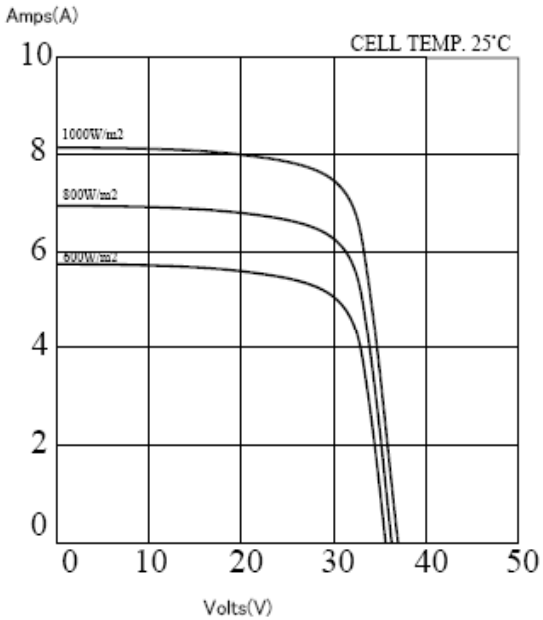

DEPENDENCE ON TEMPERATURE

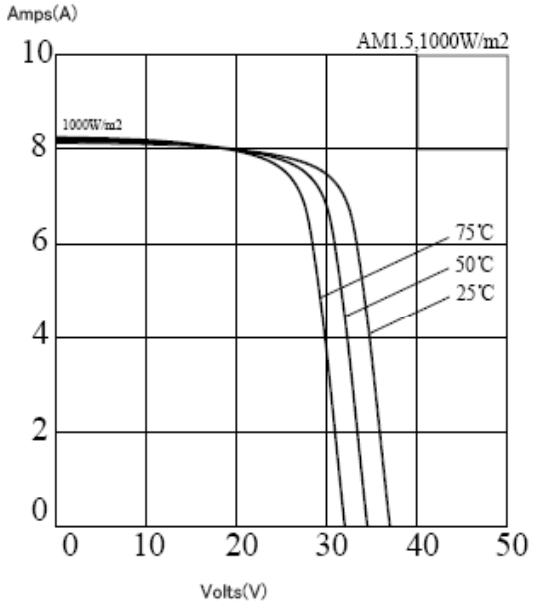

Temperature coefficient of Isc: 0.08%/℃

Power temperature coefficient: -0.38%/℃

Temperature coefficient of Voc: -0.32%/℃

NOCT:46±1℃

Limited warranty : 25 years

Walnut, CA 91789

2. HOMER Output Summary

System architecture

PV Array	3,000 kW
Wind turbine	20 Atlantis
Fuel cell	2,000 kW
Grid	9,000 kW
Inverter	1,500 kW
Rectifier	1,500 kW
Electrolyzer	2,000 kW
Hydrogen Tank	300 kg

Cost summary

Total net present cost	$ 11,771,247
Levelized cost of energy	$ 0.188/kWh
Operating cost	$ 322,783/yr

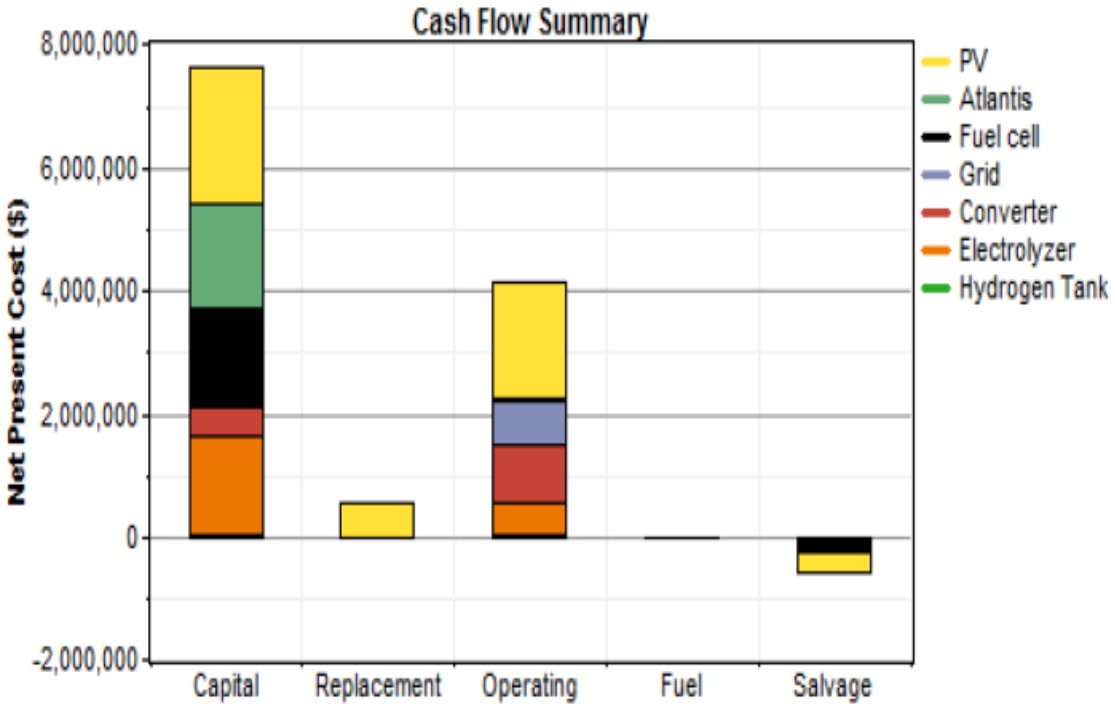

Net Present Costs

Component	Capital	Replacement	O&M	Fuel	Salvage	Total
	($)	($)	($)	($)	($)	($)
PV	2,250,000	561,249	1,917,505	0	-314,549	4,414,205
Atlantis	1,700,000	0	20,453	0	0	1,720,453
Fuel cell	1,600,000	0	0	0	-272,609	1,327,391
Grid	0	0	705,762	0	0	705,762
Converter	450,000	0	958,752	0	0	1,408,752
Electrolyzer	1,600,000	0	511,335	0	0	2,111,335
Hydrogen Tank	45,000	0	38,350	0	0	83,350
System	7,645,000	561,249	4,152,157	0	-587,157	11,771,250

Annualized Costs

Component	Capital	Replacement	O&M	Fuel	Salvage	Total
	($/yr)	($/yr)	($/yr)	($/yr)	($/yr)	($/yr)
PV	176,010	43,905	150,000	0	-24,606	345,309
Atlantis	132,985	0	1,600	0	0	134,585
Fuel cell	125,163	0	0	0	-21,325	103,837
Grid	0	0	55,209	0	0	55,209
Converter	35,202	0	75,000	0	0	110,202
Electrolyzer	125,163	0	40,000	0	0	165,163
Hydrogen Tank	3,520	0	3,000	0	0	6,520
System	598,043	43,905	324,810	0	-45,931	920,826

Electrical

Component	Production (kWh/yr)	Fraction
PV array	4,549,771	58%
Wind turbines	1,099,770	14%
Fuel cell	0	0%
Grid purchases	2,145,514	28%
Total	7,795,054	100%

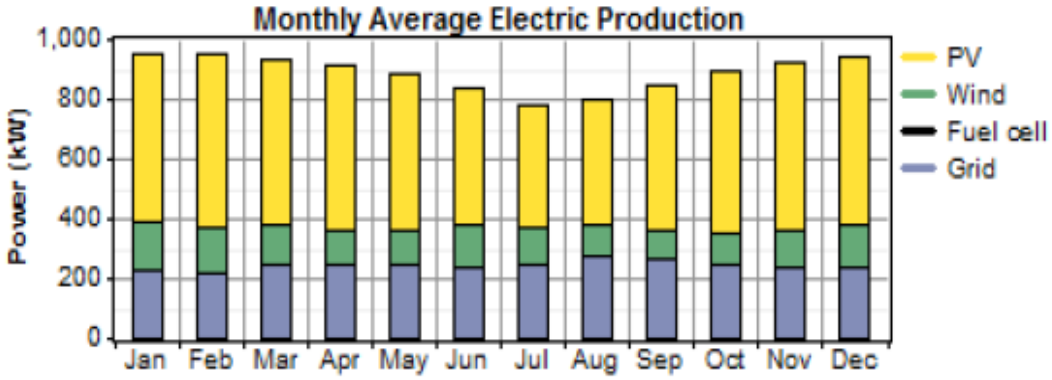

Load	Consumption (kWh/yr)	Fraction
AC primary load	4,905,604	69%
Electrolyzer load	3,075	0%
Grid sales	2,247,246	31%
Total	7,155,925	100%

Quantity	Value	Units
Excess electricity	204,959	kWh/yr
Unmet load	0.00307	kWh/yr
Capacity shortage	0.00	kWh/yr
Renewable fraction	0.725	

PV

Quantity	Value	Units
Rated capacity	3,000	kW
Mean output	519	kW
Mean output	12,465	kWh/d
Capacity factor	17.3	%
Total production	4,549,771	kWh/yr

Quantity	Value	Units
Minimum output	0.00	kW
Maximum output	2,298	kW
PV penetration	92.7	%
Hours of operation	4,387	hr/yr
Levelized cost	0.0759	$/kWh

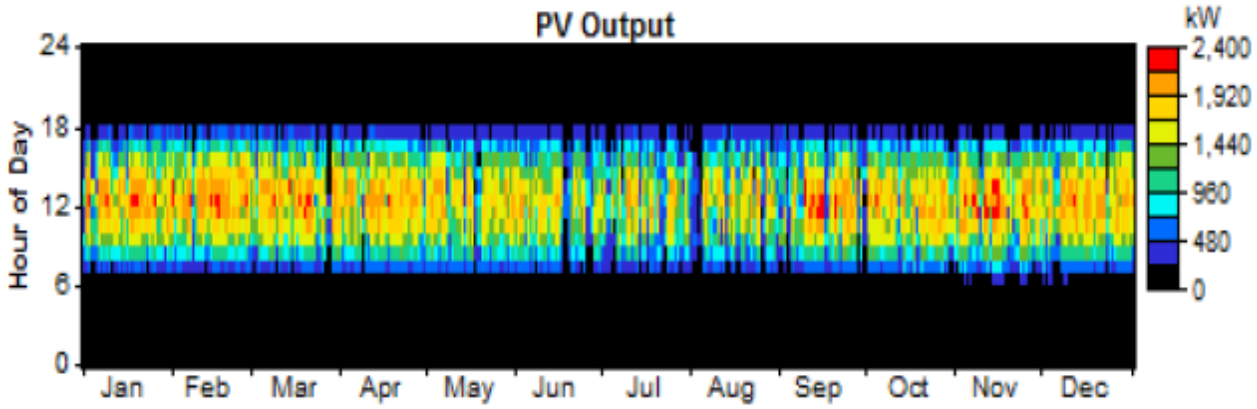

AC Wind Turbine: Atlantis

Variable	Value	Units
Total rated capacity	1,000	kW
Mean output	126	kW
Capacity factor	12.6	%
Total production	1,099,770	kWh/yr

Variable	Value	Units
Minimum output	0.00	kW
Maximum output	996	kW
Wind penetration	22.4	%
Hours of operation	7,427	hr/yr
Levelized cost	0.122	$/kWh

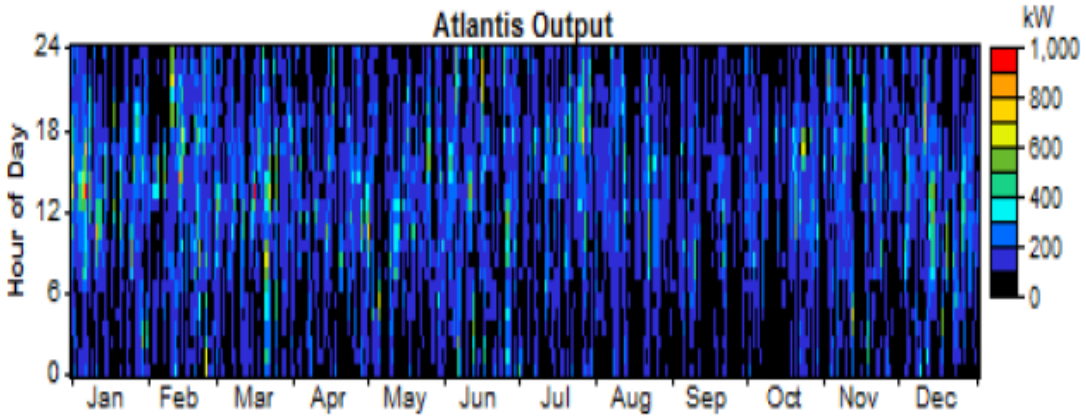

Grid

Rate: Rate 1

Month	Energy Purchased (kWh)	Energy Sold (kWh)	Net Purchases (kWh)	Peak Demand (kW)	Energy Charge ($)	Demand Charge ($)
Jan	171,795	226,607	-54,812	1,170	221	0
Feb	147,059	205,847	-58,788	1,140	-879	0
Mar	182,185	210,961	-28,776	1,186	2,876	0
Apr	176,950	199,143	-22,192	1,126	3,311	0
May	183,353	195,494	-12,141	1,067	4,408	0
Jun	174,155	162,250	11,906	1,188	6,296	0
Jul	183,011	131,491	51,520	1,044	10,127	0
Aug	204,077	134,709	69,368	1,125	12,365	0
Sep	191,329	155,030	36,299	1,138	9,007	0
Oct	184,625	198,682	-14,056	1,188	4,274	0
Nov	169,379	204,185	-34,806	1,129	1,949	0
Dec	177,595	222,848	-45,253	1,185	1,255	0
Annual	2,145,514	2,247,246	-101,733	1,188	55,209	0

3. Sub Models of Photovoltaic Array

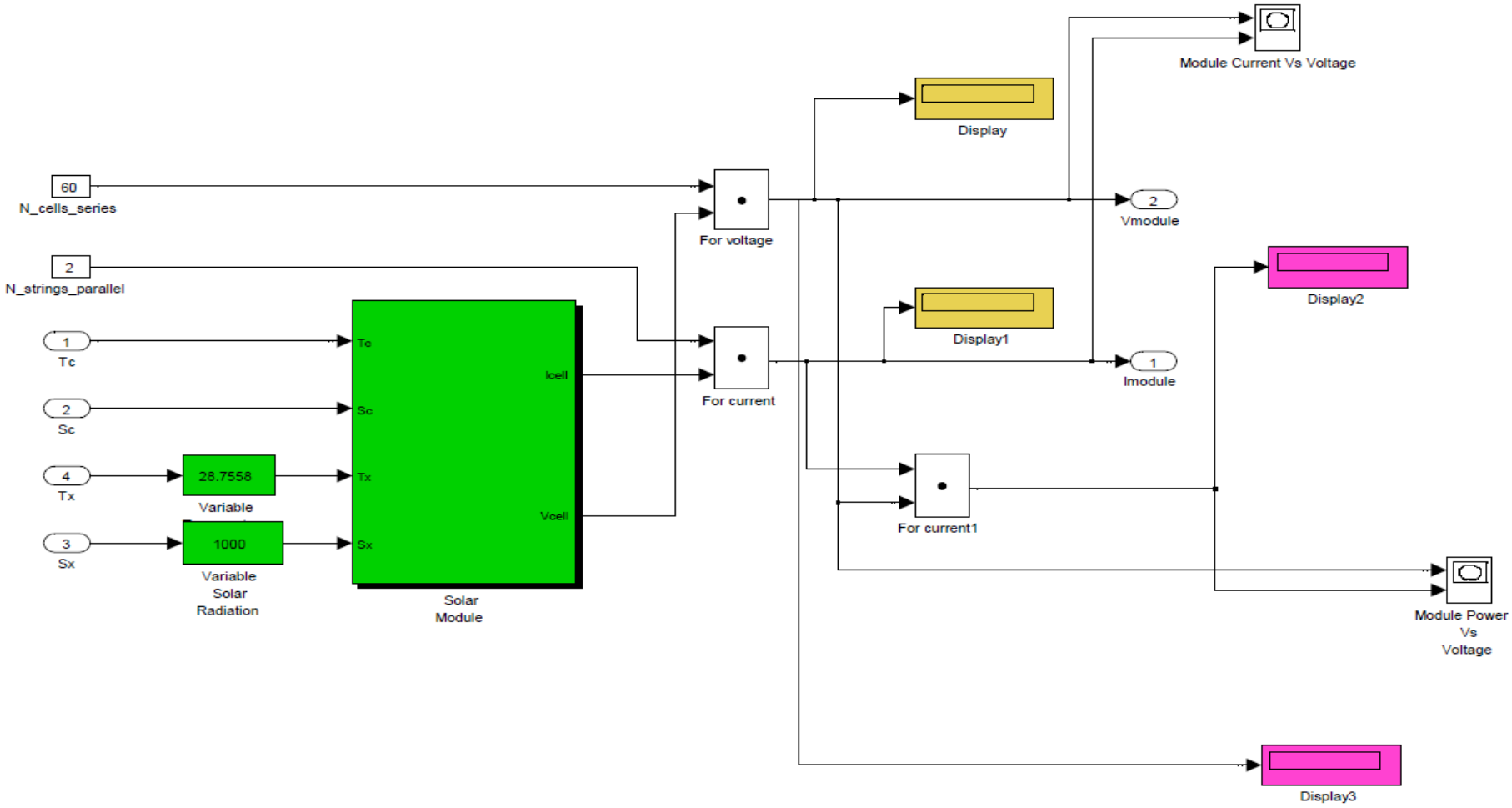

3.1 Solar Module

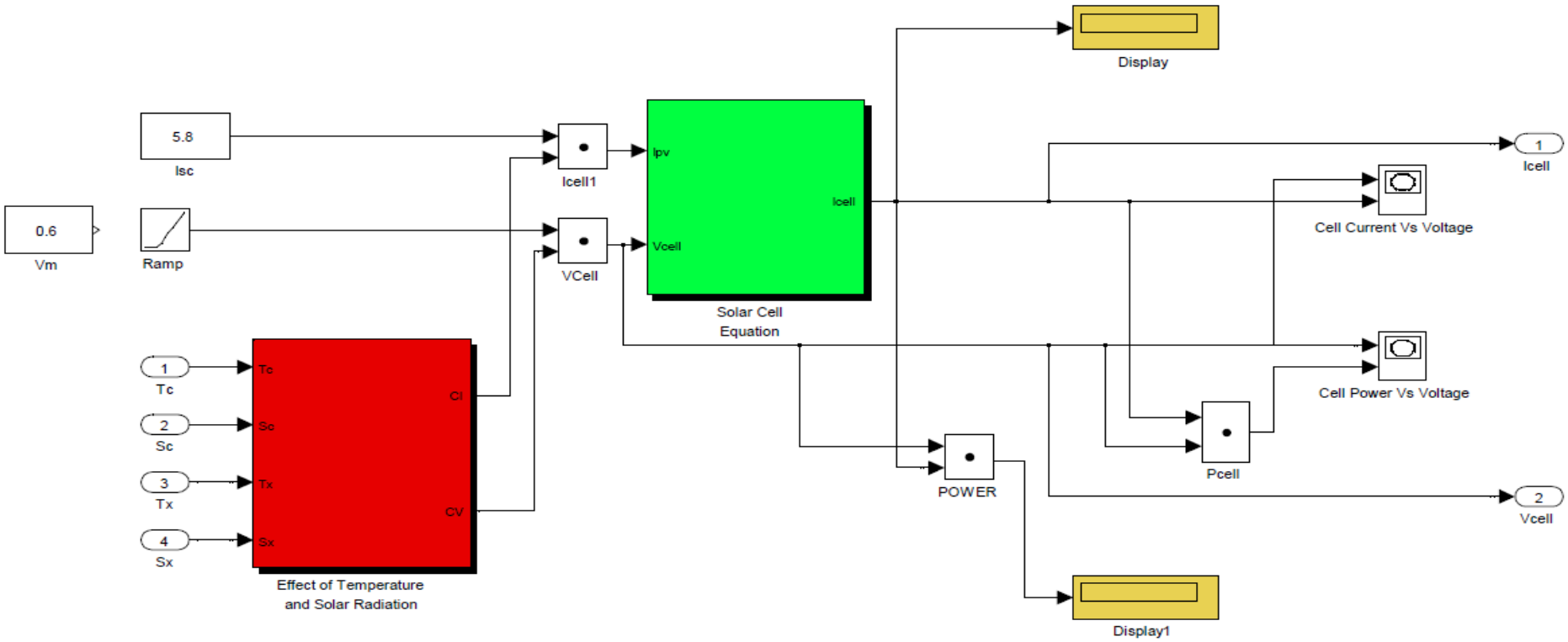

3.2 Effect of Temperature & Solar Irradiation

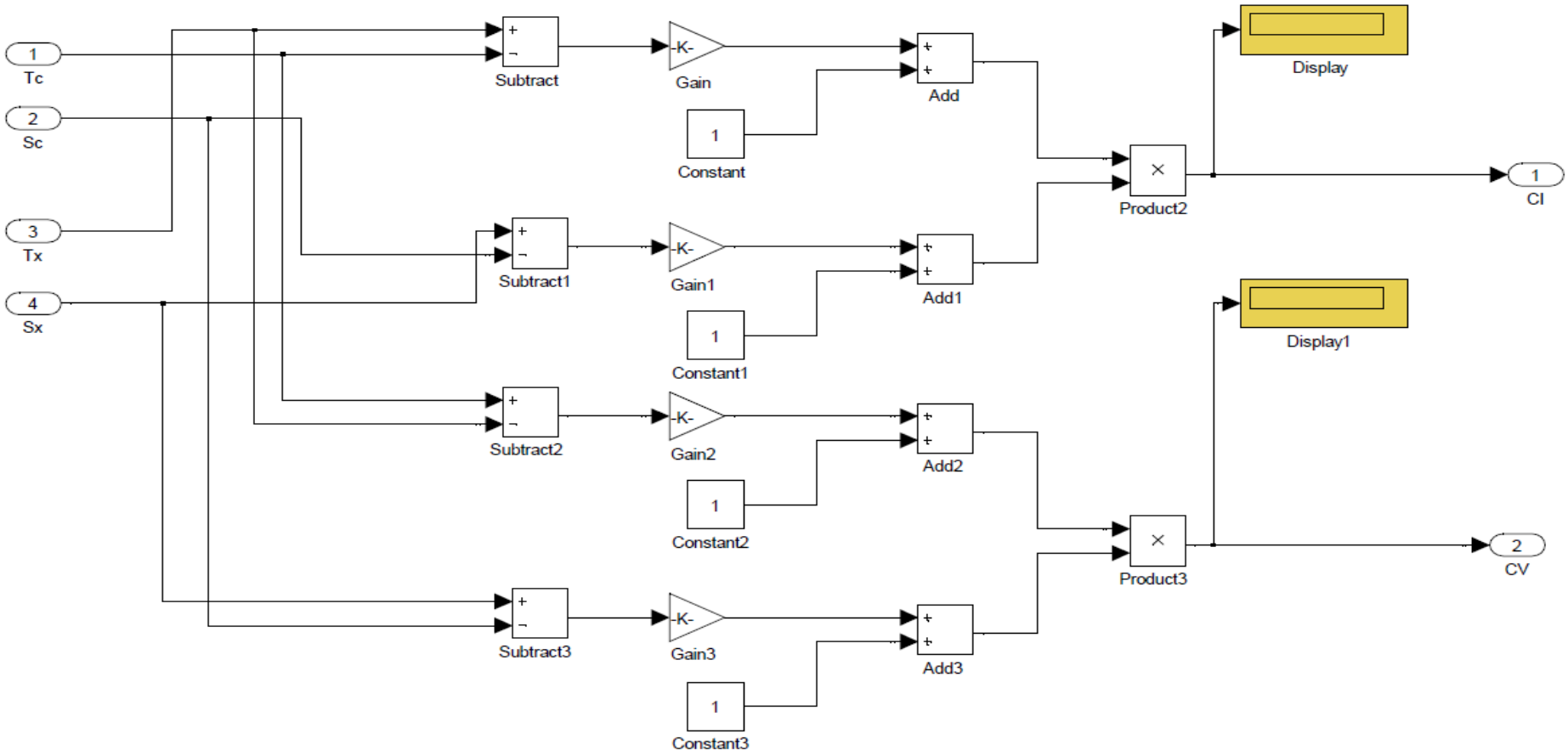

Matlab Simulink Results

4.1 PV outputs

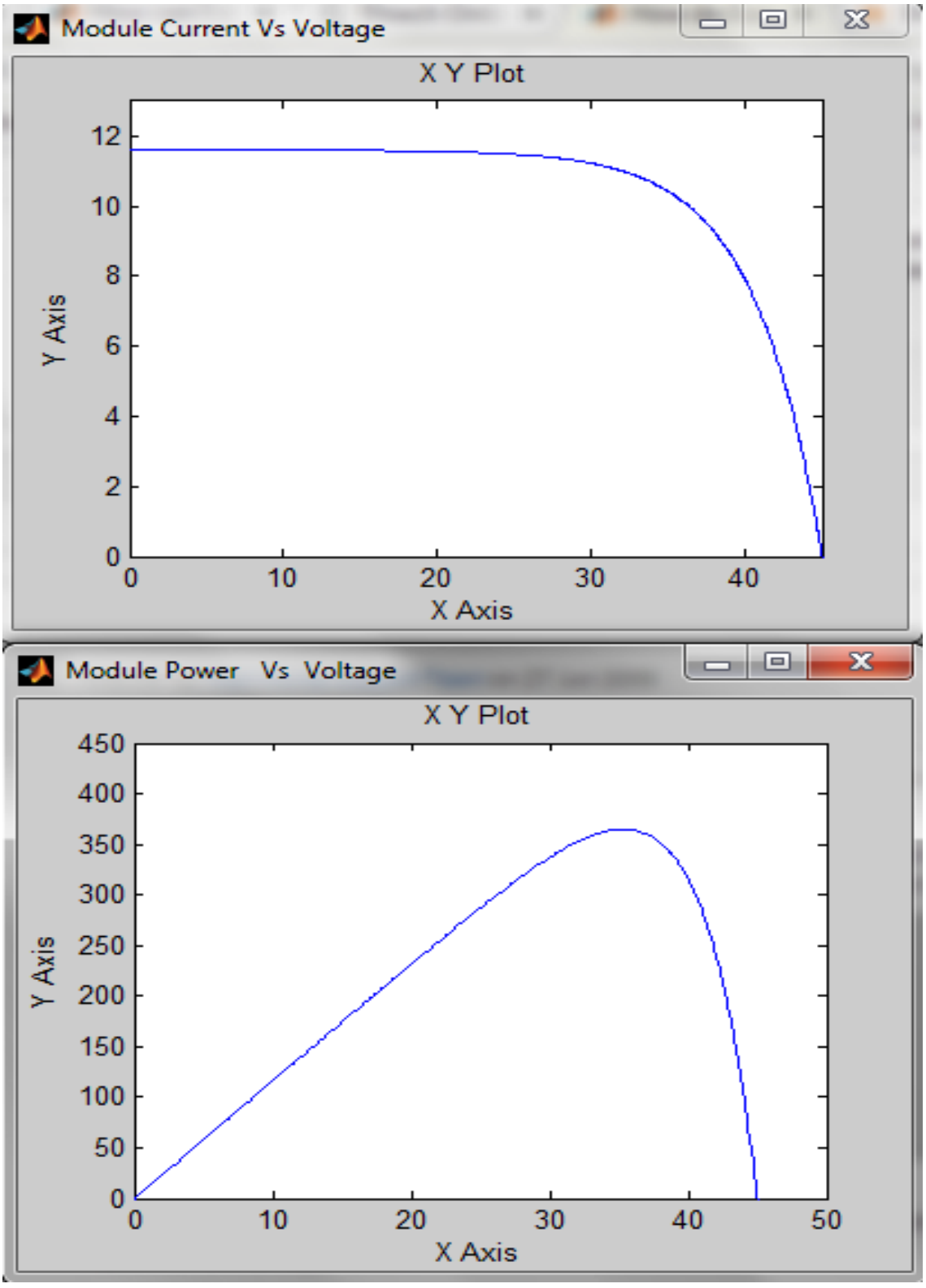

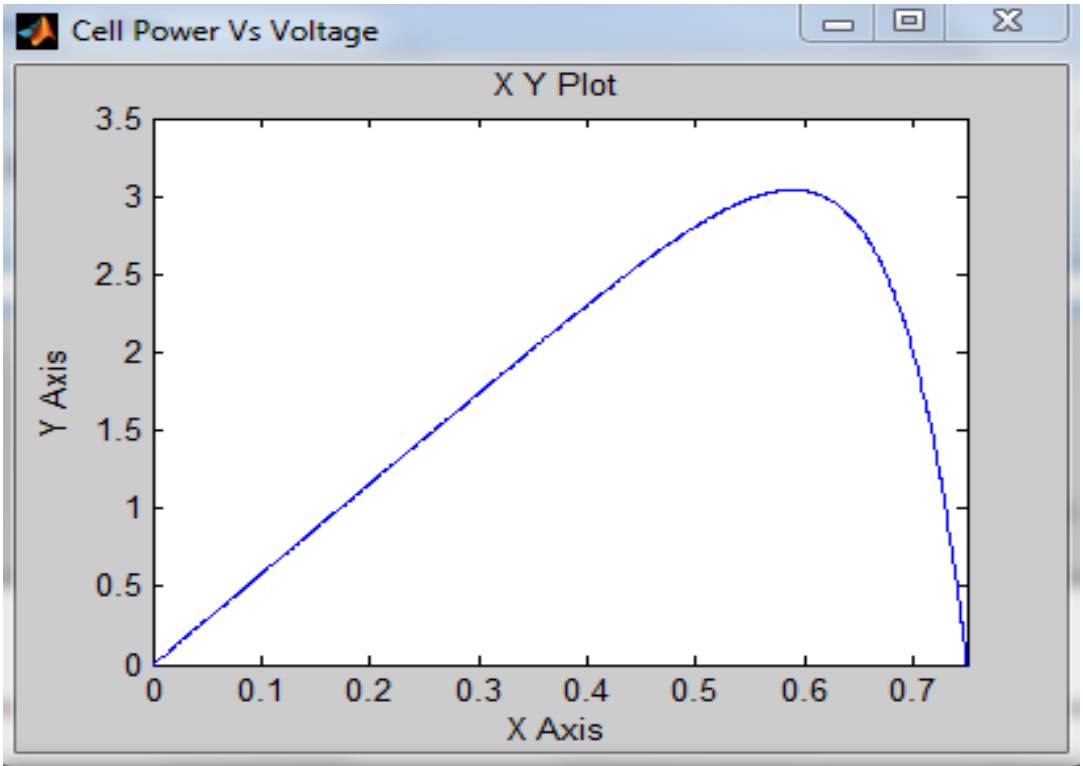
Cell Power Vs Voltage
X Y Plot
Y Axis
X Axis
0
0.5
1
1.5
2
2.5
3
3.5
0.1
0.2
0.3
0.4
0.5
0.6
0.7

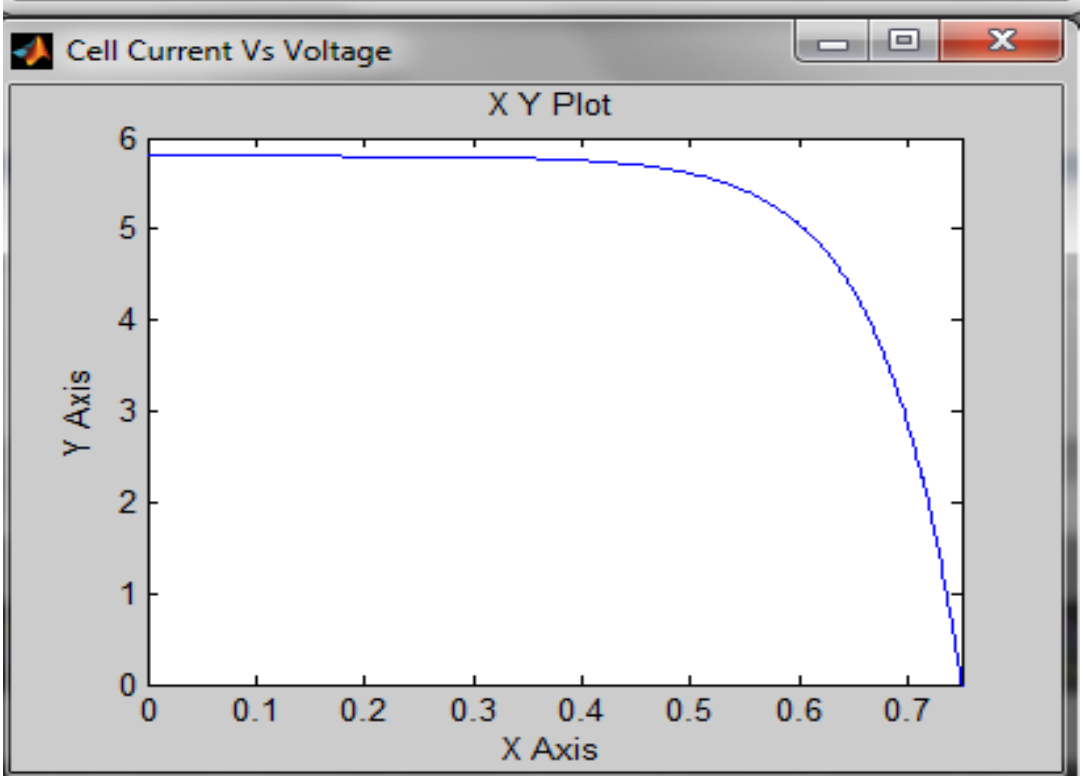
Cell Current Vs Voltage
X Y Plot
Y Axis
X Axis
0
1
2
3
4
5
6
0.1
0.2
0.3
0.4
0.5
0.6
0.7

4.2 Wind Farm Output

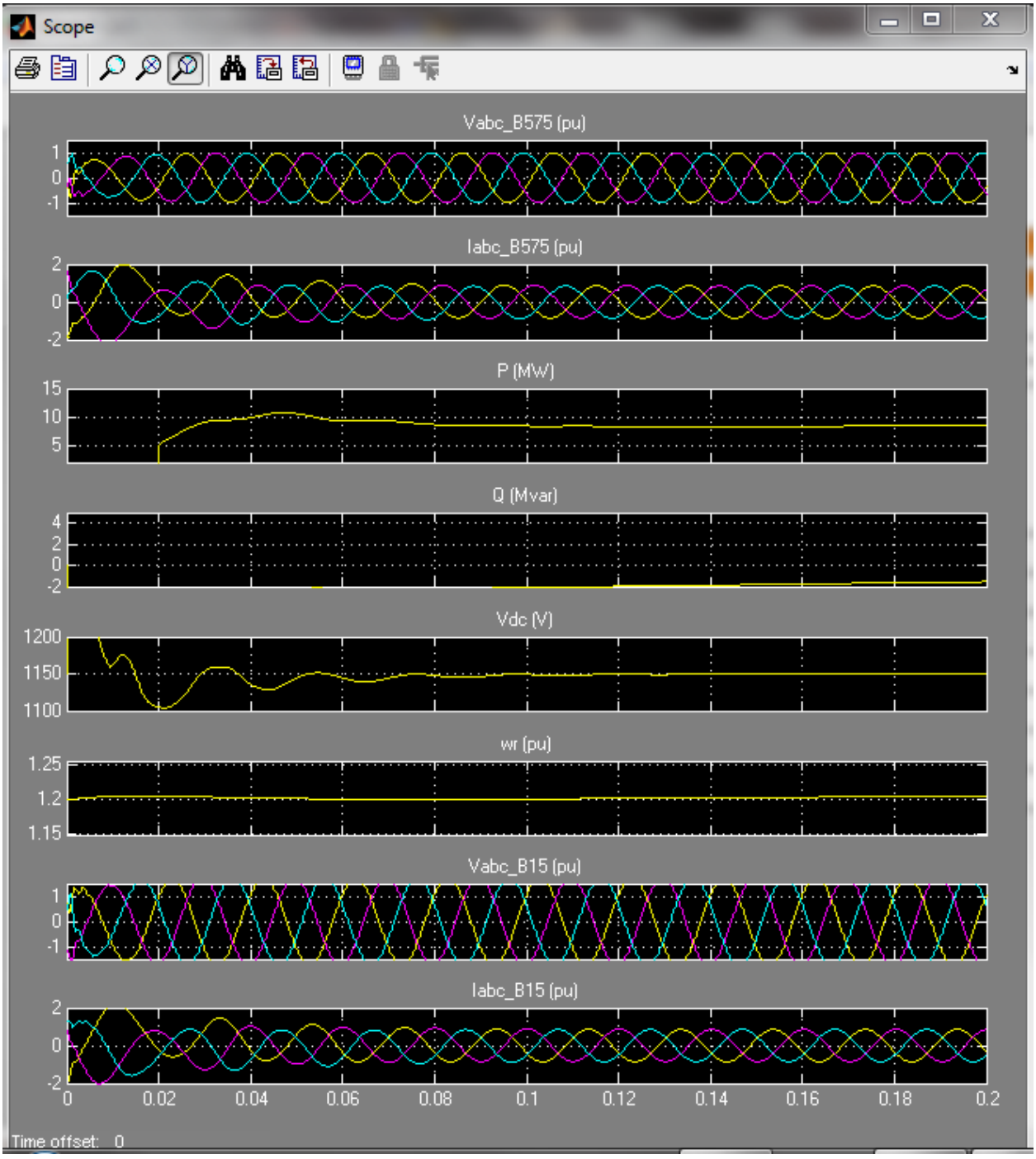

5. ABBREVIATIONS AND ACRONYMS

PV	Photovoltaic
SOFC	Solid Oxide Fuel Cells
FC	Fuel Cells
MoWE	Ministry of Water and Energy
EEPCo	Ethiopian Electric Power Corporation
TWh	Terra Watt Hour
ICS	Interconnected System
SCS	Self-Contained System
kV	Kilo Volt
DC	Direct Current
LV	Low Voltage
HV	High Voltage
GWh	Giga Watt Hour
MW	Mega Watt
UEAP	Universal Electric Access Program
REF	Rural Electrification Fund
COE	Cost of Energy
MPPT	Maximum Power Point Trucker
NASA	National Aeronautics and Space Administration
SMSE	Surface Meteorology and Solar Energy database
SWERA	Solar and Wind Energy Resource Assessment
LCE	Levelized Cost of Energy

AM	Air Mass
C	Power Coefficient of wind turbines
P	The density of the air
P	Power available in wind turbines
HAWT	Horizontal Axis Wind Turbines
VAWT	Vertical Axis Wind Turbines
F	Faraday's constant
KOH	Potassium Hydroxide
PEM	Proton Exchange Membrane
DFIG	Doubly Feed Induction Generators
IGBT	Insulated-Gated Bipolar Transistor
PWM	Pulse Width Modulation
PVA	Photovoltaic Array
GUI	Graphical User Interface
VC	Cell output voltage
Iph	Photocurrent
GSC	Grid side converter
RSC	The rotor side converter
FOC	Field Oriented Control
DTC	Direct Torque Control
CMPPT	Current Based Maximum Power Point Tracer
VMPPT	Voltage Based Maximum Power Point Tracer
V_{OC}	Open Circuit Voltage

V_mp	Maximum Power Point Voltage
Isc	Short Circuit Current
Imp	Maximum Power Point Current
DG	Distributed Generation
GIS	Geographical Information Systems
O&M	Operation and Maintenance
NPC	Net Present Cost
E.C	Ethiopian Calendar

6. Monthly and yearly load report of Metehara Substation

MONTHELY SUBSTATION LOAD REPORT

Substation :- **Metehara** **Month**:Hamle/2004 E.C

Existing Capacity:- 1X 16 MVA

No	Bay/Feeder	Power MW	Peak load Current(A)			Date	Time	Power MW	Minimum Current(A)			Date	Time
			R	S	T				R	S	T		
	132 Kv Line /Feeder												
1	Nazreth Incoming Feeder												
2	Transformer 1		23	23	23	5/11/2004	5:00		4	4	4	21/11/04	2:00
	15 Kv Line/Feeder												
1	Transformer 1 Feeder		120	120	120	5/11/2004	5:00		34	34	34	21/11/04	2:00
2	Abomsa line		85	85	85	2/11/2004	12:00		5	5	5	21/11/04	9:00
3	Suger Factory		38	38	38	5/11/2004	10:00		17	17	17	4/11/2004	2:00
4	Metehara line		12	12	12	23/11/04	8:00		5	5	5	1/11/2004	12:00
5	Industery line		12	12	12	23/11/04	8:00		5	5	5	2/11/2004	12:00

Month:-
Nehasie/2004E.C

No	Bay/Feeder	Power MW	Peak load Current(A)			Date	Time	Power MW	Minimum Current(A)			Date	Time
			R	S	T				R	S	T		
	132 Kv Line /Feeder												
1	Nazreth Incoming Feeder												
2	Transformer 1		18	18	18	7/12/2004	4:00		3	3	3	9/12/2004	2:00
	15 Kv Line/Feeder												
1	Transformer 1 Feeder		112	112	112	7/12/2004	4:00		26	26	26	9/12/2004	2:00
2	Abomsa line		12	12	12	21/12/04	7:00		7	7	7	13/12/04	10:00
3	Suger Factory		68	68	68	7/12/2004	4:00		5	5	5	9/12/2004	2:00
4	Metehara line		38	38	38	3/12/2004	7:00		6	6	6	9/12/2004	2:00
5	Industery line		12	12	12	1/12/2004	4:00		7	7	7	13/12/04	10:00

Month:-
Meskerem/2005E.C

No	Bay/Feeder	Power MW	Peak load Current(A)			Date	Time	Power MW	Minimum Current(A)			Date	Time
			R	S	T				R	S	T		
	132 Kv Line /Feeder												
1	Nazreth Incoming Feeder												
2	Transformer 1		25	25	25	26/01/05	12:00		3	3	3	14/01/05	2:00
	15 Kv Line/Feeder												
1	Transformer 1 Feeder		151	151	151	26/01/05	12:00		24	24	24	14/01/05	2:00
2	Abomsa line		10	10	10	14/01/05	10:00		5	5	5	14/01/05	12:00
3	Suger Factory		101	101	101	26/01/05	12:00		10	10	10	8/1/2005	10:00
4	Metehara line		42	42	42	10/1/2005	6:00		5	5	5	2/1/2005	2:00
5	Industery line		10	10	10	14/01/05	10:00		5	5	5	14/01/05	12:00

Month:-Tikimt/2005E.C

No	Bay/Feeder	Power MW	Peak load Current(A)			Date	Time	Power MW	Minimum Current(A)			Date	Time
			R	S	T				R	S	T		
	132 Kv Line /Feeder												
1	Nazreth Incoming Feeder												
2	Transformer 1		30	30	30	15/2/05	4:00		9	9	9	17/2/05	2:00
	15 Kv Line/Feeder												
1	Transformer 1 Feeder		174	174	174	15/2/05	4:00		50	50	50	17/2/05	2:00
2	Abomsa line		10	10	10	15/2/05	12:00		5	5	5	17/2/05	3:00
3	Suger Factory		122	122	122	15/2/05	12:00		17	17	17	17/2/05	2:00
4	Metehara line		42	42	42	8/2/2005	5:00		10	10	10	12/2/2005	2:00
5	Industery line		10	10	10	15/2/05	12:00		5	5	5	17/2/05	3:00

Month:-Hidar/2005 E.C

No	Bay/Feeder	Power MW	Peak load Current(A)			Date	Time	Power MW	Minimum Current(A)			Date	Time
			R	S	T				R	S	T		
	132 Kv Line /Feeder												
1	Nazreth Incoming Feeder												
2	Transformer 1		26	26	26	10/3/2005	11:00		6	6	6	12/3/2005	5:00
	15 Kv Line/Feeder												
1	Transformer 1 Feeder		156	156	156	10/3/2005	11:00		46	46	46	12/3/2005	5:00
2	Abomsa line		11	11	11	10/3/2005	12:00		2	2	2	14/03/05	7:00
3	Suger Factory		110	110	110	10/3/2005	11:00		34	34	34	12/3/2005	5:00
4	Metehara line		38	38	38	6/3/2005	6:00		2	2	2	14/03/05	2:00
5	Industery line		11	11	11	10/3/2005	12:00		2	2	2	14/03/05	7:00

Month:- Tahisas/2005E.C

No	Bay/Feeder	Power MW	Peak load Current(A)			Date	Time	Power MW	Minimum Current(A)			Date	Time
			R	S	T				R	S	T		
	132 Kv Line /Feeder												
1	Nazreth Incoming Feeder												
2	Transformer 1	5.447	28	28	28	26/04/05	20:00	2.335	12	12	12	7/4/2005	16:00
	15 Kv Line/Feeder												
1	Transformer 1 Feeder	3.269	148	148	148	26/04/05	20:00	1.148	52	52	52	29/04/05	17:00
2	Suger line	2.208	100	100	100	26/04/05	20:00	0.751	34	34	34	07/04/054	14:00
3	METehara line	0.928	42	42	42	7/4/2005	20:000	0.221	10	10	10	21/04/05	8:00
4	Metehara line	0.442	20	20	20	16/04/05	18:00	0.002	1	1	1	14/04/05	11:00
5	Industery line												

Month:- Tir/2005 E,C

No	Bay/Feeder	Power MW	Peak load Current(A)			Date	Time	Power MW	Minimum Current(A)			Date	Time
			R	S	T				R	S	T		
	132 Kv Line /Feeder												
1	Nazreth Incoming Feeder												
2	Transformer 1	5.447	23	23	23	23/05/05	20:00	0.584	3	3	3	10/5/2005	8:00
	15 Kv Line/Feeder												
1	Transformer 1 Feeder	2.606	118	118	118	2/5/2005	20:00	0.398	18	18	18	10/5/2008	8:00
2	Abomsa line	1.833	83	83	83	23/05/05	20:00	0.133	6	6	6	10/5/2005	8:00
3	Suger Factory	0.839	38	38	38	5-Sep	17:00	0.11	5	5	5	18/05/05	14:00
4	Metehara line	0.287	13	13	13	10/5/2005	17:00	0.022	1	1	1	5/5/2005	12:00
5	Industery line	0.243	11	11	11	1/5/2005	11:00	0.022	1	1	1	2/5/2005	10:00

Month:- Yekatit/2005 E.C

No	Bay/Feeder	Power MW	Peak load Current(A)			Date	Time	Power MW	Minimum Current(A)			Date	Time
			R	S	T				R	S	T		
	132 Kv Line /Feeder												
1	Nazreth Incoming Feeder												
2	Transformer 1	3.8911		20		14/6/05	11:00	1.1673		6		26/5/05	8:00
	15 Kv Line/Feeder												
1	Transformer 1 Feeder	2.5618		116		18/6/05	20:00	0.6405		29		26/5/05	8:00
2	Abomsa line	0.3313		15		3/6/2005	12:00	0.0442		2		26/5/05	8:00
3	Suger Factory	1.5901		76		16/6/05	12:00	0.6405		20		26/5/05	8:00
4	Metehara line	0.9276		42		14/6/05	12:00	0.2208		10		26/5/05	8:00
5	Industery line												

Monthe:Megabit/2005E.C

No	Bay/Feeder	Power MW	Peak load Current(A)			Date	Time	Power MW	Minimum Current(A)			Date	Time
			R	S	T				R	S	T		
	132 Kv Line /Feeder												
1	Nazreth Incoming Feeder												
2	Transformer 1	4.28016		22		11/7/2005	20:00	1.167		6		8/7/2005	15:00
	15 Kv Line/Feeder												
1	Transformer 1 Feeder	2.69435		122		10/7/2005	11:00	0.883		40		8/7/2005	15:00
2	Abomsa line	0.265		12		28/07/05	20:00	0.022		1		8/7/2005	8:00
3	Suger Factory	1.723		78		11/7/2005	20:00	0.375		17		24/06/05	8:00
4	Metehara line	0.972		44		12/7/2005	16:00	0.375		17		22/06/05	8:00
5	Industery line	0.243		11		7/7/2005	8:00	0.022		1		29/06/05	8:00

Monthe:Miazia/2005 E.C

No	Bay/Feeder	Power MW	Peak load Current(A)			Date	Time	Power MW	Minimum Current(A)			Date	Time
			R	S	T				R	S	T		
	132 Kv Line /Feeder												
1	Nazreth Incoming Feeder												
2	Transformer 1	4.09	21	21	21	3/8/2005	5:00	1.17	6	6	6	18/08/05	3:00
	15 Kv Line/Feeder												
1	Transformer 1 Feeder	2.72	123	123	123	8/8/2005	3:00	0.66	30	30	30	18/08/05	3:00
2	Abomsa line	1.83	83	83	83	12/8/2005	6:00	0.35	16	16	16	20/08/05	2:00
3	Suger Factory	1.13	51	51	51	18/08/05	13:00	0.38	17	17	17	20/08/05	2:00
4	Metehara line	0.18	8	8	8	8/8/2005	9:00	0.02	1	1	1	22/08/05	2:00
5	Industery line												

Month: Ginbot/2005 E.C

No	Bay/Feeder	Power MW	Peak load Current(A)			Date	Time	Power MW	Minimum Current(A)			Date	Time
			R	S	T				R	S	T		
	132 Kv Line /Feeder												
1	Nazreth Incoming Feeder												
2	Transformer 1	4.864	25	25	25	8/9/2005	8:00	0.973	5	5	5	26/09/05	15:00
	15 Kv Line/Feeder												
1	Transformer 1 Feeder	3.136	142	142	142	8/9/2005	8:00	0.4	18	18	18	8/9/2005	17:00
2	Abomsa line	0.177	8	8	8	7/9/2005	18:00	0.022	1	1	1	4/9/2005	8:00
3	Suger Factory	2.65	120	120	120	8/9/2005	8:00	0.309	14	14	14	8/9/2005	8:00
4	Metehara line	0.994	45	45	45	22/09/05	14:00	0.325	17	17	17	4/9/2005	20:00
5	Industery line	0.155	7	7	7	7/9/2005	18:00	0.022	1	1	1	4/9/2005	8:00

Month: Sene/2005 E.C

No	Bay/Feeder	Power MW	Peak load Current(A)			Date	Time	Power MW	Minimum Current(A)			Date	Time
			R	S	T				R	S	T		
	132 Kv Line /Feeder												
1	Nazreth Incoming Feeder												
2	Transformer 1	4.864	25	25	25	5/10/2005	20:00	1.362	7	7	7	18/10/05	8:00
	15 Kv Line/Feeder												
1	Transformer 1 Feeder	2.959	134	134	134	5/10/2005	20:00	0.42	19	19	19	5/10/2005	8:00
2	Abomsa line	0.111	5	5	5	4/10/2005	11:00	0.022	1	1	1	2/10/2005	9:00
3	Suger Factory	2.098	95	95	95	5/10/2005	20:00	0.221	10	10	10	10/10/2005	17:00
4	Metehara line	1.016	46	46	46	6/10/2005	12:00	0.375	17	17	17	2/10/2005	18:00
5	Industery line	0.111	5	5	5	1/10/2005	20:00	0.022	1	1	1	2/10/2005	8:00

YEARLY SUBSTATION LOAD REPORT

Year:2005E.C

No	Bay/Feeder	Power MW	Peak load Current(A)			Date	Time	Power MW	Minimum Current(A)			Date	Time
			R	S	T				R	S	T		
	132 Kv Line /Feeder												
1	Nazreth Incoming Feeder												
2	Transformer 1	5.447	30	30	30	26/04/05	20:00	0.584	3	3	3	10/5/2005	8:00
	15 Kv Line/Feeder												
1	Transformer 1 Feeder	2.959	134	134	134	5/10/2005	20:00	0.42	19	19	19	5/10/2005	8:00
2	Abomsa line	0.111	5	5	5	4/10/2005	11:00	0.022	1	1	1	2/10/2005	9:00
3	Suger Factory	2.65	122	122	122	8/9/2005	8:00	0.11	5	5	5	18/05/05	14:00
4	Metehara line	1.016	46	46	46	6/10/2005	12:00	0.002	1	1	1	5/5/2005	12:00
5	Industery line	0.243	12	12	12	7/7/2005	8:00	0.022	1	1	1	2/5/2005	10:00

7. Price schedule for substation extension

Item	Description	Unit	Qty	Plant and Mandaytory Spare Part supplied from the Abroad (CIP)				Installation Services(Works/Erection) and Other Services including design				Total (excluding VAT)		VAT	TOTAL
				Foreign		Local Services		Foreign		Local		Foreign	Local	Local	Local + Foreign
				Unit Price	Total Price	Unit Price	Total Price	Unit Price	Total Price	Unit Price	Total Price			(USD)	(USD)
			①	②	③ (①*②)	④	⑤ (①*④)	⑧	⑨ (①*⑧)	⑩	⑪ (①*⑩)	⑫ (③+⑨)	⑬ (⑤+⑦+⑪)		
SUB-TOTAL (CARRIED TO SUMMARY OF PRICES)												-	-	-	
1.00	**1*132 kV SIDE, of 132/33 TRANSFORMER BAY**														
1.10	Bus bar Disconnectors, center break type, 3-pole, 1250 A	Set	1.00	7,500.00	7,500.0	621.91	621.91			1,160.27	1,160.27	7,500	1,782.18	267.33	7,602.48
1.20	Set of Circuit Breakers, SF6, three pole operation type, 3150A, 31.5kA	set	1.00	37,500.00	37,500.0	3,109.53	3,109.53			5,801.36	5,801.36	37,500	8,910.89	1,336.63	38,012.38
1.30	Current Transformers, 150-300/1/1/1A, 3 core,	No.	3.00	7,500.00	22,500.0	621.91	1,865.72			1,160.27	3,480.82	22,500	5,346.53	801.98	22,807.43
1.40	Lightening Arrestors with discharge counter, 120 kV, 10 kA,	No.	3.00	1,500.00	4,500.0	124.38	373.14			232.05	696.16	4,500	1,069.31	160.40	4,561.49
1.50	Post Insulators, out door type	No.	1.00	625.00	625.0	51.83	51.83			96.69	96.69	625	148.51	22.28	633.54
1.60	Conductors, Insulator strings, connectors, Clamps & hardware for equipment interconnections	lot	1.00	20,000.00	20,000.0	3,316.00	3,316.00			4,406.00	4,406.00	20,000	7,722.00	1,158.30	20,444.02
SUB-TOTAL (CARRIED TO SUMMARY OF PRICES)					92,625		9,338.12				15,641.30	92,625.00	24,979.43	3,746.91	94,061.32
2.00	OUTDOOR TERMINAL CABINETS														
2.10	Outdoor Terminal Cabinets complete with auxiliary devices and terminal blocks	No.	1.00	6,250.00	6,250.0	518.25	518.25			966.89	966.89	6,250	1,485.15	222.77	6,335.40
SUB-TOTAL (CARRIED TO SUMMARY OF PRICES)					6,250.0		518.25				966.89	6,250	1,485.15	222.77	6,335.40
3.00	CONTROL & PROTECTION PANELS														
3.01	Control and signalling panel for 132 kV side of 132/33 power transformer	No.	1.00	28,750.00	28,750.0	2,383.97	2,383.97			3,166.77	3,166.77	28,750	5,550.74	832.61	29,069.17
3.02	Common Control and signalling panel	No.	1.00	28,750.00	28,750.0	2,383.97	2,383.97			3,166.77	3,166.77	28,750	5,550.74	832.61	29,069.17
3.03	Protection panel for 132/33/15 kV auto transformers circuit protection	No.	1.00	60,000.00	60,000.0	4,975.25	4,975.25			6,608.91	6,608.91	60,000	11,584.16	1,737.62	60,666.09
SUB-TOTAL (CARRIED TO SUMMARY OF PRICES)					117,500		9,743.19				12,942.45	117,500.00	22,685.64	3,402.85	118,804.42
4.00	33 KV METAL CLAD SWITCHGEAR (INDOOR)														
4.10	33 KV transformer incoming feeder switchgear compartements with 33 kV VT (cubicle)	No.	1.00	40,000.00	40,000.0	2,600.00	2,600.00			3,500.00	3,500.00	40,000	6,100.00	915.00	40,350.75
SUB-TOTAL (CARRIED TO SUMMARY OF PRICES)					40,000		2,600.00				3,500.00	40,000.00	6,100.00	915.00	40,350.75
5.00	33 KV OUTDOOR SWITCHGEAR														
5.10	33 kV lightning arresters, outdoor, for tranformer feeder, 36 KV, complete with accessories 10KA and common discharge counters for three phases	No.	3.00	800.00	2,400.0	52.00	156.00			97.00	291.00	2,400	447.00	67.05	2,425.70
5.20	33 kV disconnector with earthing switch, three pole, motor operated, 2000 A for 33 kV side of transformer	No.	1.00	6,900.00	6,900.0	570.00	570.00			1,060.00	1,060.00	6,900	1,630.00	244.50	6,993.73
5.30	33 kV interconnectors, support structures, conductors, insulators, fittings, and hardware for the interconnection of 33 kV system. etc	Lot	1.00	11,250.00	11,250.0	1,000.00	1,000.00			1,750.00	1,750.00	11,250	2,750.00	412.50	11,408.13

5.40	33 kV power cable and accessories	Lot	1.00	223,805.32	223,805.3	1,347.16	1,347.16			781.46	781.46	223,805	2,128.62	319.29	223,927.72
	SUB-TOTAL (CARRIED TO SUMMARY OF PRICES)				**244,355**		**3,073.16**				**3,882.46**	**244,355.32**	**6,955.62**	**1,043.34**	**244,755.27**
6.00	**STEEL STRUCTURES**														
6.10	Steel fabricated structure for, 132 and 33kV equipment and switch yard bus bar support, line termination gantries, etc.	Lot	1.00	100,000.00	100,000.0	830.00	830.00			24,000.00	24,000.00	100,000	24,830.00	3,724.50	101,427.73
	SUB-TOTAL (CARRIED TO SUMMARY OF PRICES)				100,000.0		830				**24,000.00**	**100,000**	**24,830.00**	**3,724.50**	**101,427.73**
7.00	**AUTO TRANSFORMERS**														
7.10	Auto transformer Power,132/33KV, 12/16 MVA complete with rails and accessories	No.	1.00	360,420.00	360,420.0	18,918.46	18,918.46			8,205.24	8,205.24	360,420	27,123.71	4,068.56	361,979.61
	SUB-TOTAL (CARRIED TO SUMMARY OF PRICES)				360,420.0		18,918.5				8,205.2	360,420.0	27,123.7	4,068.6	361,979.6
8.00	**CIVIL WORKS**														
8.10	General site preparation, excavation and top	Lot	0.25							693,609.06	173,402.27	-	173,402.27	26,010.34	9,970.63
8.20	Cable trenches, ducts & covers and other equipment foundations those are not mentioned in the above item 1 to 25.	Lot	0.25							590,191.64	147,547.91	-	147,547.91	22,132.19	8,484.00
8.30	Landscaping and surface finishing	Lot	0.25							1,205.96	301.49	-	301.49	45.22	17.34
8.40	Gravelling of the switchyard area	Lot	0.25							121,452.70	30,363.18	-	30,363.18	4,554.48	1,745.88
8.50	Final site clearing	Lot	0.25							13,494.56	3,373.64	-	3,373.64	506.05	193.98
	SUB-TOTAL (CARRIED TO SUMMARY OF PRICES)				-		-				**354,988.48**		**354,988.48**	**53,248.27**	**20,411.84**
	Total				**961,150.3**		**45,021.2**				**424,126.8**	**961,150.3**	**469,148.0**	**70,372.2**	**988,126.3**